

ELECTRONIC SUPPLEMENTARY INFORMATION

Bimetallic Scorpionate-based Helical Organoaluminums for the Efficient Carbon Dioxide Fixation into a Variety of Cyclic Carbonates

*Marta Navarro,^a Luis F. Sánchez-Barba,^{*a} Andrés Garcés,^{*a} Juan Fernández-Baeza,^b Israel*

*Fernández,^{*c} Agustín Lara-Sánchez,^b and Ana M. Rodríguez^b*

^aDepartamento de Biología y Geología, Física y Química Inorgánica, Universidad Rey Juan Carlos, Móstoles-28933-Madrid, Spain.

^bUniversidad de Castilla-La Mancha, Departamento de Química Inorgánica, Orgánica y Bioquímica- Centro de Innovación en Química Avanzada (ORFEO-CINQA), Campus Universitario, 13071-Ciudad Real, Spain.

^cDepartamento de Química Orgánica I and Centro de Innovación en Química Avanzada (ORFEO-CINQA), Facultad de Ciencias Químicas, Universidad Complutense de Madrid, 28040, Madrid, Spain.

E-mail: luisfernando.sanchezbarba@urjc.es, andres.garces@urjc.es; israel@quim.ucm.es

ELECTRONIC SUPPLEMENTARY INFORMATION

Table of Contents

1) Spectroscopy details

Figures S1–S9. ^1H and ^{13}C - ^1H NMR spectra of complexes **1–9** S3

2) Selective 1D NOESY Experiments

Figure S10. 1D NOESY responses for complex **3** S12

3) X-Ray Diffraction Studies: Crystallographic Structure Determination for the Complexes **1, 3·0.5(C₅H₁₂)**, **4, 6**, and **8·0.5 C₇H₈**.

Details for crystallographic studies and structural refinement S13

Figure S11. ORTEP view of the *P*-enantiomer [AlMe₂(κ^2 -pbpamd)] (**1**) S13

Figure S12. ORTEP view of the *M*-enantiomer of [AlMe₂(tbpamd⁻)AlMe₂] (**6**) S14

Figure S13. ORTEP view of the *P*-enantiomer of [AlMe₂(phbpamd⁻)AlMe₂] (**8**) S15

Figure S14a-b. ORTEP views of *P* and *M* enantiomers and their alternating disposition along the c axis in the unit cell of [AlMe₂(tbpamd⁻)AlMe₂] (**3**) S16

Table S1. Selected distances (Å) and angles (degrees) for **1** and **3·0.5(C₅H₁₂)** S17

Table S2. Crystal data and structure refinement for **1** and **3·0.5(C₅H₁₂)** S18

Table S3. Selected distances (Å) and angles (degrees) for **4, 6** and **8** S19

Table S4. Crystal data and structure refinement for **4, 6** and **8·0.5(C₇H₈)** S20

4) Experimental details for the synthesis of cyclic carbonates

General procedures for catalytic tests S21

^1H and ^{13}C - ^1H NMR spectroscopic data of compounds **11a-j, 13a-f** and **15** S22

Figures S15–S30. ^1H and ^{13}C - ^1H NMR spectra of compounds **11a-j** and **13a-f** S24

Figure S31. ^1H NMR spectra of commercial available *cis/trans* mixture of limonene oxide and *trans* isomer isolated. S40

Figure S32. ^1H and ^{13}C - ^1H NMR spectra of compound **15** S41

5) Kinetic studies to determine the order with respect the catalyst and co-catalyst:

Typical kinetic experiment procedure S42

Kinetics analysis S42

Figures S33 and S34. Kinetic Plots to determine order with respect **4** and TBAB S43

Table S5 Reaction rate constant and associated error for cycloaddition reaction of

10a and CO₂ S45

6) References S46

ELECTRONIC SUPPLEMENTARY INFORMATION

1. Spectroscopic Details

Figures S1–S11. ^1H and ^{13}C - ^1H NMR spectra of complexes **1–9**.

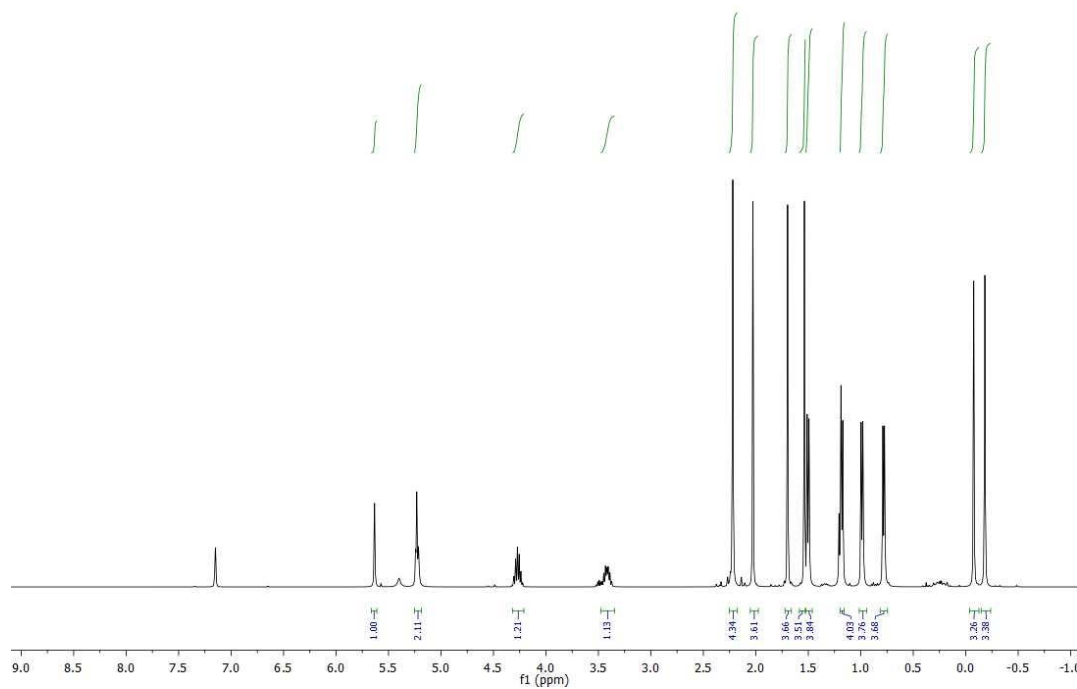


Figure S1a. ^1H -NMR spectrum (400 MHz, 297 K, C_6D_6) for complex $[\text{AlMe}_2(\kappa^2\text{-pbpam})]$ (**1**).

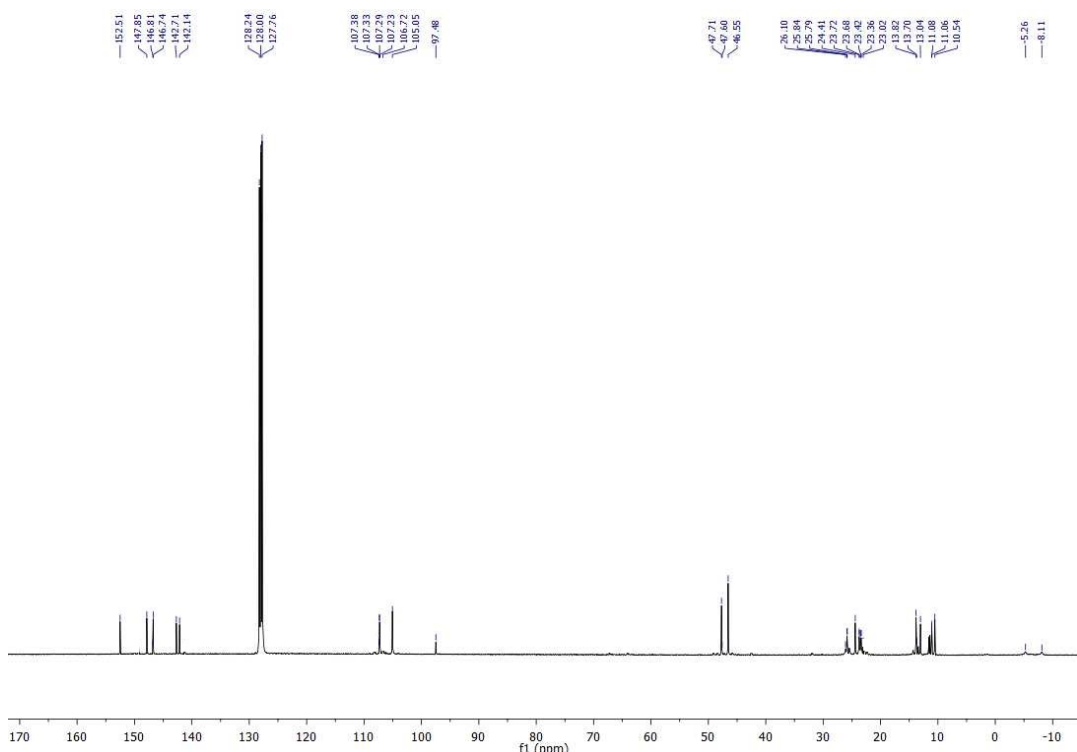
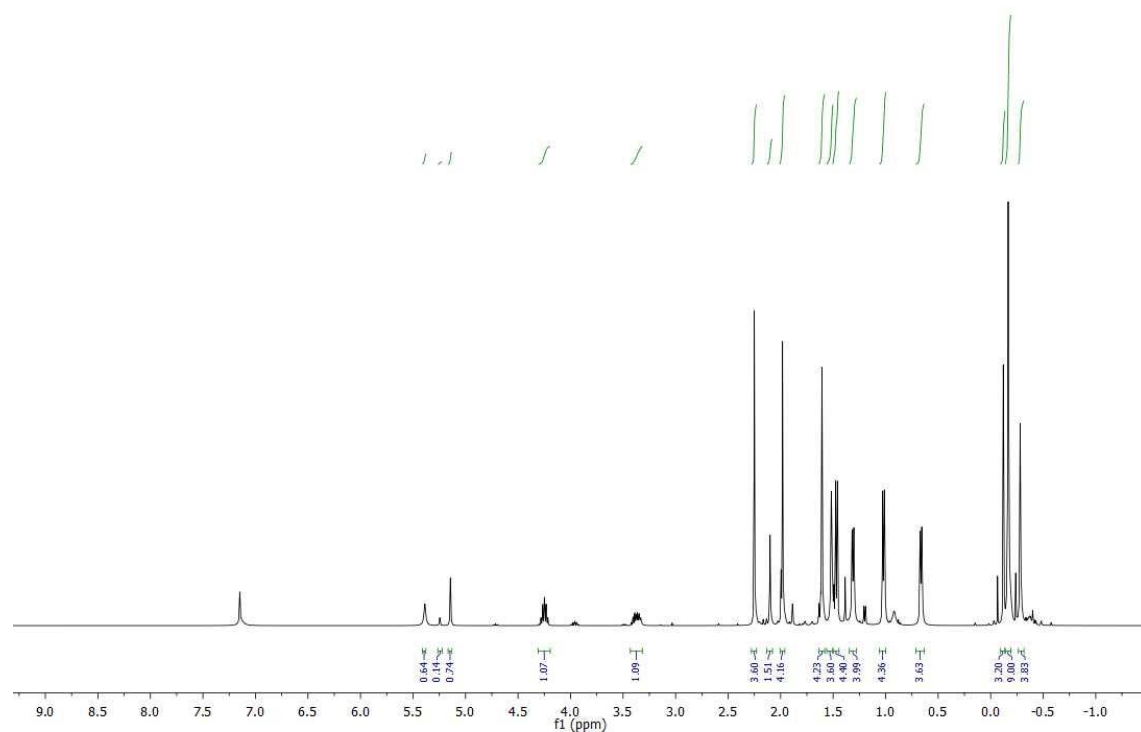


Figure S1b. ^{13}C - $\{^1\text{H}\}$ -NMR spectrum (400 MHz, 297 K, C_6D_6) for complex $[\text{AlMe}_2(\kappa^2\text{-pbpam})]$ (**1**).

ELECTRONIC SUPPLEMENTARY INFORMATION



ELECTRONIC SUPPLEMENTARY INFORMATION

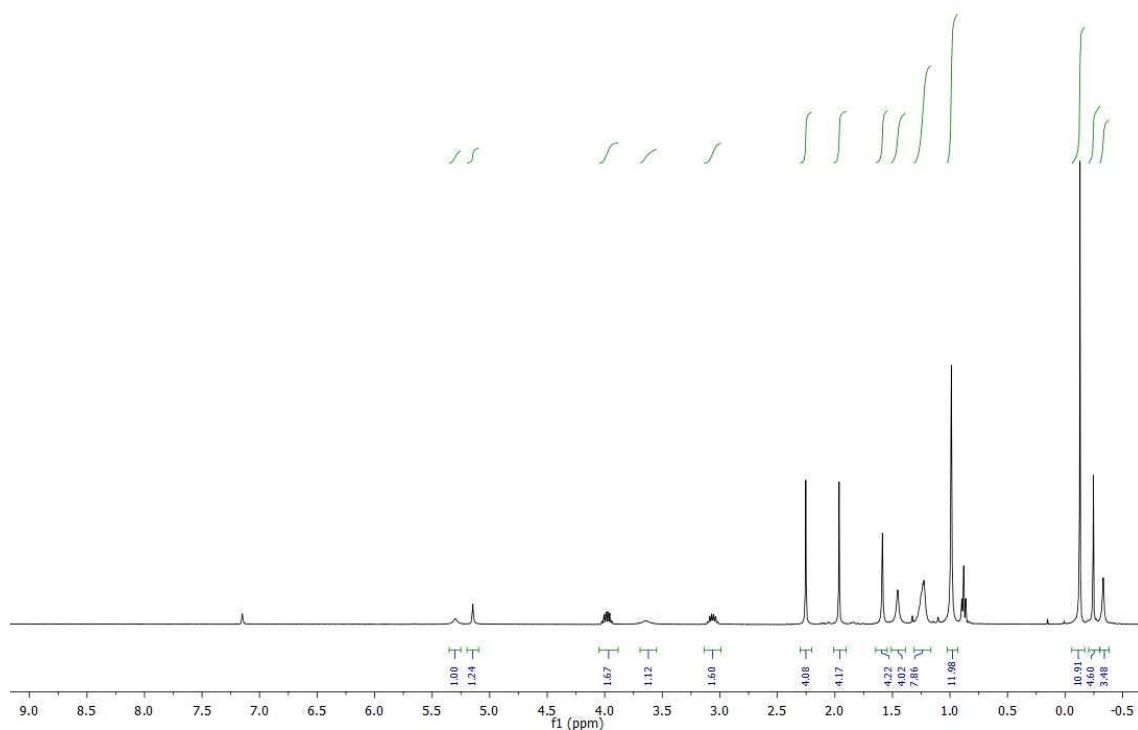


Figure S3a. ¹H NMR spectrum (400 MHz, 297 K, C₆D₆) for complex [AlMe₂(κ^2 -tbpamd)AlMe₃] (**3**).

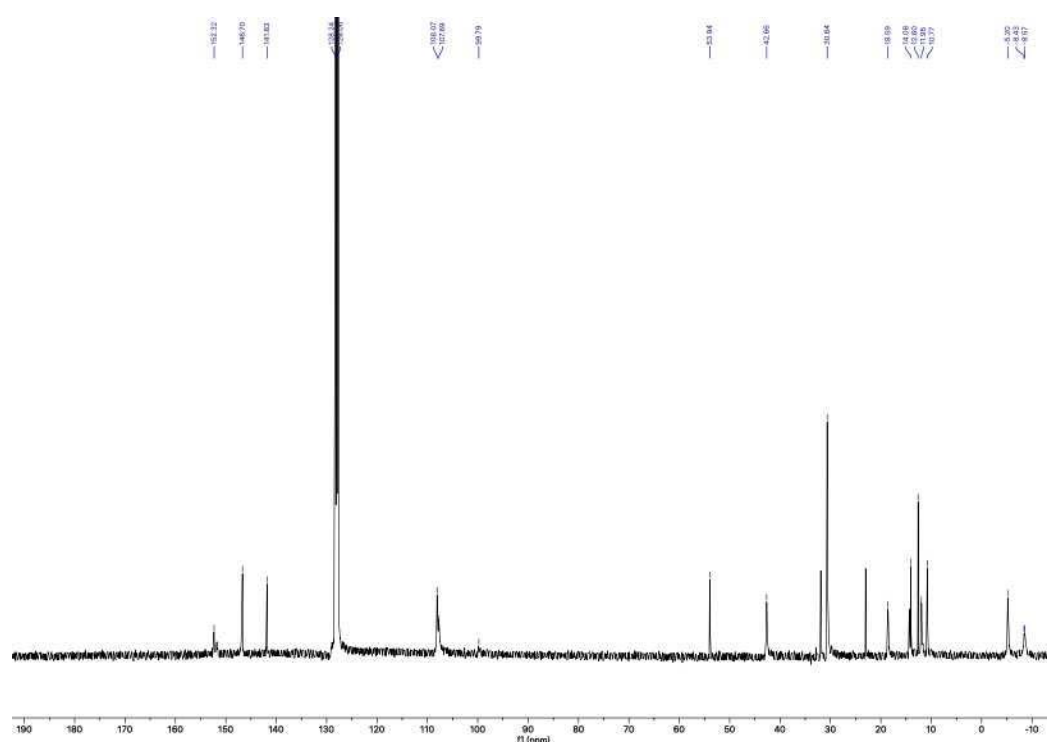


Figure S3b. ¹³C-^{1}H-NMR spectrum (400 MHz, 297 K, C₆D₆) for complex [AlMe₂(κ^2 -tbpamd)AlMe₃] (**3**).

ELECTRONIC SUPPLEMENTARY INFORMATION

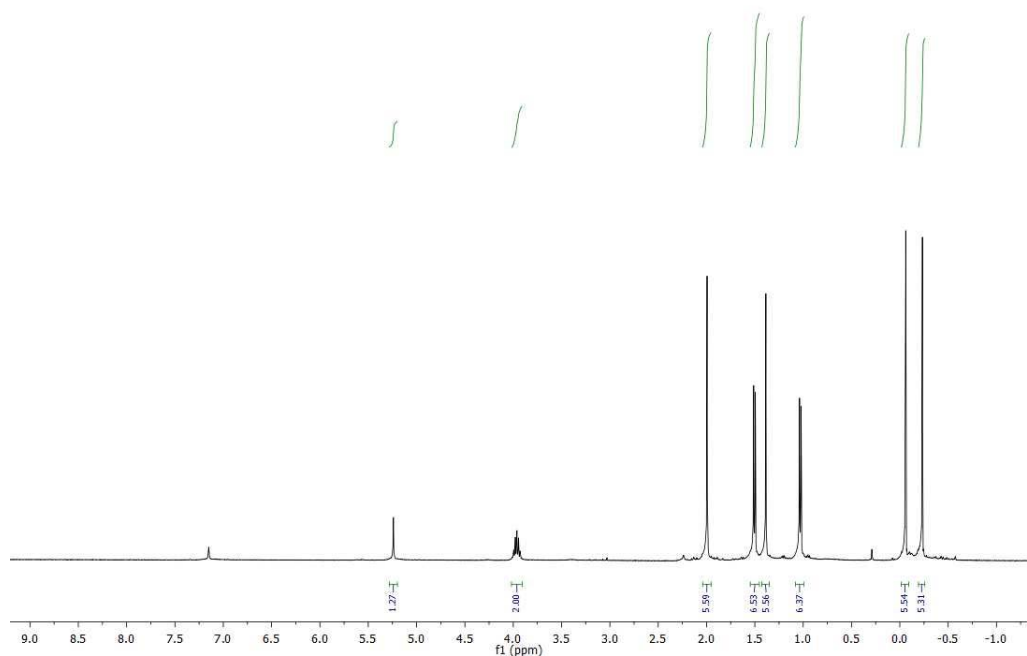


Figure S4a. ¹H-NMR spectrum (400 MHz, 297 K, C₆D₆) for complex [AlMe₂(pbpamd⁻)AlMe₂] (**4**).

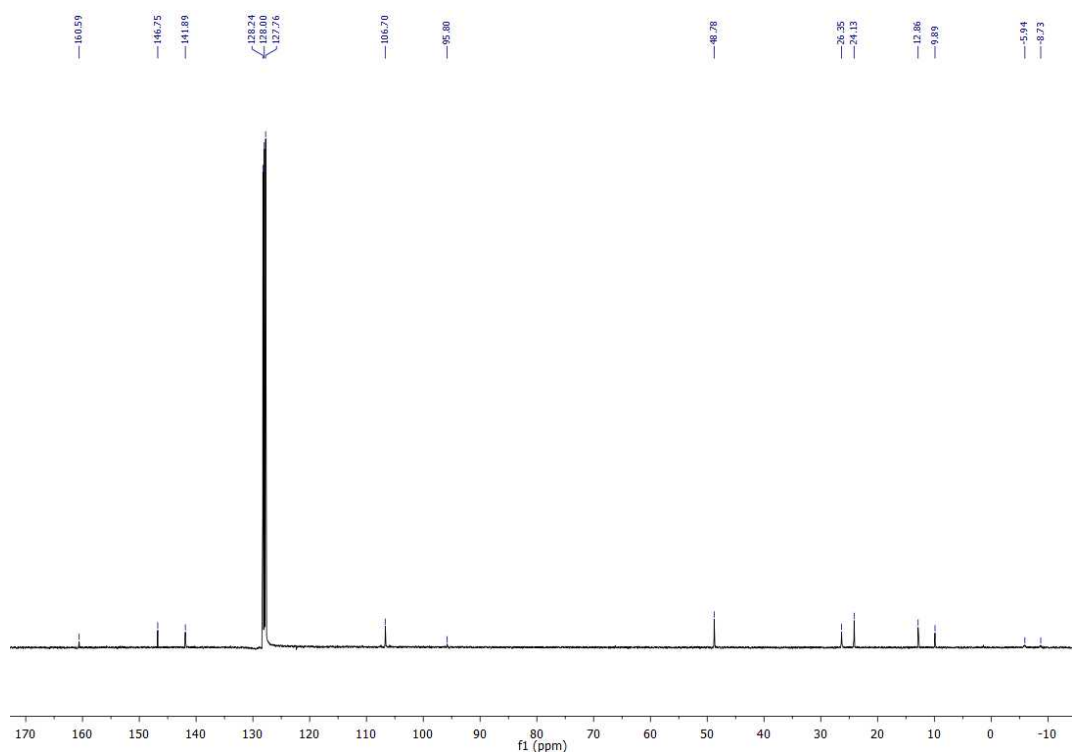


Figure S4b. ¹³C-{¹H}-NMR spectrum (400 MHz, 297 K, C₆D₆) for complex [AlMe₂(pbpamd⁻)AlMe₂] (**4**).

ELECTRONIC SUPPLEMENTARY INFORMATION

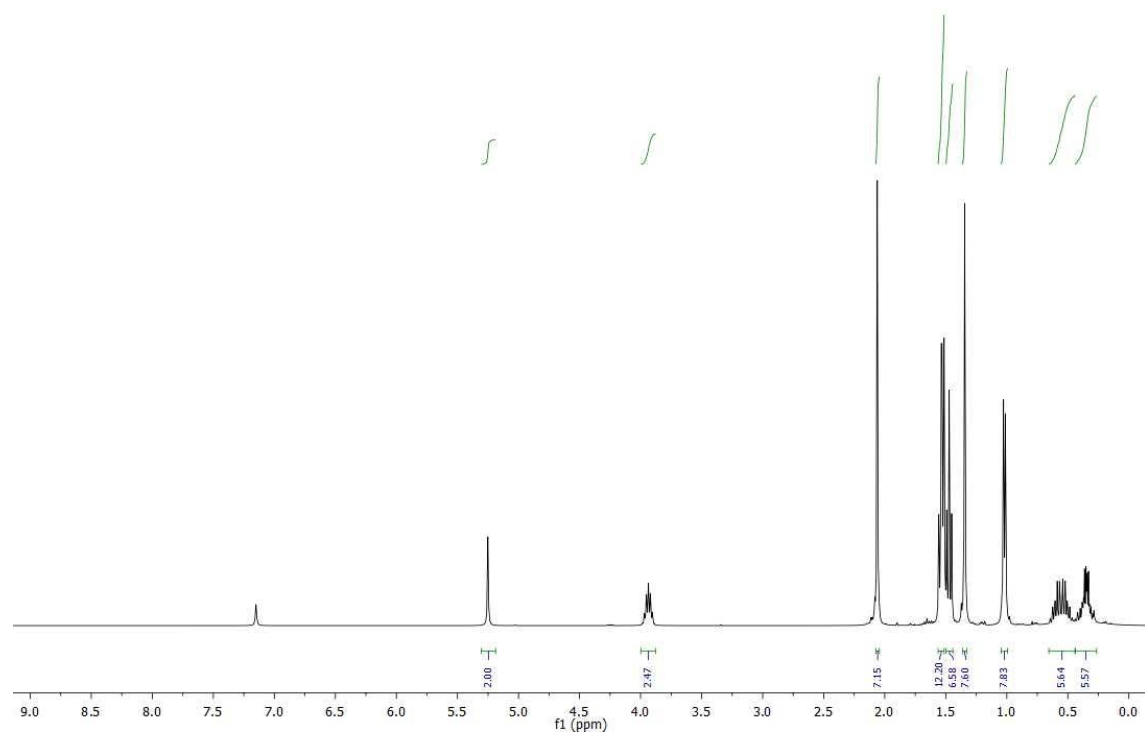


Figure S5a. ¹H-NMR spectrum (400 MHz, 297 K, C₆D₆) for complex [AlEt₂(pbpamd⁻)AlEt₂] (**5**).

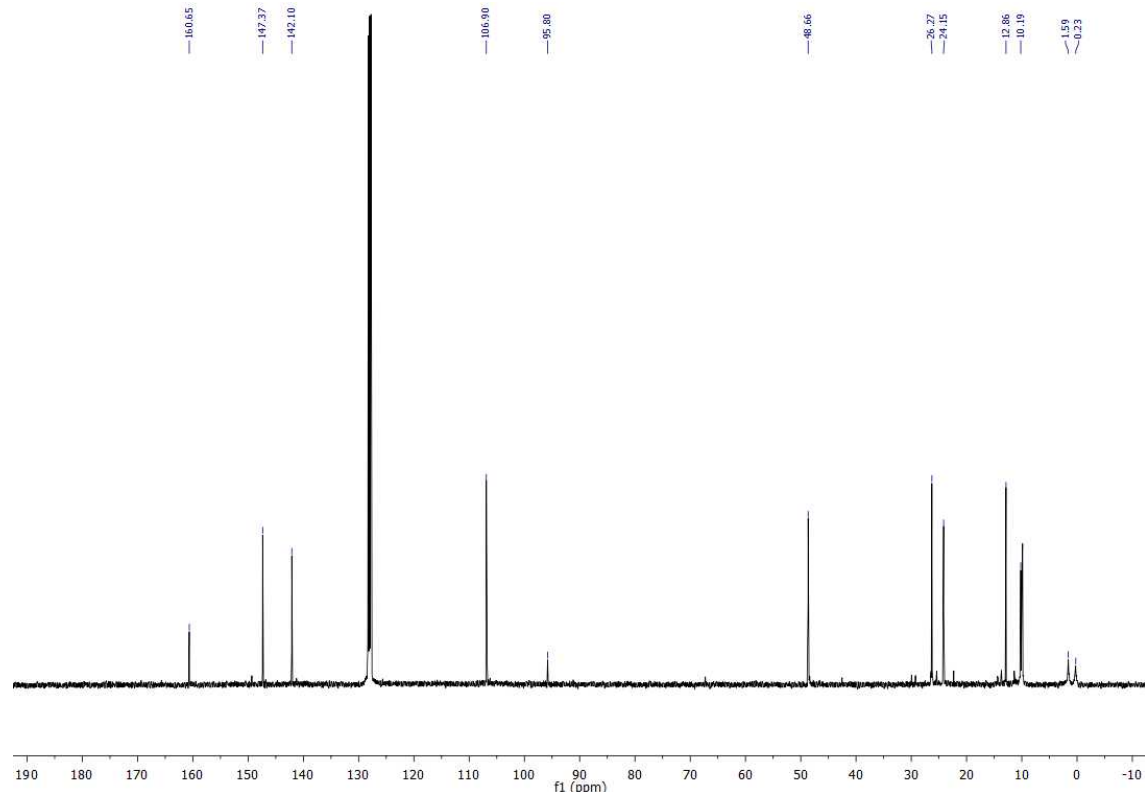


Figure S5b. ¹³C-{¹H}-NMR spectrum (400 MHz, 297 K, C₆D₆) for complex [AlEt₂(pbpamd⁻)AlEt₂] (**5**).

ELECTRONIC SUPPLEMENTARY INFORMATION

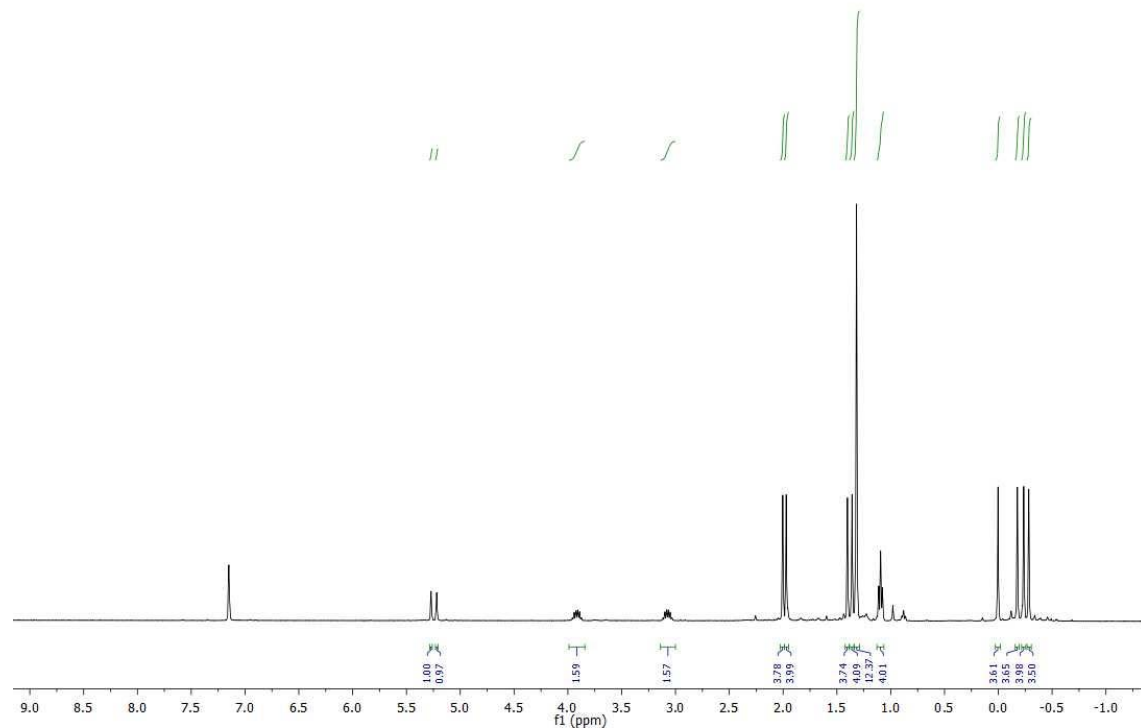


Figure S6a. ¹H-NMR spectrum (400 MHz, 297 K, C₆D₆) for complex [AlMe₂(tbpaMD⁻)AlMe₂] (**6**).

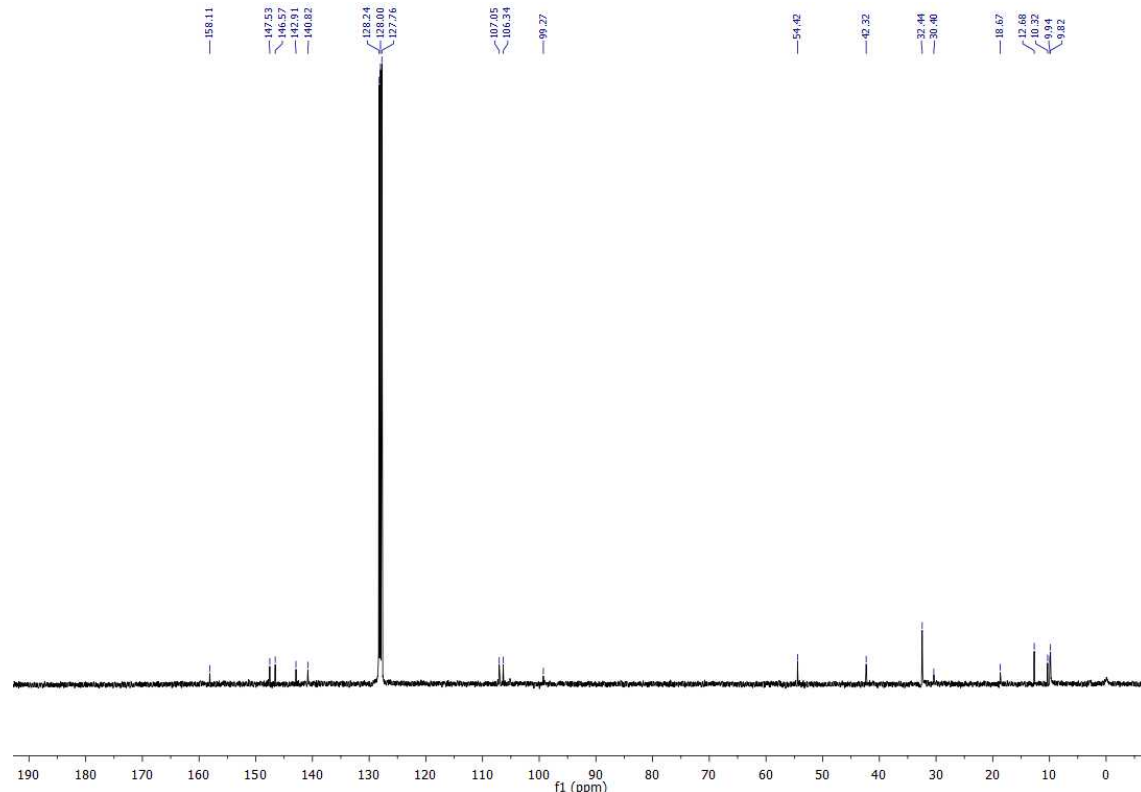


Figure S6b. ¹³C-{¹H}-NMR spectrum (400 MHz, 297 K, C₆D₆) for complex [AlMe₂(tbpaMD⁻)AlMe₂] (**6**).

ELECTRONIC SUPPLEMENTARY INFORMATION

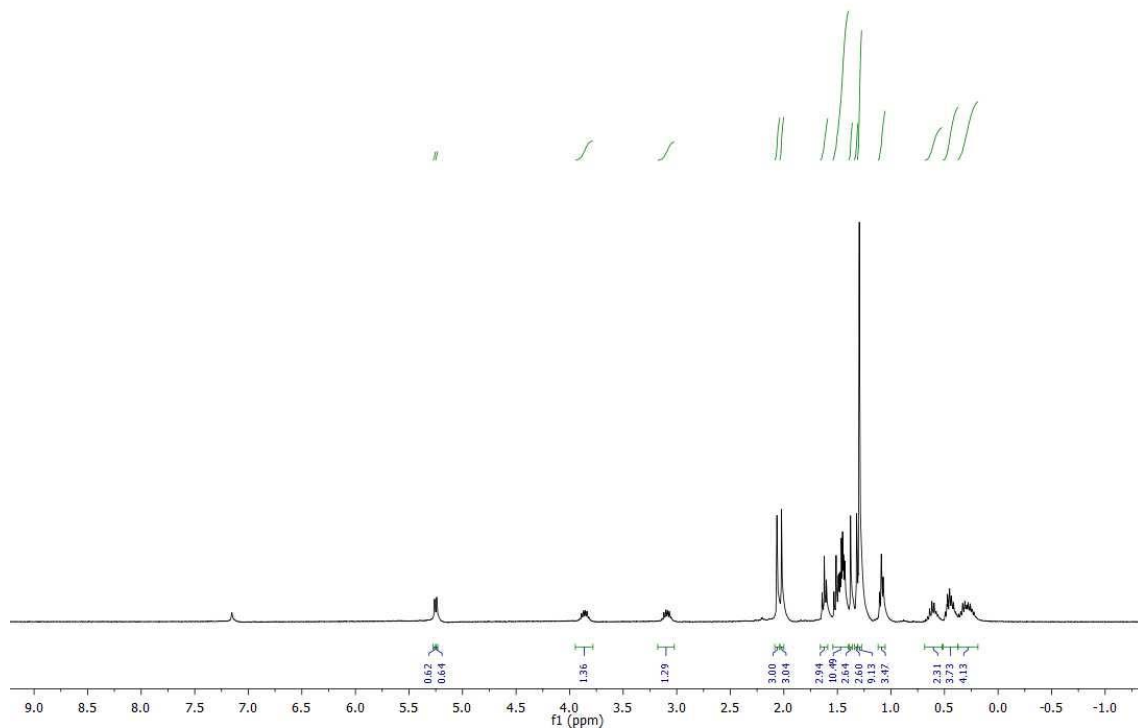


Figure S7a. ¹H-NMR spectrum (400 MHz, 297 K, C₆D₆) for complex [AlEt₂(tbpaMD⁻)AlEt₂] (7).

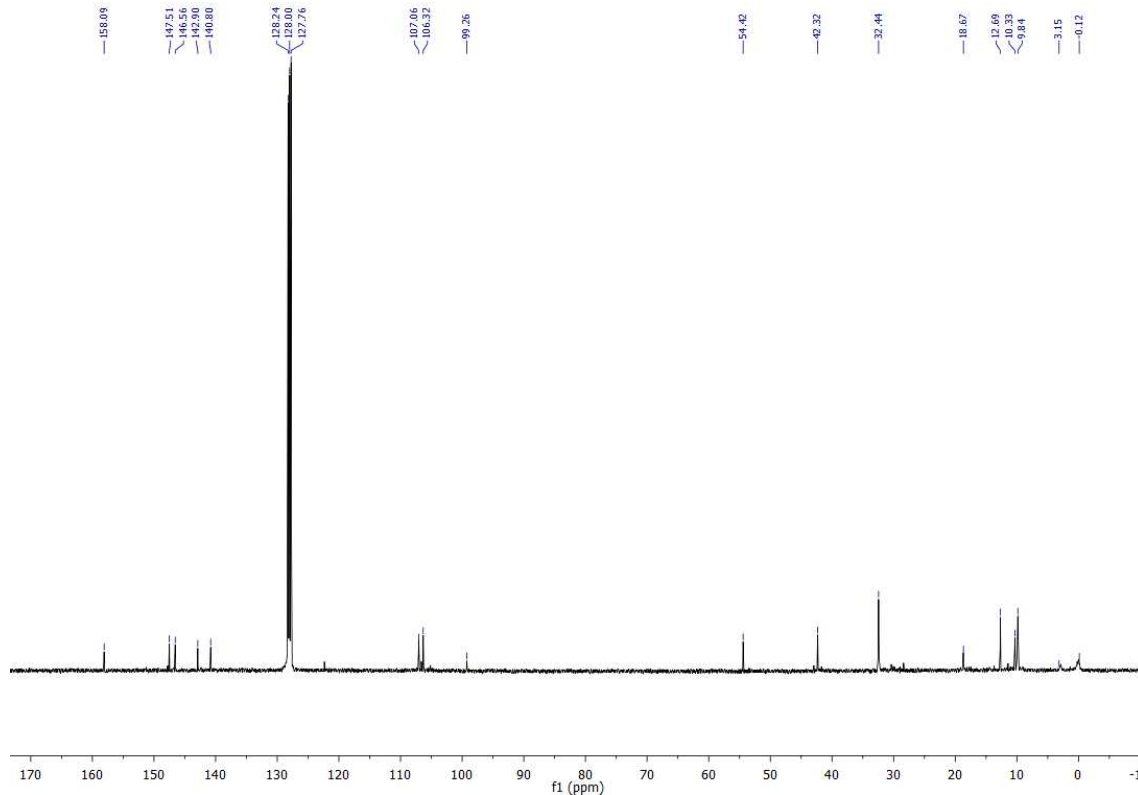


Figure S7b. ¹³C-{¹H}-NMR spectrum (400 MHz, 297 K, C₆D₆) for complex [AlEt₂(tbpaMD⁻)AlEt₂] (7).

ELECTRONIC SUPPLEMENTARY INFORMATION

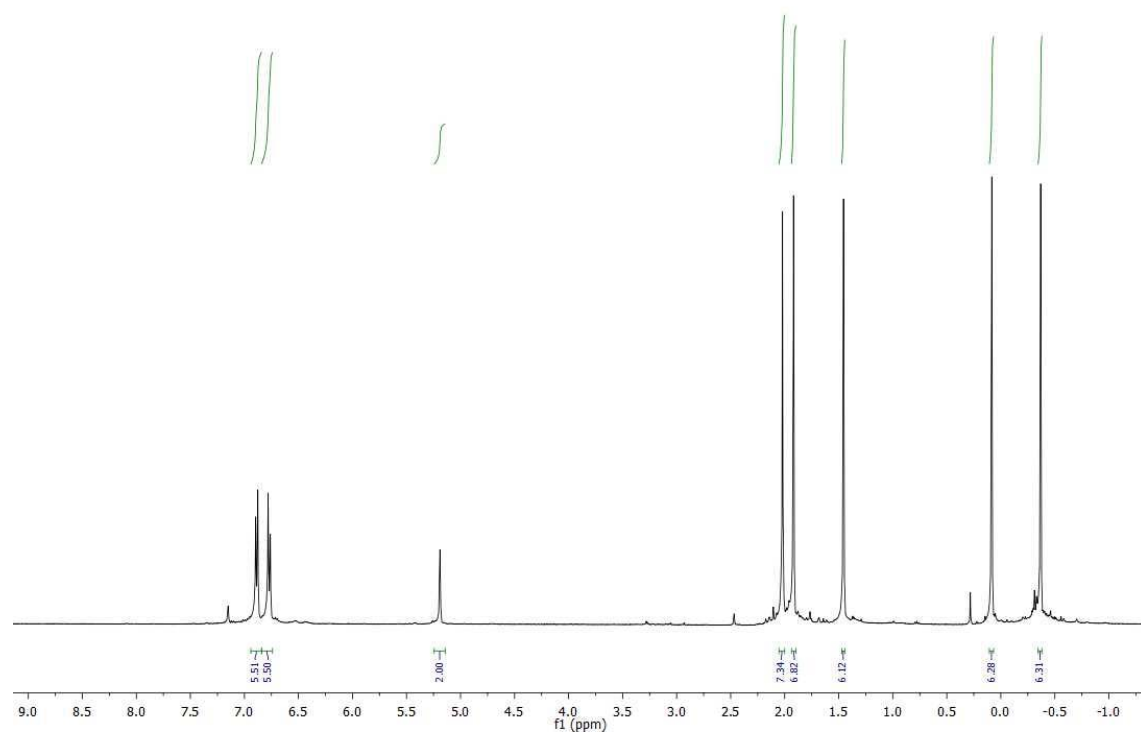


Figure S8a. ¹H-NMR spectrum (400 MHz, 297 K, C₆D₆) for complex [AlMe₂(phbpamD⁻)AlMe₂] (**8**).

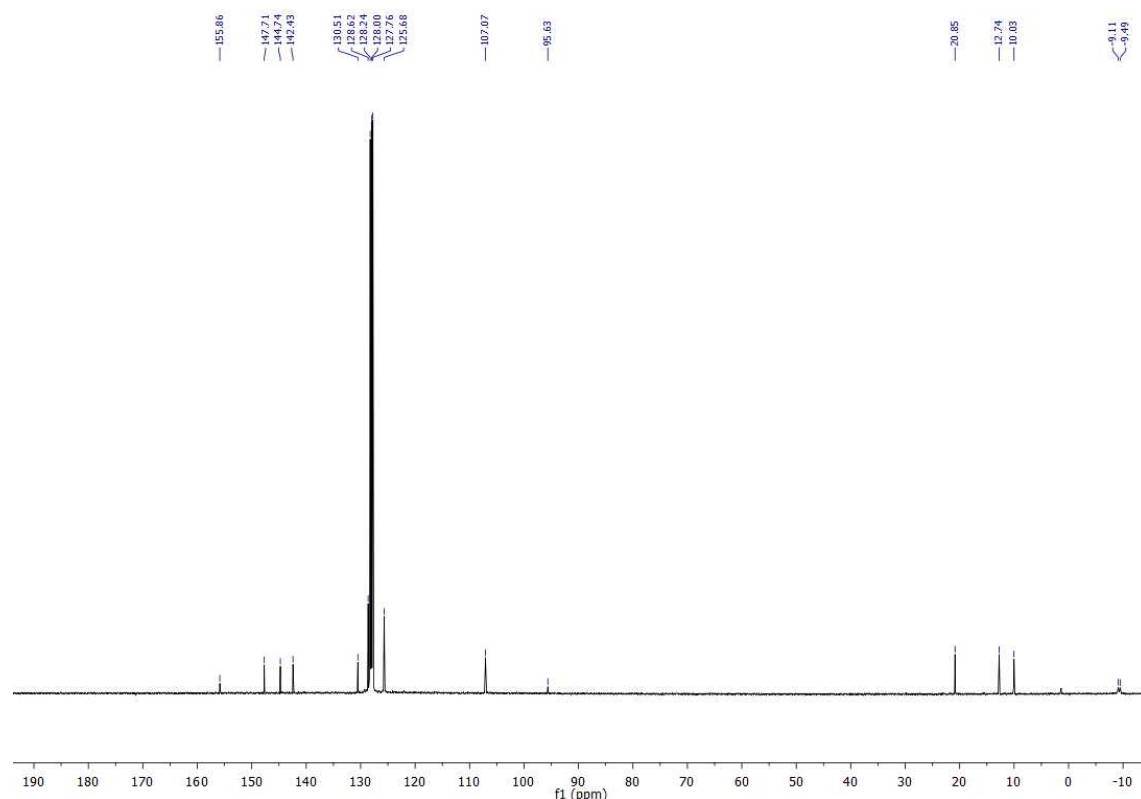


Figure S8b. ¹³C-^{1}H-NMR spectrum (400 MHz, 297 K, C₆D₆) for complex [AlMe₂(phbpamD⁻)AlMe₂] (**8**).

ELECTRONIC SUPPLEMENTARY INFORMATION

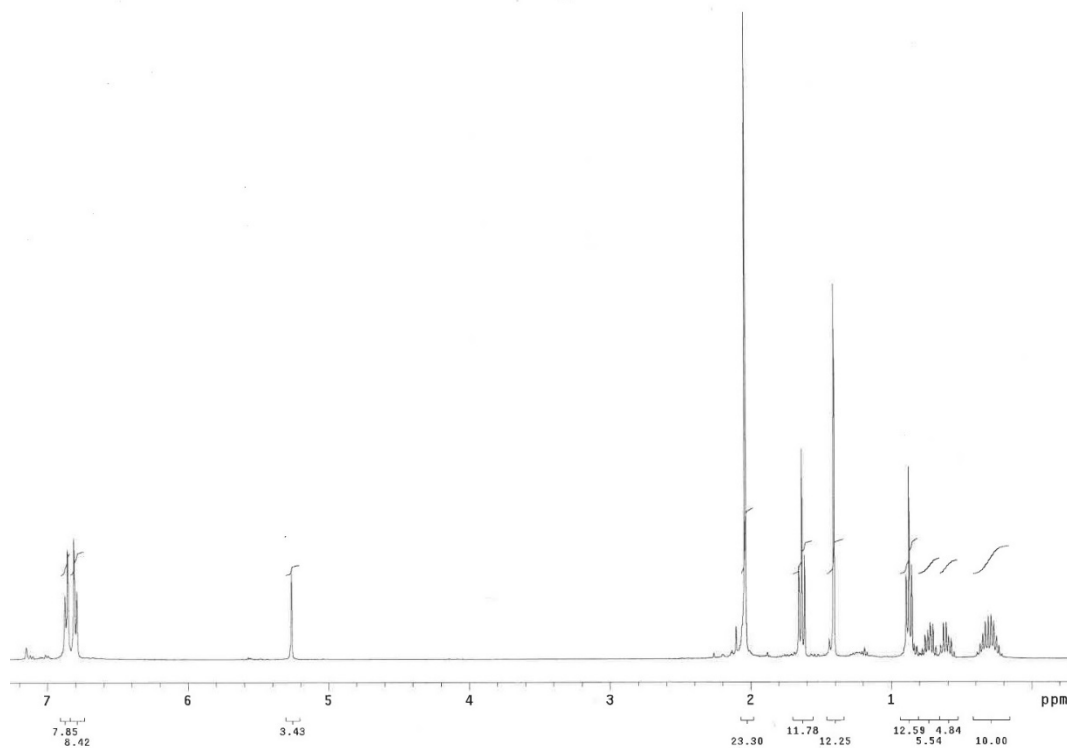


Figure S9a. ¹H-NMR spectrum (400 MHz, 297 K, C₆D₆) for complex [AlEt₂(phbpamd⁻)AlEt₂] (**9**).

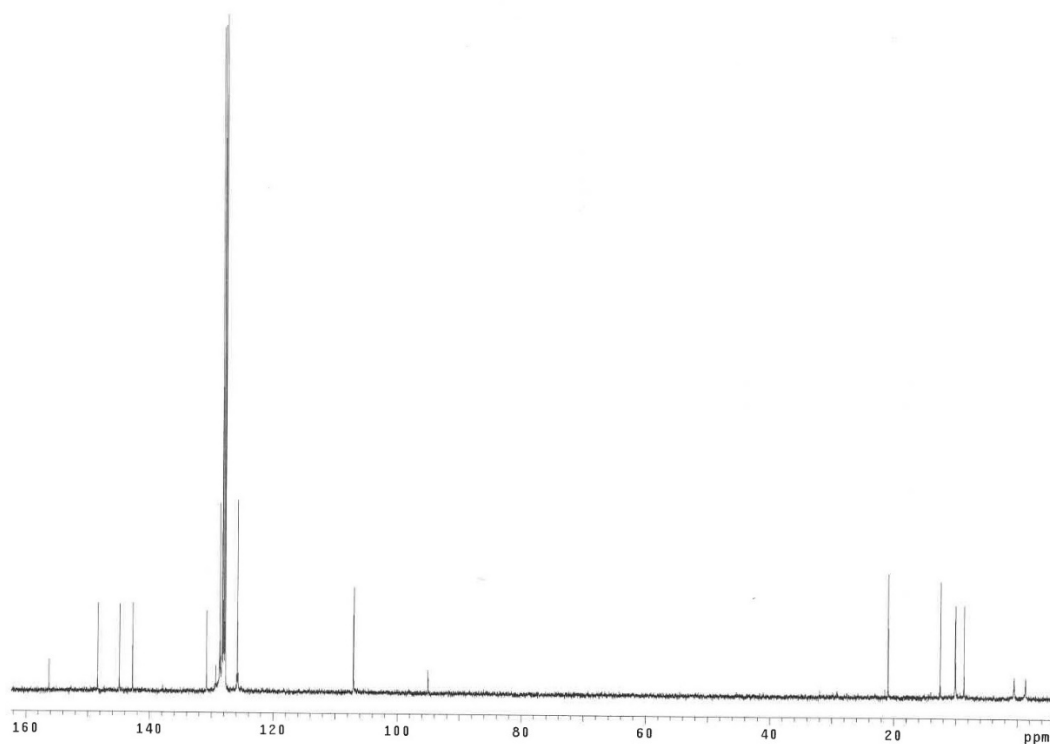


Figure S9b. ¹³C-{¹H}-NMR spectrum (400 MHz, 297 K, C₆D₆) for complex [AlEt₂(phbpamd⁻)AlEt₂] (**9**).

ELECTRONIC SUPPLEMENTARY INFORMATION

2. Selective 1D NOESY Experiment

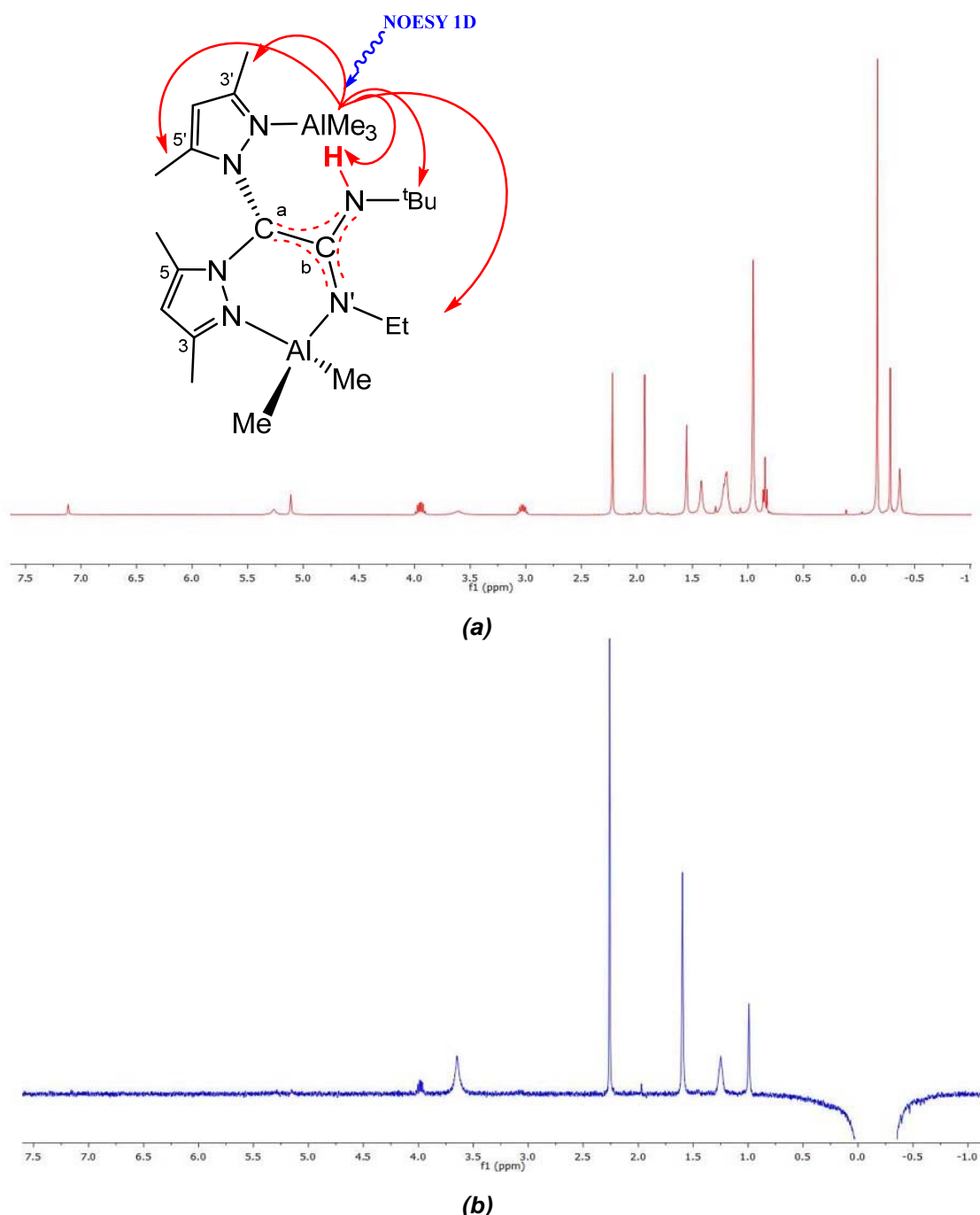


Figure S10. (a) ¹H NMR spectrum (400 MHz, 297 K, C₆D₆) of complex [AlMe₂(κ^2 -tbpamd)AlMe₃] (**3**). (b) ¹H NOESY-1D responses on irradiating the methyl groups of AlMe₃.

ELECTRONIC SUPPLEMENTARY INFORMATION

3. X-Ray Diffraction Studies: Crystallographic Structure Determination for the Complexes **1**, **3·0.5(C₅H₁₂)**, **4**, **6**, and **8·0.5(C₇H₈)**.

Details for crystallographic studies and structural refinement

Crystals suitable for X-ray diffraction were obtained for **1**, **3·0.5(C₅H₁₂)**, **4**, **6**, and **8·0.5(C₇H₈)**. The crystals were selected under oil and attached to the tip of a nylon loop. The crystals were mounted in a stream of cold nitrogen at 240–250 K and centred in the X-ray beam.

The crystal evaluation and data collection were performed on a Bruker X8 APEX II CCD-based diffractometer with MoK α ($\lambda = 0.71073 \text{ \AA}$) radiation. The initial cell constants were obtained from three series of scans at different starting angles. The reflections were successfully indexed by an automated indexing routine built in the SAINT program². The absorption correction was based on fitting a function to the empirical transmission surface as sampled by multiple equivalent measurements³. A successful solution by the direct methods⁴ provided most non-hydrogen atoms from the E-map. The remaining non-hydrogen atoms were located in an alternating series of least-squares cycles and difference Fourier maps. All non-hydrogen atoms were refined with anisotropic displacement coefficients unless specified otherwise. All hydrogen atoms were included in the structure factor calculation at idealized positions and were allowed to ride on the neighbouring atoms with relative isotropic displacement coefficients.

The compound **8** crystallized with half of a disordered molecule of toluene and compound **3** crystallized with half of a molecule of pentane. The disordered toluene was refined with soft restraints and constraints and isotropic displacement coefficients.

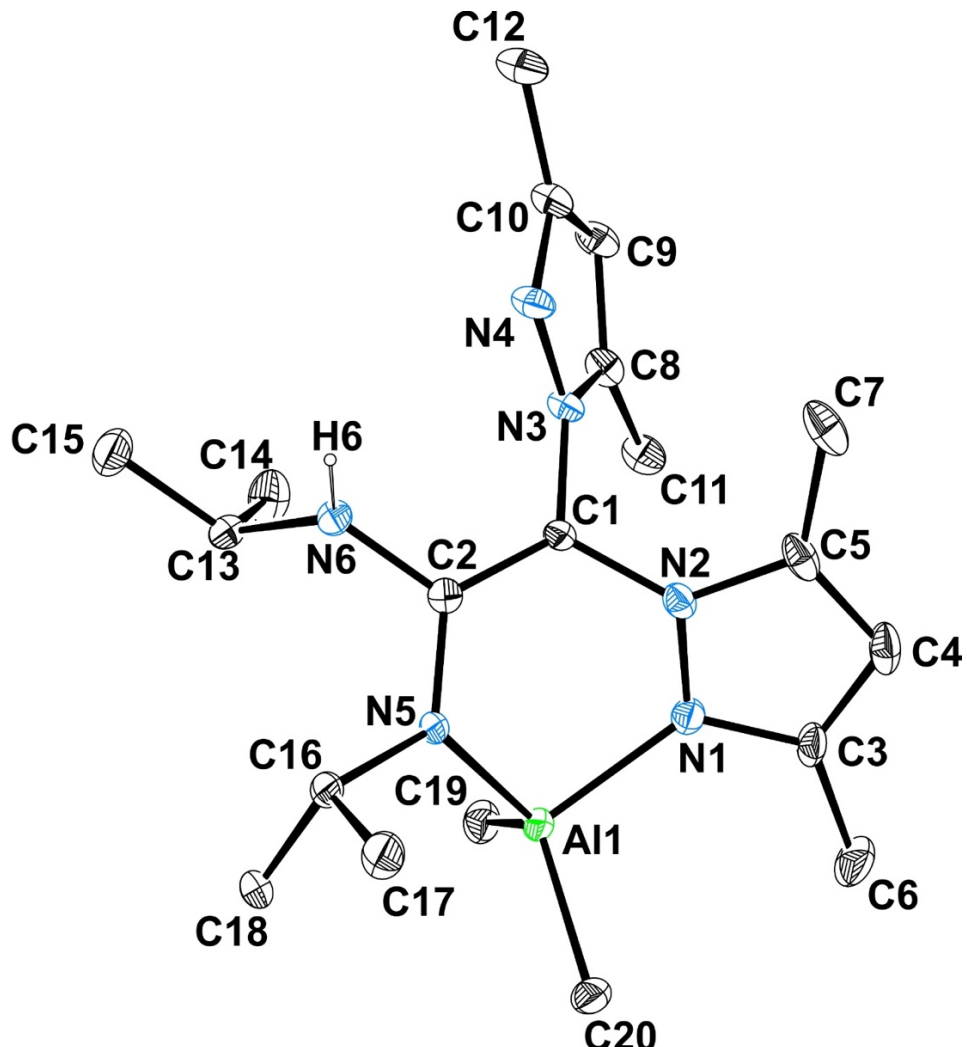


Figure S11. ORTEP view of the *P*-enantiomer of [AlMe₂(κ^2 -pbpamid)] (**1**). Hydrogen atoms have been omitted for clarity. Thermal ellipsoids are drawn at the 30 % probability level.

ELECTRONIC SUPPLEMENTARY INFORMATION

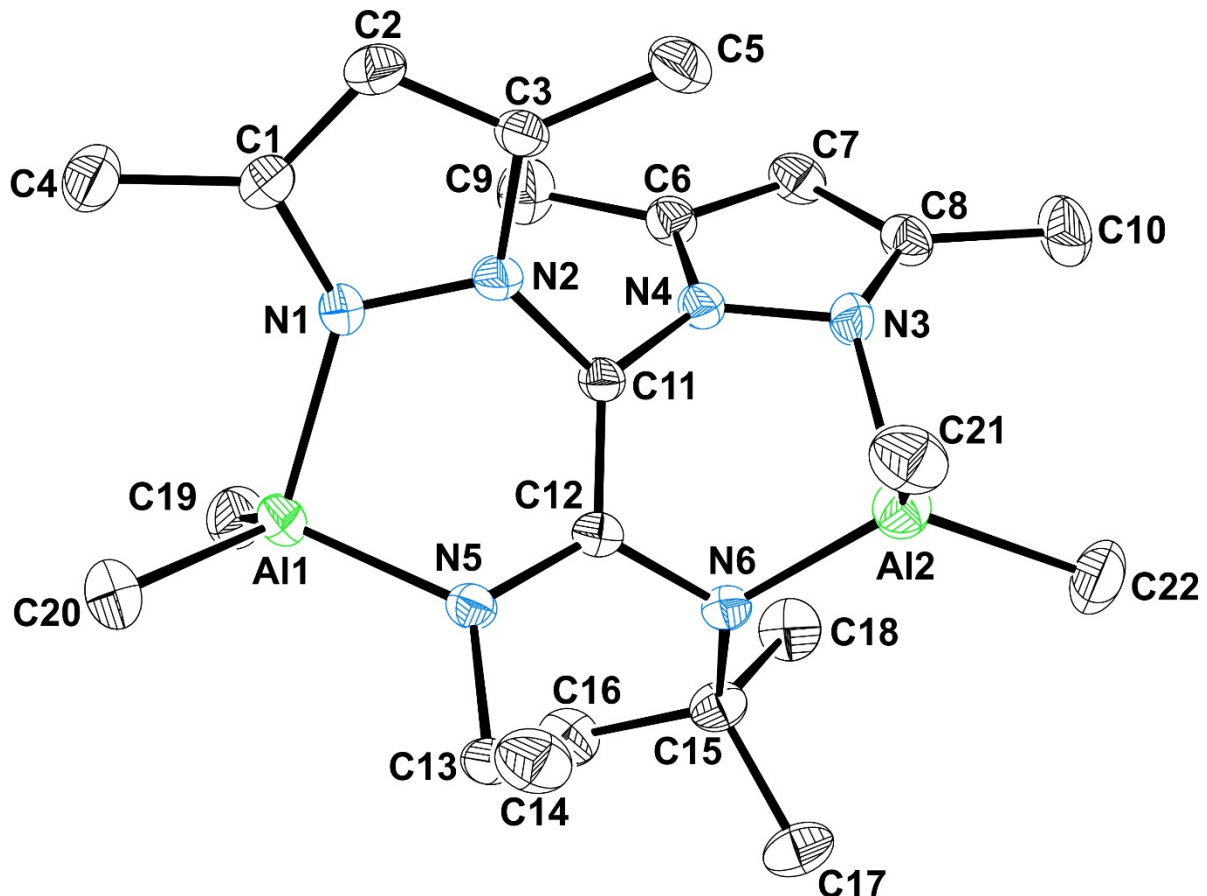


Figure S12. ORTEP view of the *M* enantiomer of $[\text{AlMe}_2(\text{tbpamd}^-)\text{AlMe}_2]$ (**6**). Hydrogen atoms have been omitted for clarity. Thermal ellipsoids are drawn at the 30 % probability level.

ELECTRONIC SUPPLEMENTARY INFORMATION

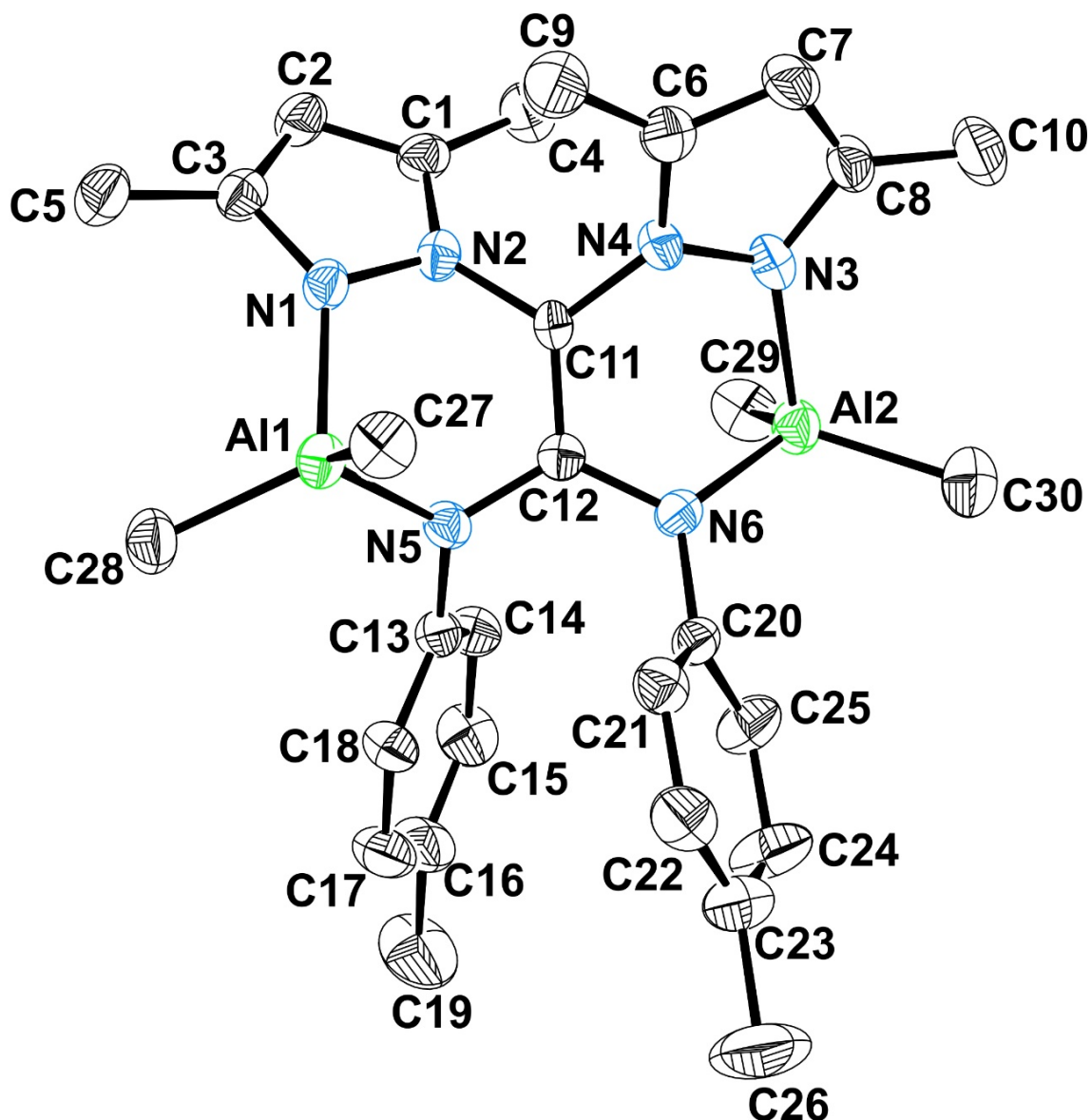
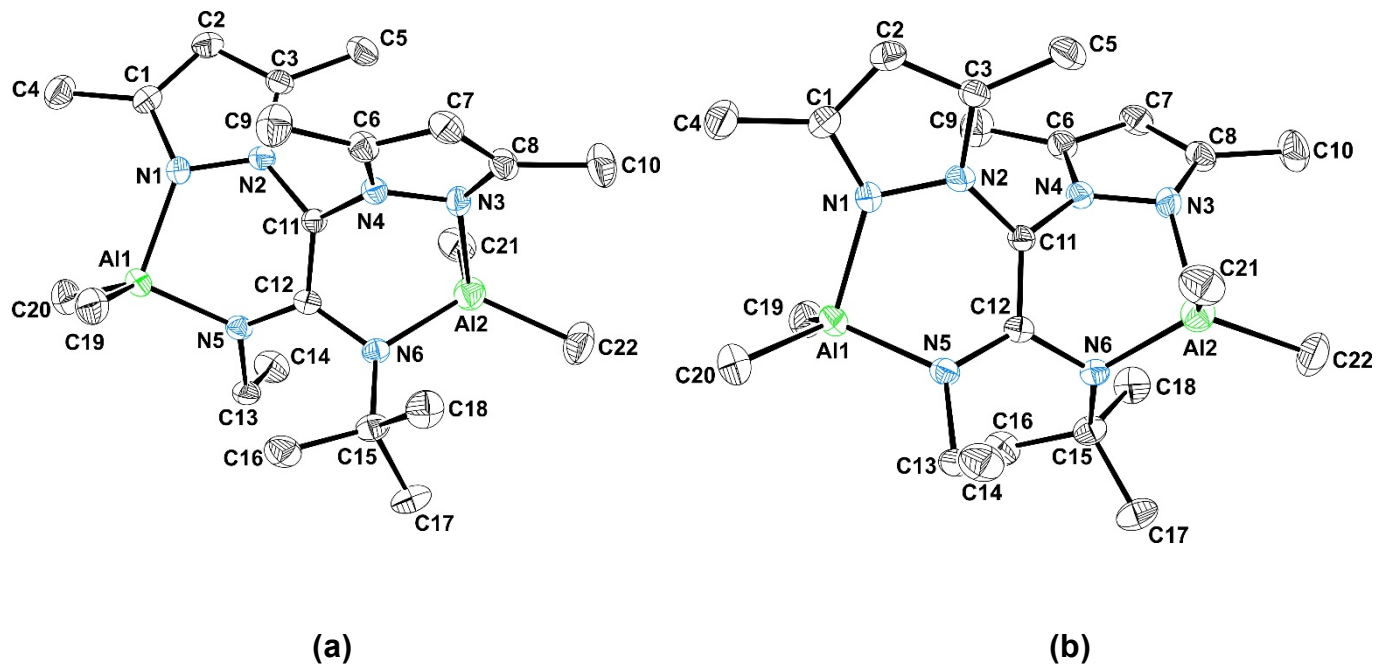


Figure S13. ORTEP view of the *P* enantiomer of $[\text{AlMe}_2(\text{phbpamd}^-)\text{AlMe}_2]$ (8). Hydrogen atoms have been omitted for clarity. Thermal ellipsoids are drawn at the 30 % probability level.

ELECTRONIC SUPPLEMENTARY INFORMATION



(a)

(b)

Figure S14a. ORTEP views of $[\text{AlMe}_2(\kappa^2\text{-tbpamd})\text{AlMe}_2]$ (**6**) for the (a) *P* enantiomer and (b) *M* enantiomer.

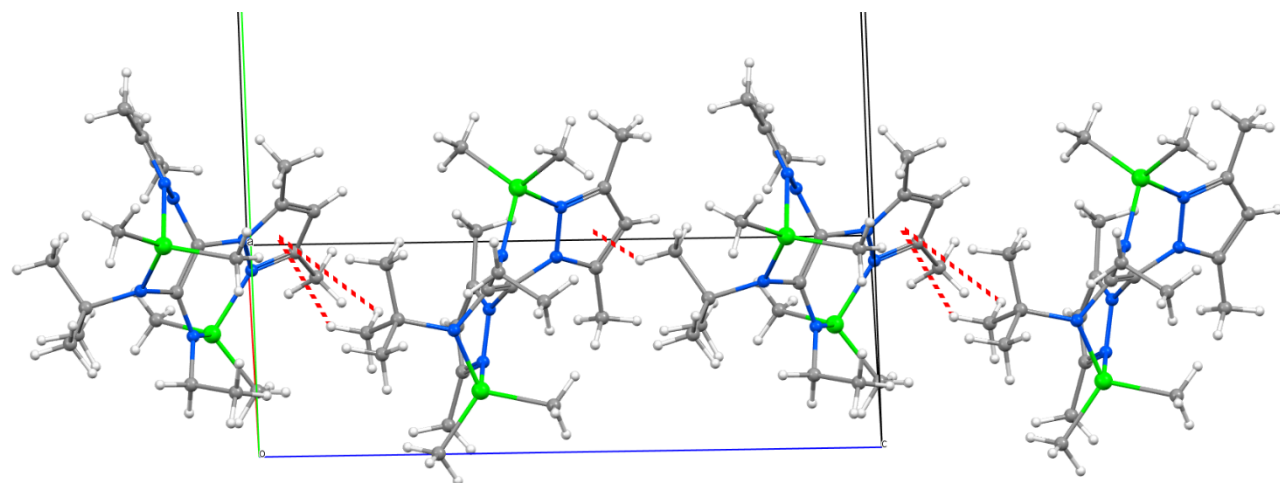


Figure S14b. Alternating disposition of both enantiomers along the *c* axis in the unit cell.

ELECTRONIC SUPPLEMENTARY INFORMATION

Table S1. Selected distances (Å) and angles (degrees) for complexes **1** and **3·0.5(C₅H₁₂)**

Distances					
1 (mole 1)		1 (mole 2)		3·0.5(C ₅ H ₁₂)	
Al(1)-N(1)	1.950(3)	Al(2)-N(11)	1.866(4)	Al(1)-N(3)	2.051(3)
Al(1)-N(5)	1.878(3)	Al(2)-C(39)	1.950(4)	Al(2)-N(1)	1.950(3)
Al(1)-C(19)	1.959(5)	Al(2)-C(40)	1.961(5)	Al(2)-N(6)	1.865(3)
Al(1)-C(20)	1.963(4)	Al(2)-N(7)	1.975(4)	Al(1)-C(25)	1.960(4)
C(1)-C(2)	1.367(5)	C(21)-C(22)	1.359(6)	Al(1)-C(26)	1.975(5)
C(1)-N(2)	1.417(5)	C(21)-N(8)	1.418(5)	Al(1)-C(27)	1.977(5)
C(1)-N(3)	1.418(5)	C(21)-N(9)	1.418(5)	Al(2)-C(23)	1.954(5)
C(2)-N(5)	1.360(5)	C(22)-N(11)	1.365(5)	Al(2)-C(24)	1.958(5)
C(2)-N(6)	1.402(5)	C(22)-N(12)	1.394(5)	N(2)-C(6)	1.431(4)
C(16)-N(5)	1.478(5)	C(36)-N(11)	1.479(5)	N(5)-C(12)	1.401(4)
				C(12)-N(6)	1.360(4)
				C(12)-C(6)	1.369(5)

Angles					
1 (mole 1)		1 (mole 2)		3·0.5(C ₅ H ₁₂)	
N(5)-Al(1)-N(1)	95.65(14)	N(11)-Al(2)-C(39)	111.26(18)	C(25)-Al(1)-C(26)	111.6(2)
N(5)-Al(1)-C(19)	114.00(18)	N(11)-Al(2)-C(40)	116.8(2)	C(25)-Al(1)-C(27)	112.5(2)
N(1)-Al(1)-C(19)	109.29(18)	C(39)-Al(2)-C(40)	114.9(2)	C(26)-Al(1)-C(27)	115.4(2)
N(5)-Al(1)-C(20)	115.24(18)	N(11)-Al(2)-N(7)	94.36(16)	C(25)-Al(1)-N(3)	111.20(17)
N(1)-Al(1)-C(20)	105.86(18)	C(39)-Al(2)-N(7)	109.81(19)	C(26)-Al(1)-N(3)	103.25(18)
C(19)-Al(1)-C(20)	114.5(2)	C(40)-Al(2)-N(7)	107.6(2)	C(27)-Al(1)-N(3)	101.97(19)
C(2)-C(1)-N(2)	123.0(3)	C(22)-C(21)-N(8)	123.4(4)	N(6)-Al(2)-N(1)	94.29(13)
C(2)-C(1)-N(3)	122.7(4)	C(22)-C(21)-N(9)	122.4(3)	N(6)-Al(2)-C(23)	112.4(2)
N(2)-C(1)-N(3)	114.0(3)	N(8)-C(21)-N(9)	114.0(3)	N(1)-Al(2)-C(23)	109.20(19)
N(5)-C(2)-C(1)	122.3(4)	C(21)-C(22)-N(11)	121.9(4)	N(6)-Al(2)-C(24)	114.6(2)
N(5)-C(2)-N(6)	119.7(3)	C(21)-C(22)-N(12)	118.7(3)	N(1)-Al(2)-C(24)	108.2(2)
C(1)-C(2)-N(6)	118.0(3)	N(11)-C(22)-N(12)	119.4(4)	C(23)-Al(2)-C(24)	115.7(3)
C(2)-N(5)-C(16)	118.6(3)	C(22)-N(11)-C(36)	117.8(3)	C(12)-C(6)-N(4)	122.4(3)
C(2)-N(5)-Al(1)	119.6(2)	C(22)-N(11)-Al(2)	114.1(3)	C(12)-C(6)-N(2)	123.7(3)
C(16)-N(5)-Al(1)	121.5(2)	C(36)-N(11)-Al(2)	127.9(3)	N(4)-C(6)-N(2)	113.0(3)
				N(6)-C(12)-C(6)	121.4(3)
				N(6)-C(12)-N(5)	120.1(3)
				C(6)-C(12)-N(5)	118.5(3)
				C(12)-N(6)-Al(2)	122.1(3)
				C(28)-N(6)-Al(2)	119.8(2)

ELECTRONIC SUPPLEMENTARY INFORMATION

Table S2. Crystal data and structure refinement for **1** and **3·0.5(C₅H₁₂)**

	1	3 · 0.5(C₅H₁₂)
Empirical formula	C ₂₀ H ₃₅ Al N ₆	C _{24.50} H ₄₇ Al ₂ N ₆
Formula weight	386.52	479.64
Temperature (K)	110(2)	240(2)
Wavelength (Å)	0.71073	0.71073
Crystal system	Orthorhombic	Triclinic
Space group	<i>P n a 2₁</i>	<i>P ̄1</i>
a(Å)	18.8949(6)	9.509(4)
b(Å)	10.1078(4)	9.662(4)
c(Å)	23.9918(7)	19.196(10)
α(°)	90	104.121(10)
β(°)	90	95.484(10)
γ(°)	90	108.221(7)
Volume(Å ³)	4582.1(3)	1596.2(13)
Z	8	2
Density (calculated) (g/cm ³)	1.121	0.998
Absorption coefficient (mm ⁻¹)	0.104	0.111
F(000)	1680	524
Crystal size (mm ³)	0.15 x 0.14 x 0.09	0.19 x 0.17 x 0.09
Index ranges	-22 ≤ h ≤ 22 -12 ≤ k ≤ 12 -28 ≤ l ≤ 23	-11 ≤ h ≤ 11 -11 ≤ k ≤ 10 -22 ≤ l ≤ 22
Reflections collected	55093	10647
Independent reflections	7935 [R(int) = 0.1100]	5524 [R(int) = 0.0443]
Data / restraints / parameters	7935 / 1 / 507	5524 / 0 / 321
Goodness-of-fit on F ²	1.003	1.009
Final R indices [I>2σ(I)]	R1 = 0.0463 wR2 = 0.0949	R1 = 0.0787 wR2 = 0.2180
Absolute structure parameter	-0.08(12)	
Largest diff. peak / hole (e.Å ⁻³)	0.316 / -0.331	0.607 / -0.353

ELECTRONIC SUPPLEMENTARY INFORMATION

Table S3. Selected distances (Å) and angles (degrees) for complexes **4**, **6** and **8 0.5(C₇H₈)**

Distances					
4	6	8 0.5(C₇H₈)			
Al(1)-N(1)	1.977(2)	Al(1)-N(1)	1.963(4)	Al(1)-N(1)	1.967(5)
Al(2)-N(3)	1.971(2)	Al(2)-N(3)	2.002(4)	Al(2)-N(3)	1.959(5)
Al(1)-N(5)	1.866(2)	Al(1)-N(5)	1.872(4)	Al(1)-N(5)	1.871(5)
Al(2)-N(6)	1.871(2)	Al(2)-N(6)	1.888(4)	Al(2)-N(6)	1.873(5)
Al(1)-C(19)	1.956(2)	Al(1)-C(19)	1.953(6)	Al(1)-C(27)	1.954(6)
Al(1)-C(20)	1.959(2)	Al(1)-C(20)	1.954(6)	Al(1)-C(28)	1.935(6)
Al(2)-C(21)	1.974(3)	Al(2)-C(21)	2.009(6)	Al(2)-C(29)	1.944(6)
Al(2)-C(22)	1.974(3)	Al(2)-C(22)	1.968(6)	Al(2)-C(30)	1.960(7)
N(5)-C(12)	1.376(2)	N(5)-C(12)	1.364(6)	C(12)-N(5)	1.389(6)
N(5)-C(13)	1.474(2)	N(5)-C(13)	1.472(6)	C(13)-N(5)	1.404(6)
N(6)-C(12)	1.379(2)	N(6)-C(12)	1.394(6)	C(12)-N(6)	1.374(6)
N(6)-C(16)	1.475(3)	N(6)-C(15)	1.521(6)	C(20)-N(6)	1.416(7)
C(11)-C(12)	1.378(2)	C(11)-C(12)	1.377(6)	C(11)-C(12)	1.377(7)
Angles					
4	6	8 0.5(C₇H₈)			
N(5)-Al(1)-N(1)	94.62(7)	N(5)-Al(1)-N(1)	94.9(2)	N(5)-Al(1)-N(1)	94.1(2)
C(19)-Al(1)-C(20)	115.6(1)	C(19)-Al(1)-C(20)	115.8(3)	C(28)-Al(1)-C(27)	116.7(3)
N(6)-Al(2)-N(3)	95.36(7)	N(6)-Al(2)-N(3)	94.8(2)	N(6)-Al(2)-N(3)	94.5(2)
C(22)-Al(2)-C(21)	115.7(2)	C(22)-Al(2)-C(21)	111.7(3)	N(6)-Al(2)-C(29)	113.8(3)
C(12)-N(5)-Al(1)	113.9(1)	C(12)-N(5)-Al(1)	119.0(3)	C(12)-N(5)-Al(1)	115.1(3)
C(12)-N(6)-Al(2)	114.8(1)	C(12)-N(6)-Al(2)	110.1(3)	C(12)-N(6)-Al(2)	118.0(4)
C(12)-C(11)-N(4)	123.9(2)	C(12)-C(11)-N(4)	122.0(4)	C(12)-C(11)-N(4)	122.9(5)
C(12)-C(11)-N(2)	122.8(2)	C(12)-C(11)-N(2)	124.8(4)	C(12)-C(11)-N(2)	123.5(5)
N(4)-C(11)-N(2)	113.3(1)	N(4)-C(11)-N(2)	113.0(4)	N(4)-C(11)-N(2)	113.6(4)
N(5)-C(12)-C(11)	117.8(2)	N(5)-C(12)-C(11)	119.4(4)	N(6)-C(12)-C(11)	119.3(5)
N(5)-C(12)-N(6)	123.7(2)	N(5)-C(12)-N(6)	124.2(4)	N(6)-C(12)-N(5)	123.7(5)
C(11)-C(12)-N(6)	118.4(2)	C(11)-C(12)-N(6)	116.3(4)	C(11)-C(12)-N(5)	117.0(5)

ELECTRONIC SUPPLEMENTARY INFORMATION

Table S4. Crystal data and structure refinement for **4**, **6** and **8·0.5(C₇H₈)**

	4	6	8·0.5(C₇H₈)
Empirical formula	C ₂₂ H ₄₀ Al ₂ N ₆	C ₂₂ H ₄₀ Al ₂ N ₆	C _{33.5} H ₄₄ Al ₂ N ₆
Formula weight	442.56	442.56	584.70
Temperature (K)	250(2)	250(2)	240(2)
Wavelength (Å)	0.71073	0.71073	0.71073
Crystal system	Monoclinic	Monoclinic	Monoclinic
Space group	<i>P</i> 2 ₁ /c	<i>P</i> 2 ₁ /c	<i>P</i> 2 ₁ /c
a(Å)	17.326(2)	8.970(3)	18.637(3)
b(Å)	9.3088(11)	17.914(5)	9.3840(19)
c(Å)	19.085(2)	16.198(5)	26.354(4)
α(°)	90	90	90
β(°)	116.679(5)	92.816(15)	125.3250(12)
γ(°)	90	90	90
Volume(Å ³)	2750.5(6)	2599.9(13)	3760.4(12)
Z	4	4	4
Density (calculated) (g/cm ³)	1.069	1.131	1.033
Absorption coefficient (mm ⁻¹)	0.124	0.131	0.105
F(000)	960	960	1252
Crystal size (mm ³)	0.22 x 0.19 x 0.12	0.26 x 0.19 x 0.12	0.18 x 0.16 x 0.11
Index ranges	-21 ≤ h ≤ 24 -8 ≤ k ≤ 13 -26 ≤ l ≤ 27	-10 ≤ h ≤ 9 -21 ≤ k ≤ 16 -18 ≤ l ≤ 19	-22 ≤ h ≤ 16 -11 ≤ k ≤ 10 -31 ≤ l ≤ 30
Reflections collected	22833	13354	17044
Independent reflections	8244	4578	6577
	[R(int) = 0.0691]	[R(int) = 0.0824]	[R(int) = 0.1102]
Data / restraints / parameters	8244 / 0 / 283	4578 / 0 / 283	6577 / 78 / 412
Goodness-of-fit on F ²	0.963	1.028	0.983
Final R indices [I>2σ(I)]	R1 = 0.0578 wR2 = 0.1251	R1 = 0.0773 wR2 = 0.2020	R1 = 0.0827 wR2 = 0.2149
Largest diff. peak/hole (e.Å ⁻³)	0.176 / -0.247	1.155 / -0.558	0.635 / -0.226

ELECTRONIC SUPPLEMENTARY INFORMATION

4. Experimental details for cyclic carbonates

General procedures for catalytic tests.

General procedure for catalyst screening at 1 bar pressure

Styrene oxide **10a** (1.66 mmol) and complexes **1–9** (83.0 µmol) were placed in a sample vial fitted with a magnetic stirrer bar and placed in a large conical flask. Cardice pellets were added to the conical flask, which was fitted with a rubber stopper pierced by a deflated balloon. The reaction mixture was stirred at 25 °C for 18 h, then the conversion of styrene oxide **10a** to styrene carbonate **11a** was determined by analysis of a sample by ¹H-NMR spectroscopy.

General procedure for the synthesis of cyclic carbonates **11a–j** at 1 bar pressure

An epoxide **11a–j** (1.66 mmol), catalyst **4** (36.8 mg, 83.0 µmol) and TBAB (27 mg, 83.0 µmol) were placed in a sample vial fitted with a magnetic stirrer bar and placed in a large conical flask. Cardice pellets were added to the conical flask which was fitted with a rubber stopper pierced by a deflated balloon. The reaction mixture was stirred for 18 h at the temperature of interest. The conversion of epoxide into cyclic carbonate was then determined by analysis of a sample by ¹H-NMR spectroscopy. The remaining sample was filtered through a plug of silica, eluting with CH₂Cl₂ to remove the catalyst. The eluent was evaporated *in vacuo* to give either the pure cyclic carbonate or a mixture of cyclic carbonate and unreacted epoxide. In the latter case, the mixture was purified by flash chromatography using a solvent gradient as follows: hexane, hexane-EtOAc (9:1), hexane-EtOAc (6:1), hexane-EtOAc (3:1) and finally EtOAc to give the pure cyclic carbonate. Cyclic carbonates **11a–j** are all known compounds and the spectroscopic data for samples prepared using catalyst **4** were consistent with those reported in the literature.^{5,6}

General procedure for the synthesis of cyclic carbonates **11a–j** and **13a–f** at 10 bar pressure

An epoxide **11a–j** or **13a–f** (12–2.4 mmol), catalyst **4** (26.6 mg, 60.2 µmol) and TBAB (20 mg, 60.2 µmol) were placed in stainless steel reactor with a magnetic stirrer bar. The reactor was pressurized to 10 bar of carbon dioxide and the reaction mixture was stirred at 50–70 °C for 8–18 h. After that, the reactor have been cooled down to ambient temperature and depressurized, and the conversion of epoxide into cyclic carbonate **11a–j** or **13a–f** was determined by analysis of a sample by ¹H-NMR spectroscopy. The remaining sample was filtered through a plug of silica, eluting with CH₂Cl₂ to remove the catalyst. The eluent was evaporated *under vacuum* to give either the pure cyclic carbonate or a mixture of cyclic carbonate and unreacted epoxide. In the latter case, the mixture was purified by flash chromatography using a solvent gradient as follows: hexane, hexane-EtOAc (9:1), hexane-EtOAc (6:1), hexane-EtOAc (3:1) and finally EtOAc to give the pure cyclic carbonate. Cyclic carbonates **11a–j** and **13a–f** are all known compounds and the spectroscopic data for samples prepared using catalyst **4** were consistent with those reported in the literature.^{5,6}

General procedure for the synthesis of cyclic carbonate **15**

Previously, (*R*)-Limonene oxide (*cis* and *trans* mixture) and pure *trans*-(*R*)-limonene oxide⁷ were each distilled from calcium hydride under vacuum and stored under nitrogen whilst co-catalyst PPNCI (PPNCI = bis(triphenylphosphoranylidene)ammonium chloride) was recrystallized in a 3:1 dichloromethane/toluene mixture. Stainless-steel reactor was dried under vacuum at 80 °C for 18 hours.

In a representative experiment, 0.929 g of (*R*)-Limonene oxide (*cis/trans* mixture or solely *trans*) (1 mL, 6.10 mmol), catalyst **4** (27 mg, 61 µmol) and PPNCI (105 mg, 183 µmol) were placed in the dried stainless-steel reactor with a magnetic stirrer bar. The reactor was pressurized to 10 bar of carbon dioxide and the reaction mixture was stirred at 70 °C for 66 h. After that, the reactor has been cooled down to ambient temperature and depressurized, and the conversion of epoxide into cyclic carbonate **15** was determined by analysis of a sample by ¹H-NMR spectroscopy. The remaining sample was filtered through a plug of silica, eluting with CH₂Cl₂ to remove the catalyst. The eluent was evaporated *under vacuum* and later purified by flash chromatography using a

ELECTRONIC SUPPLEMENTARY INFORMATION

solvent gradient as follows: hexane, hexane-EtOAc (9:1), hexane-EtOAc (6:1), hexane-EtOAc (3:1) and finally EtOAc to give the pure cyclic carbonate. Cyclic carbonate **15** is a known compound and the spectroscopic data for samples prepared using catalyst **4** were consistent with those reported in the literature.⁸

¹H and ¹³C-{¹H} NMR spectroscopic data of compounds **11a-j**, **13a-f** and **15**

Styrene carbonate (11a**)**. Isolated in 86 % yield as a white solid (1.78 g, 90 %). ¹H NMR (CDCl₃, 298 K) δ 7.45-7.33 (m, 5H, Ar-H), ¹³C {¹H} (CDCl₃, 298 K) δ 154.8 (C=O), 135.7 (C^{ipso}), 129.7, 129.2, 125.8 (Ph), 78.0 (PhCHO), 71.1 (OCH₂).

1,2-hexylene carbonate (11b**)**. Isolated in 90 % yield as a colourless liquid (1.65 g, 95 %). ¹H NMR (CDCl₃, 298 K) δ 4.68 (m, 1 H, OCH), 4.51 (m, 1 H, OCH₂), 4.05 (m, 1 H, OCH₂), 1.73 (m, 2 H, CH₂), 1.40 (m, 4 H, CH₂), 0.91 [t, 3 H, ³J_{H-H} = 8 Hz, CH₃]. ¹³C {¹H} (CDCl₃, 298 K) δ 155.1 (C=O), 77.0 (OCH), 69.4 (OCH₂), 33.6, 26.4, 22.2 (-CH₂-), 13.8 (CH₃).

1,2-decylene carbonate (11c**)**. Isolated in 96 % yield as a colourless liquid (1.20 g, 100 %). ¹H NMR (CDCl₃, 298 K) δ 4.68 (m, 1 H, OCH), 4.50 (m, 1 H, OCH₂), 4.04 (m, 1 H, OCH₂), 1.71 (m, 2 H, CH₂), 1.37 (m, 12 H, CH₂), 0.86 [t, 3 H, ³J_{H-H} = 8 Hz, CH₃]. ¹³C {¹H} (CDCl₃, 298 K) δ 155.1 (C=O), 77.0 (OCH), 69.4 (OCH₂), 33.9, 31.8, 29.3, 29.2, 29.1, 24.3, 22.6 (-CH₂-), 14.1 (CH₃).

1,2-dodecene carbonate (11d**)**. Isolated in 67 % yield as a colourless liquid (0.96 g, 70 %). ¹H NMR (CDCl₃, 298 K) δ 4.68 (m, 1 H, OCH), 4.50 (m, 1 H, OCH₂), 4.04 (m, 1 H, OCH₂), 1.72 (m, 2 H, -CH₂-), 1.23 (m, 16 H, -CH₂-), 0.85 [t, 3 H, ³J_{H-H} = 8 Hz, CH₃]. ¹³C {¹H} (CDCl₃, 298 K) δ 155.1 (C=O), 77.0 (OCH), 69.4 (OCH₂), 33.9, 31.9, 29.5, 29.4, 29.3, 29.2, 29.1, 24.3, 22.6 (-CH₂-), 14.1 (CH₃).

3-chloropropylene carbonate (11e**)**. Isolated in 90 % yield as a colourless liquid (1.55 g, 95 %). ¹H NMR (CDCl₃, 298 K) δ 4.94 (m, 1 H, OCH), 4.57 (m, 1 H, OCH₂), 4.40 (dd, 1 H, ³J_{H-H} = 9 Hz, 8.7 Hz, OCH₂), 3.73 (m, 2 H, CH₂Cl). ¹³C {¹H} (CDCl₃, 298 K) δ 154.1 (C=O), 74.16 (OCH), 66.9 (OCH₂), 43.5 (CH₂Cl).

Glycerol carbonate (11f**)**. Isolated in 89 % yield as a colourless liquid (1.33 g, 94 %). ¹H NMR (CDCl₃, 298 K) δ 4.80 (m, 1 H, OCH), 4.49 (m, 2 H, OCH₂), 3.99 (m, 1 H, CH₂OH), 3.71 (m, 1 H, CH₂OH), 2.59 (m, 1 H, OH). ¹³C {¹H} (CDCl₃, 298 K) δ 155.2 (C=O), 76.5 (OCH), 65.7 (OCH₂), 61.6 (CH₂OH).

3-phenoxypropylene carbonate (11g**)**. Isolated in 80 % yield as a white solid (1.98 g, 85 %). ¹H NMR (CDCl₃, 298 K) δ 7.29 (m, 2 H, Ar-H), 7.00 (m, 1 H, Ar-H), 6.89 (m, 2 H, Ar-H), 5.01 (m, 1 H, OCH), 4.60 (m, 1 H, PhOCH₂), 4.52 (m, 1 H, PhOCH₂), 4.22 (dd, 1 H, ³J_{H-H} = 10.6 Hz, 4.2 Hz, OCH₂), 4.12 (dd, 1 H, ³J_{H-H} = 12 Hz, 4 Hz, OCH₂). ¹³C {¹H} (CDCl₃, 298 K) δ 157.7 (OPh^{ipso}), 154.7 (OCOO), 129.7, 121.9, 114.5 (Ph), 74.1 (CH₂OPh), 66.8 (OCH), 66.2 (-CH₂O).

3-vinyloxypropylene carbonate (11h**)**. Isolated in 87 % as a white solid (0.89 g, 94 %). ¹H NMR (CDCl₃, 298 K) δ 5.85 (m, 1 H, -CH=CH₂), 5.23 (m, 2 H, CH₂=CH-), 4.80 (m, 1 H, OCH), 4.48 (m, 1 H, OCH₂), 4.38 (m, 1 H, OCH₂), 4.03 (m, 2 H, =CH-CH₂O), 3.67 (dd, 1 H, ³J_{H-H} = 10.6 Hz, 4 Hz, CH₂O-Allyl), 3.59 (dd, 1 H, ³J_{H-H} = 10.6 Hz, 4 Hz, CH₂O-Allyl). ¹³C {¹H} (CDCl₃, 298 K) δ 154.9 (C=O), 133.6, 118.0 (C=C), 74.9 (OCH), 72.6 (=CH-CH₂O), 68.8 (OCH₂), 66.2 (CH₂O-Allyl).

4-bromostyrene carbonate (11i**)**. Isolated in 94 % yield as a white solid (1.46 g, 100 %). ¹H NMR (CDCl₃, 298 K) δ 7.57 (dd, 2 H, ³J_{H-H} = 8.4 Hz, Ar-H), 7.23 (dd, 2 H, ³J_{H-H} = 8.4 Hz, Ar-H), 5.62 (m, 1 H, OCH), 4.78 (m, 1 H, OCH₂), 4.28 (m, 1 H, OCH₂). ¹³C {¹H} (CDCl₃, 298 K) δ 154.5 (C=O), 134.8 (C^{ipso}), 132.5, 127.4, 123.9 (Ph), 77.2 (OCH), 70.9 (OCH₂).

4,4'-(butane-1,4-diylbis(oxy))bis(methylene))bis(1,3-dioxolan-2-one) (11j**)**. Isolated in 70 % yield as a colourless liquid (0.66 g, 75 %). ¹H NMR (CDCl₃, 298 K) δ 4.80 (m, 2 H, OCH), 4.49 (m, 2 H, OCH₂), 4.39 (m, 2 H, OCH₂), 3.68 (dd, 2 H, ³J_{H-H} = 12 Hz, 4 Hz, CH₂O-R), 3.58 (dd, 2 H, J_{H-H} = 12 Hz, 4 Hz, CH₂O-R), 3.52 (m, 4 H, -CH₂O-CH₂-), 1.63 (m, 4 H, -CH₂-CH₂-). ¹³C {¹H} (CDCl₃, 298 K) δ 155.1 (C=O), 75.2 (OCH), 71.6 (OCH₂), 69.6 (CH₂O-R), 66.2 (-CH₂O-CH₂), 26.0 (-CH₂-).

Cis-1,2-cyclohexene carbonate (13a**)**. Isolated in 65 % yield as a white solid (0.39 g, 91 %). ¹H NMR (CDCl₃, 298 K) δ 4.65 (m, 2 H, OCH), 1.86 (m, 4 H, CH₂), 1.58 (m, 4 H, CH₂), 1.39 (m, 4 H, CH₂). ¹³C {¹H} (CDCl₃, 298 K) δ 155.3 (C=O), 75.7 (OCH), 26.7 (CH₂), 19.1 (CH₂).

ELECTRONIC SUPPLEMENTARY INFORMATION

Cis-1,2-cyclopentene carbonate (13b). Isolated in 68 % yield as a white solid (0.26 g, 83 %). ^1H NMR (CDCl_3 , 298 K) δ 5.09 (m, 2 H, OCH), 2.13 (m, 2 H, CH_2), 1.72 (m, 4 H, CH_2). ^{13}C { ^1H } (CDCl_3 , 298 K) δ 155.5 ($\text{C}=\text{O}$), 81.8 (OCH), 33.2 (CH_2), 21.5 (CH).

4-(furan-2-ylmethoxy)-1,3-dioxolan-2-one (13c). Isolated in 81 % yield as an orange liquid (4.38 g, 92%). ^1H NMR (CDCl_3 , 298 K) δ 7.40 (m, 1 H, $\text{OCH}=\text{CH}$), 6.33 (m, 2 H, $\text{CH}=\text{CH}$), 4.76 (m, 1 H, OCH), 4.42 (m, 4 H, OCH_2), 3.64 (m, 2 H, CH_2). ^{13}C { ^1H } (CDCl_3 , 298 K) δ 154.8 ($\text{C}=\text{O}$), 150.6 ($\text{O}=\text{C}(\text{=CHR})\text{CH}_2$), 143.7 ($\text{OCH}=\text{CHR}$), 110.4, 110.1 ($\text{RHC}-\text{CH}_2\text{R}$), 74.8 (OCH_2), 68.4 (OCH_2CHOR) 66.3 ($\text{C}_4\text{H}_3\text{O}-\text{CH}_2$) 65.3 (OCH_2).

bis((2-oxo-1,3-dioxolan-4-yl)methyl) fumarate (13d). Isolated in 99 % yield as a white solid (1.71 g, 100 %). ^1H NMR (DMSO-d^6 , 298 K) δ 6.81 (m, 2 H, $-\text{CH}=\text{CH}-$), 5.08 (m, 2 H, OCH), 4.57 (m, 4 H, OCH_2), 4.44 (m, 4 H, OCH_2), 4.34 (m, 4 H, $-\text{CH}_2-$). ^{13}C { ^1H } (DMSO-d^6 , 298 K) δ 163.2 ($\text{O}=\text{CO}$), 154.2 ($\text{O}=\text{COO}$), 132.6 ($-\text{CH}=\text{CH}-$), 73.6 (OCH), 65.5 (OCH_2), 64.0 ($-\text{CH}_2-$).

bis((2-oxo-1,3-dioxolan-4-yl)methyl) succinate (13e). Isolated in 99 % yield as a white solid (1.72 g, 100 %). ^1H NMR (DMSO-d^6 , 298 K) δ 5.02 (m, 2 H, OCH), 4.56 (m, 4 H, OCH_2), 4.28 (m, 4 H, OCH_2), 4.27 (m, 8 H, OCH_2), 2.61 (m, 4 H, COCH_2-). ^{13}C { ^1H } (DMSO-d^6 , 298 K) δ 171.1 ($\text{O}=\text{CO}$), 154.2 ($\text{O}=\text{COO}$), 73.7 (OCH), 65.5 (OCH_2), 63.1 (COCH_2-), 27.9 ($-\text{CH}_2-$).

bis((2-oxo-1,3-dioxolan-4-yl)methyl) glutarate (13f). Isolated in 99 % yield as a white solid (1.79 g, 100 %). ^1H NMR (DMSO-d^6 , 298 K) δ 5.03 (m, 2 H, OCH), 4.40 (m, 8 H, OCH_2), 2.40 (m, 4 H, COCH_2), 1.77 (m, 2 H, COCH_2CH_2). ^{13}C { ^1H } (CDCl_3 , 298 K) δ 172.3 ($\text{O}=\text{CO}$), 154.9 ($\text{O}=\text{COO}$), 74.5 (OCH), 66.2 (OCH_2), 63.6 ($-\text{CH}_2\text{OC(O)-}$), 32.5 ($-\text{O}=\text{C(O)CH}_2-$), 19.9 ($-\text{CH}_2-$).

trans-(R)- -(+)-Limonene carbonate (15). Isolated in 76 % yield from *trans*-(*R*)-(+)Limonene oxide as a colourless oil (0.95 g, 79 %). ^1H NMR (CDCl_3 , 298 K) δ 4.69 (m, 1 H, $\text{MeC}=\text{CH}_2$), 4.66 (m, 1 H, $\text{MeC}=\text{CH}_2$), 4.33 (dd, $^3\text{J}_{\text{HH}}=9.6$ Hz and 7.0 Hz, 1 H, OCH), 2.36-2.21 (m, 2 H, $-\text{CH}_2-$), 1.87 (tt, $^3\text{J}_{\text{HH}}=12.0$ Hz and 3.2 Hz, CH), 1.65 (s, 3 H, $-\text{C(Me)}=\text{CH}_2$), 1.64-1.55 (m, 2 H, $-\text{CH}_2-$), 1.40 (s, 3 H, $-\text{CO(Me)}$), 1.38-1.31 (m, 2 H, $-\text{CH}_2-$). ^{13}C { ^1H } (CDCl_3 , 298 K) δ 154.9 ($\text{O}=\text{COO}$), 147.4 ($-\text{C(Me)}=\text{CH}_2$), 110.3 ($-\text{C(Me)}=\text{CH}_2$), 82.2 ($-\text{C(O)Me}$), 80.7 ($-\text{CO}$), 40.1 ($\text{C-C(Me)}(=\text{CH}_2)$), 34.1, 33.2, 25.8 ($-\text{CH}_2-$), 26.3 ($-\text{CO(Me)}$), 20.7 ($\text{C-C(Me)}(=\text{CH}_2)$).

ELECTRONIC SUPPLEMENTARY INFORMATION

Figures S15–S24. ^1H and ^{13}C - $\{^1\text{H}\}$ NMR spectra of compounds **11a-j** and **13a-f**

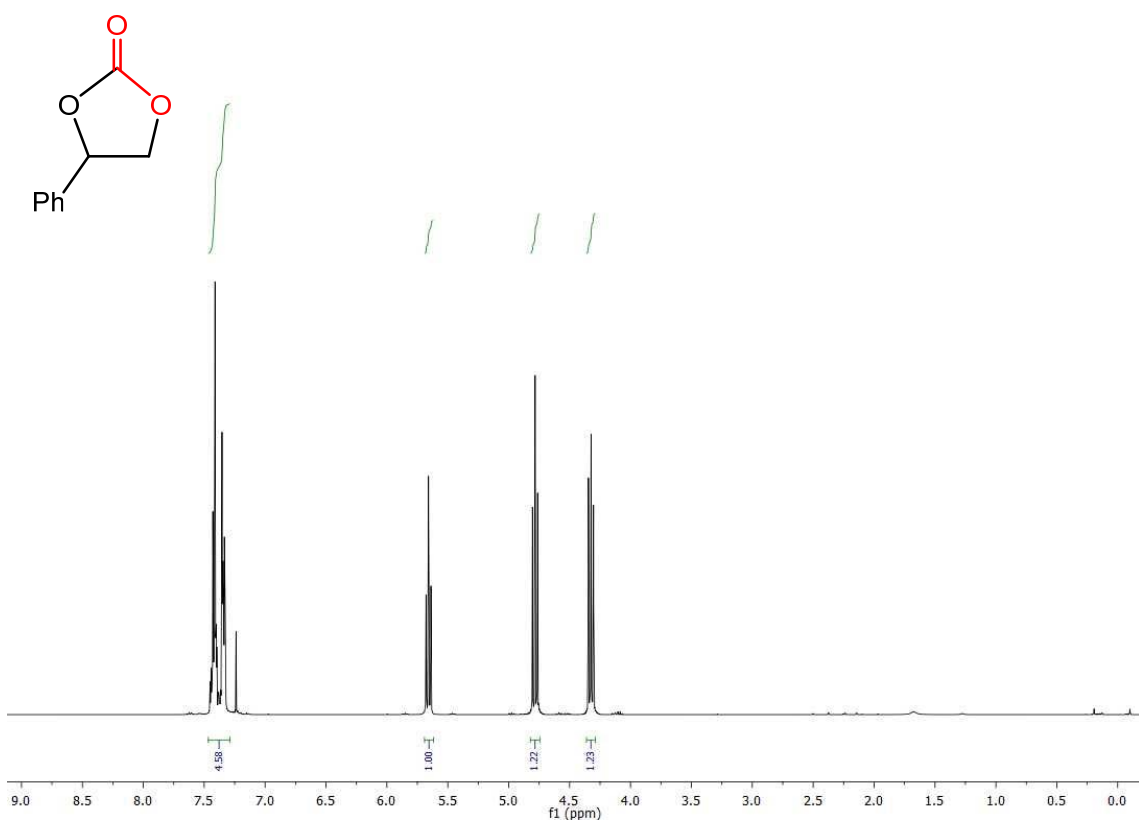


Figure S15a. ^1H NMR spectrum (400 MHz, 297 K, CDCl_3) for styrene carbonate **11a**.

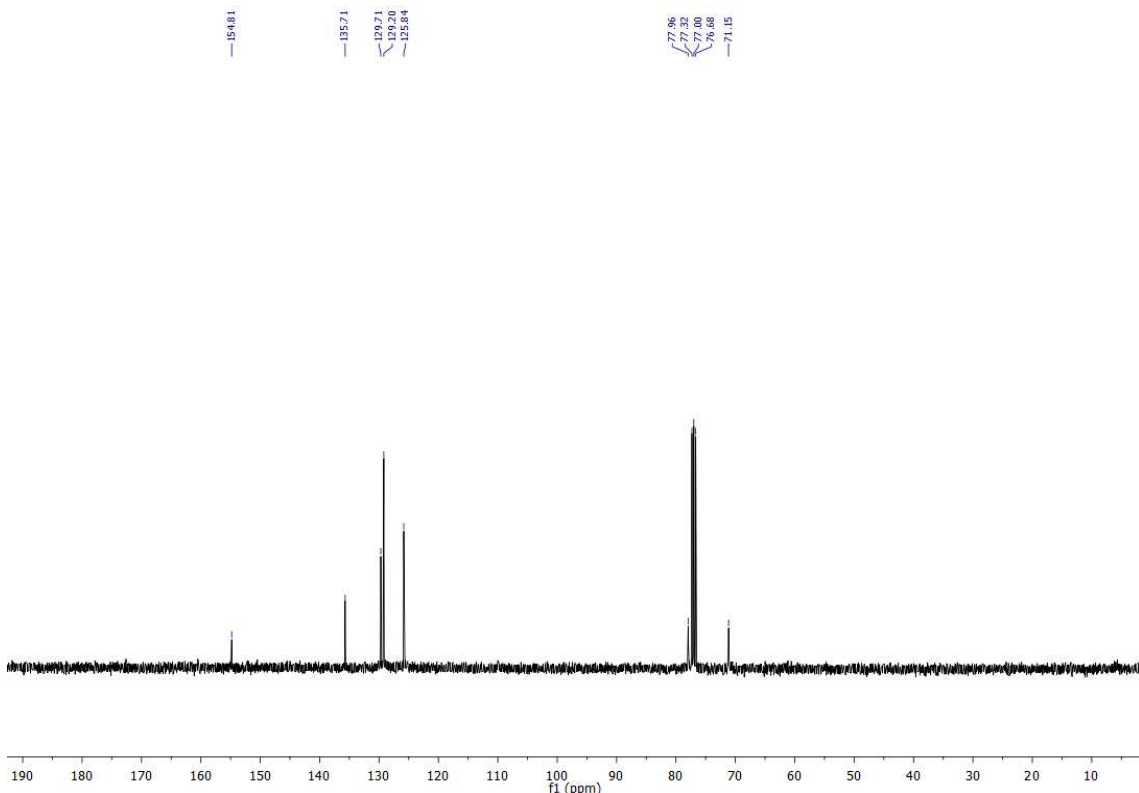


Figure S15b. ^{13}C - $\{^1\text{H}\}$ -NMR spectrum (400 MHz, 297 K, CDCl_3) for styrene carbonate **11a**.

ELECTRONIC SUPPLEMENTARY INFORMATION

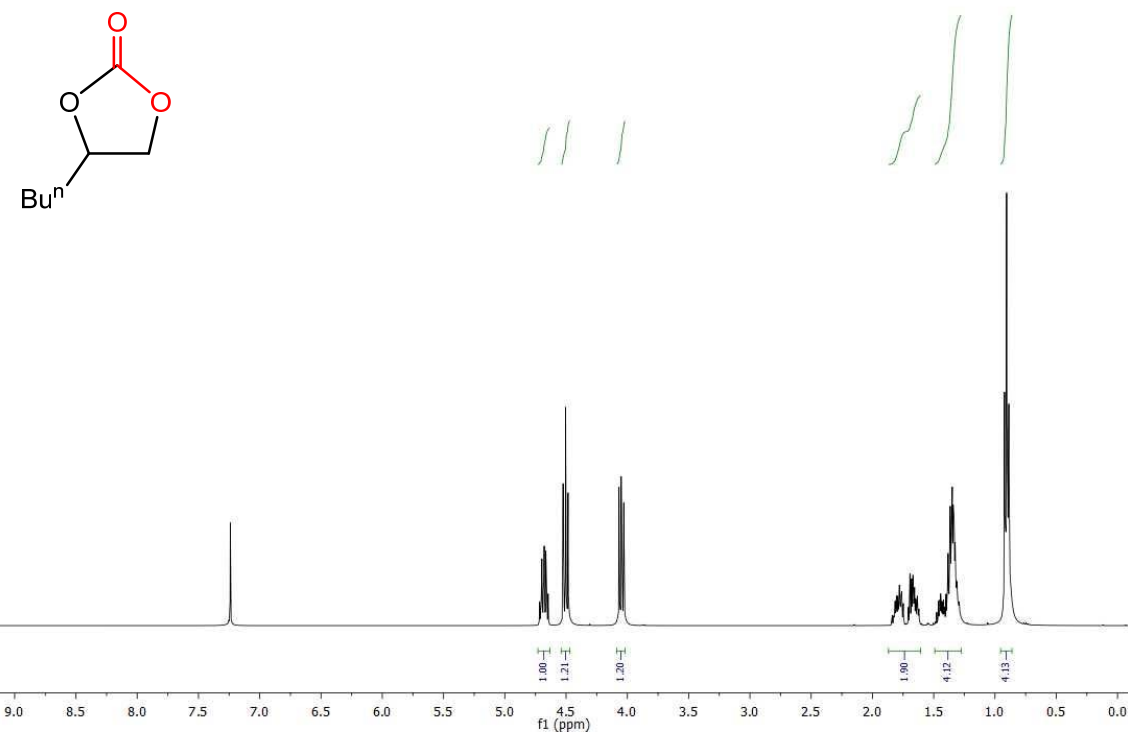


Figure S16a. ^1H NMR spectrum (400 MHz, 297 K, CDCl_3) for 1,2-hexylene carbonate **11b**.

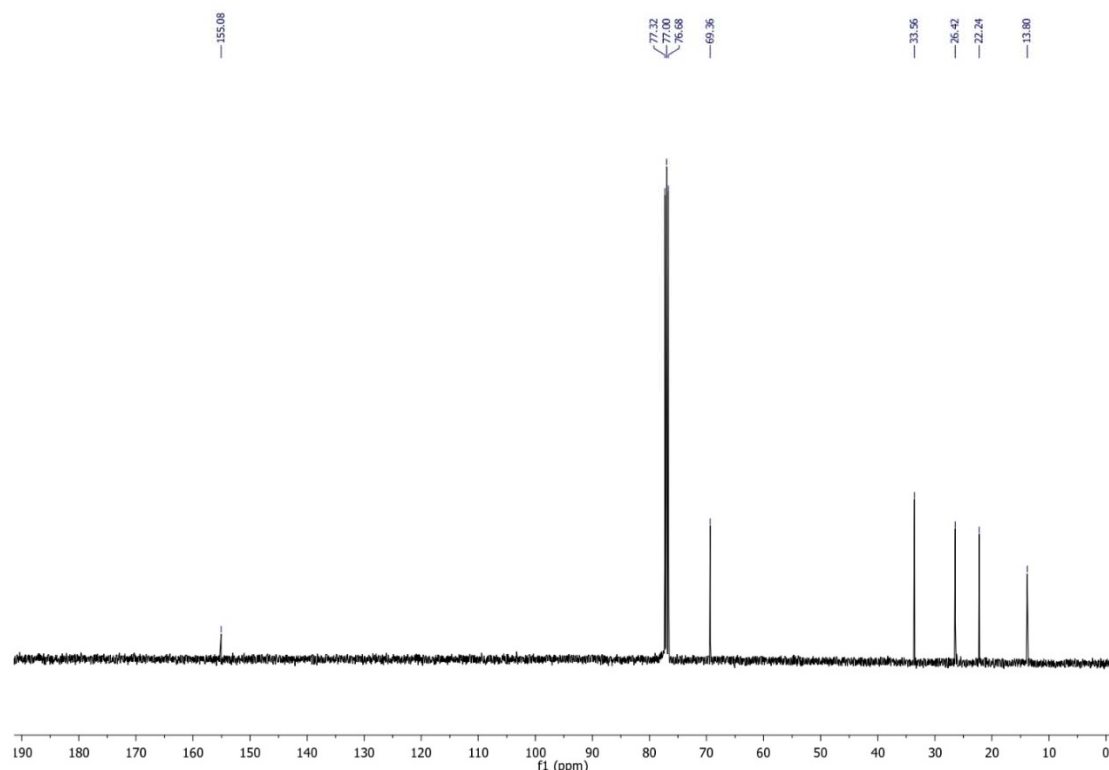


Figure S16b. ^{13}C - $\{{}^1\text{H}\}$ -NMR spectrum (400 MHz, 297 K, CDCl_3) for 1,2-hexylene carbonate **11b**.

ELECTRONIC SUPPLEMENTARY INFORMATION

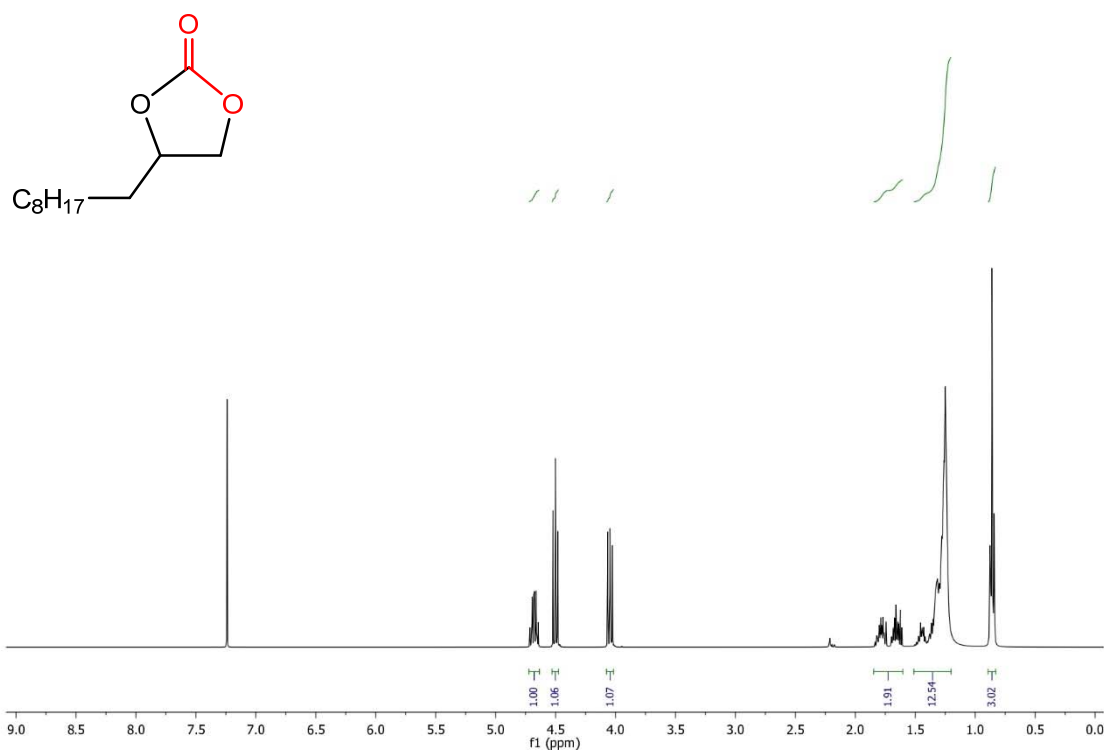


Figure S17a. ¹HNMR spectrum (400 MHz, 297 K, CDCl₃) for 1,2-decylene carbonate **11c**.

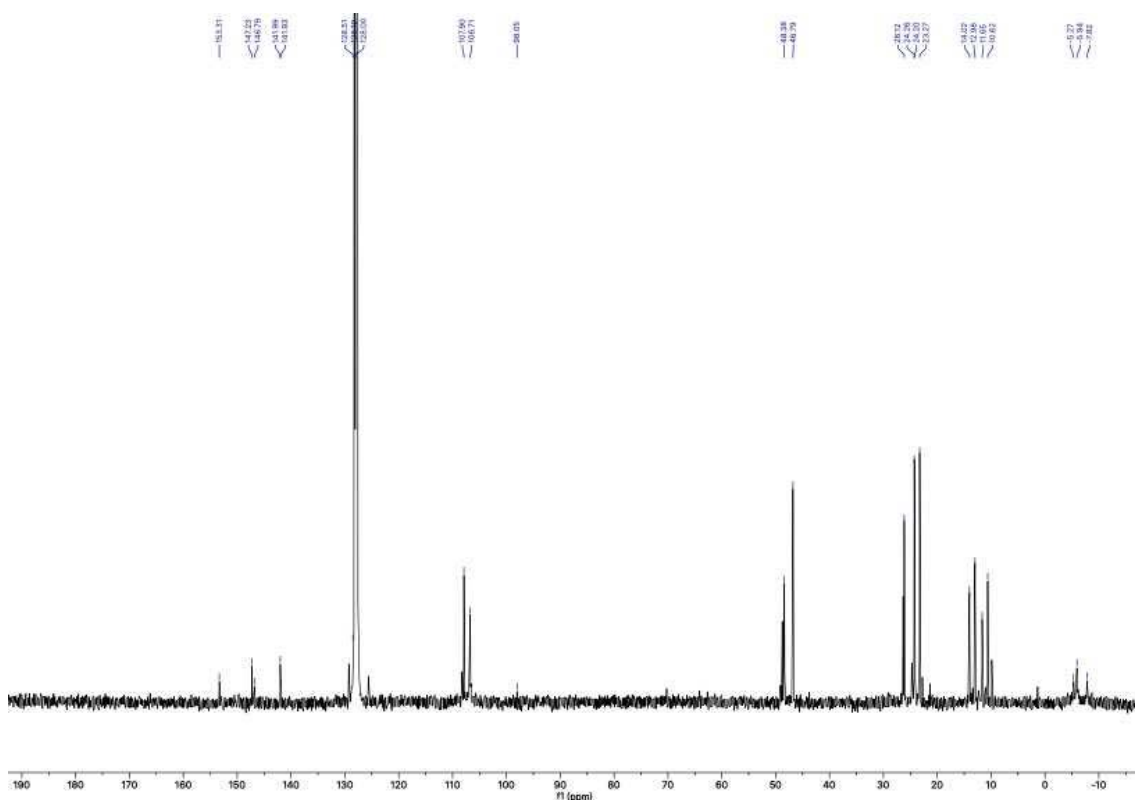


Figure S17b. ¹³C-{¹H}-NMR spectrum (400 MHz, 297 K, CDCl₃) for 1,2-decylene carbonate **11c**.

ELECTRONIC SUPPLEMENTARY INFORMATION

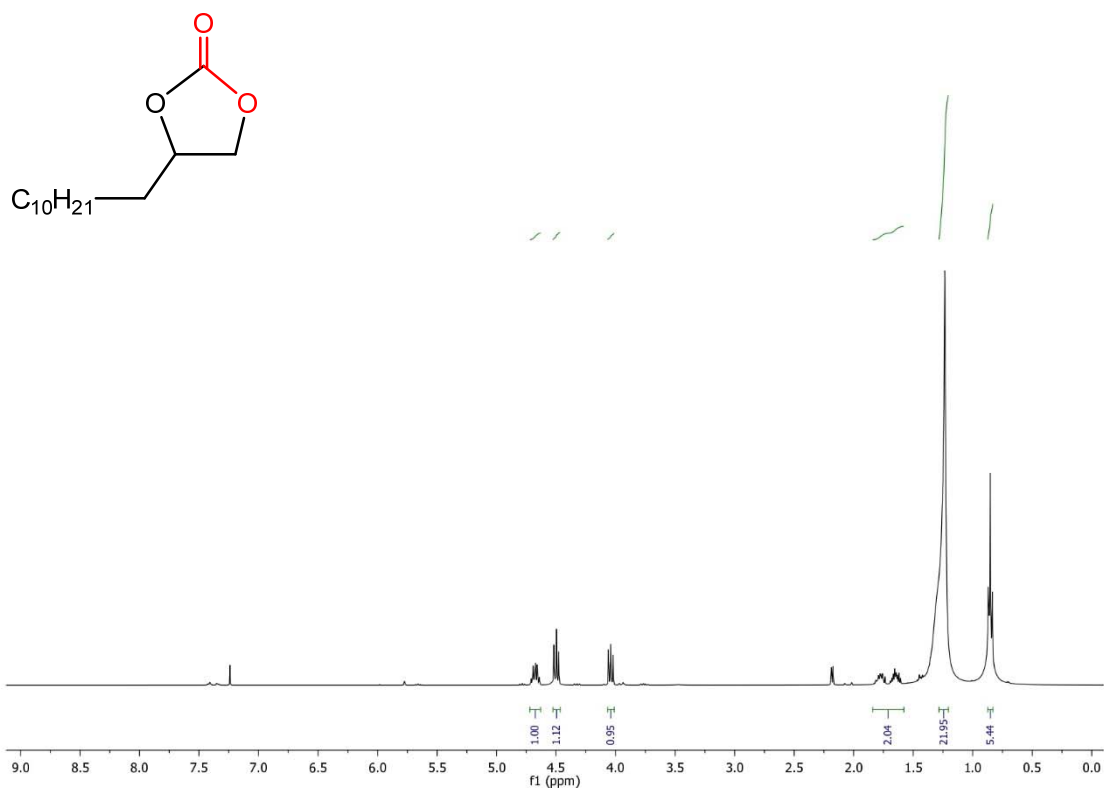


Figure S18a. ^1H NMR spectrum (400 MHz, 297 K, CDCl_3) for 1,2-dodecylene carbonate **11d**.

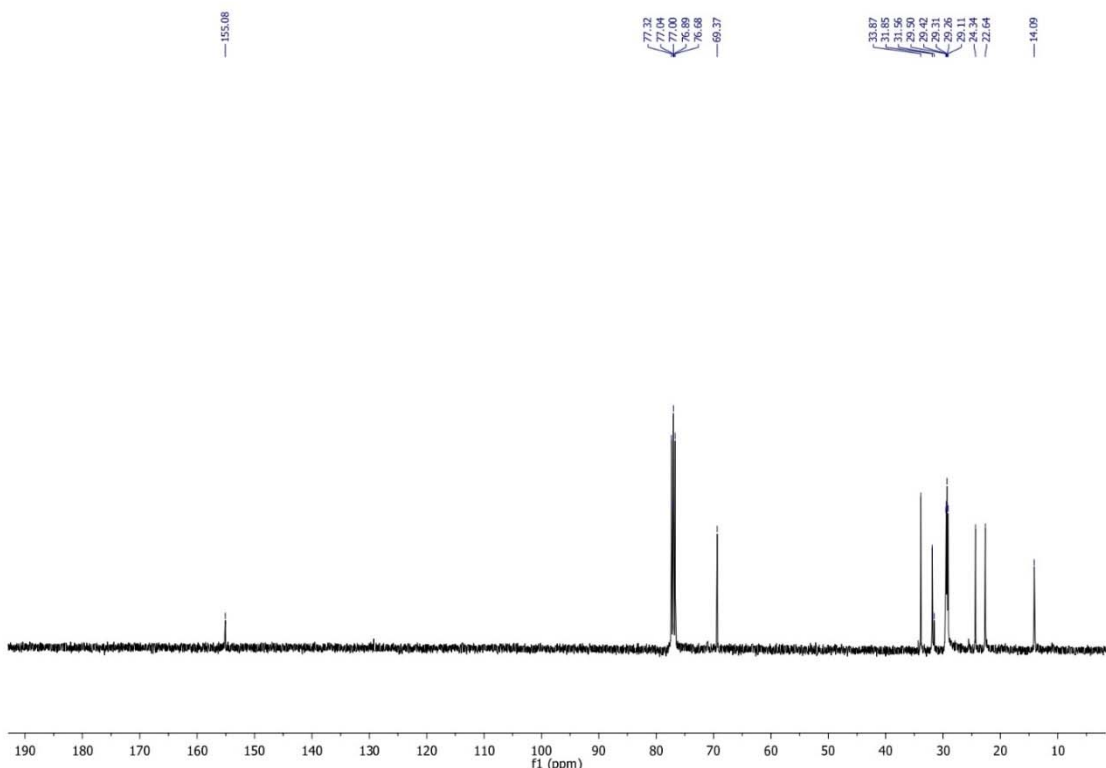


Figure S18b. ^{13}C -{ ^1H }-NMR spectrum (400 MHz, 297 K, CDCl_3) for 1,2-dodecylene carbonate 11d.

ELECTRONIC SUPPLEMENTARY INFORMATION

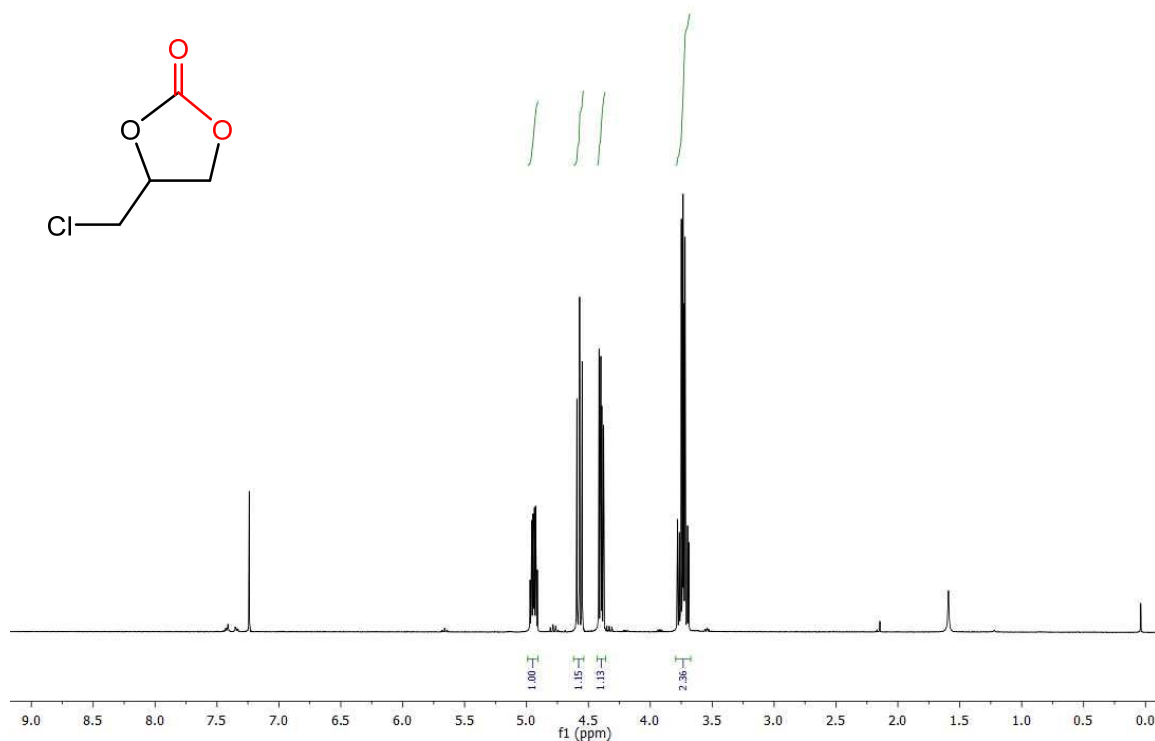


Figure S19a. ^1H NMR spectrum (400 MHz, 297 K, CDCl_3) for 3-chloropropylene carbonate **11e**.

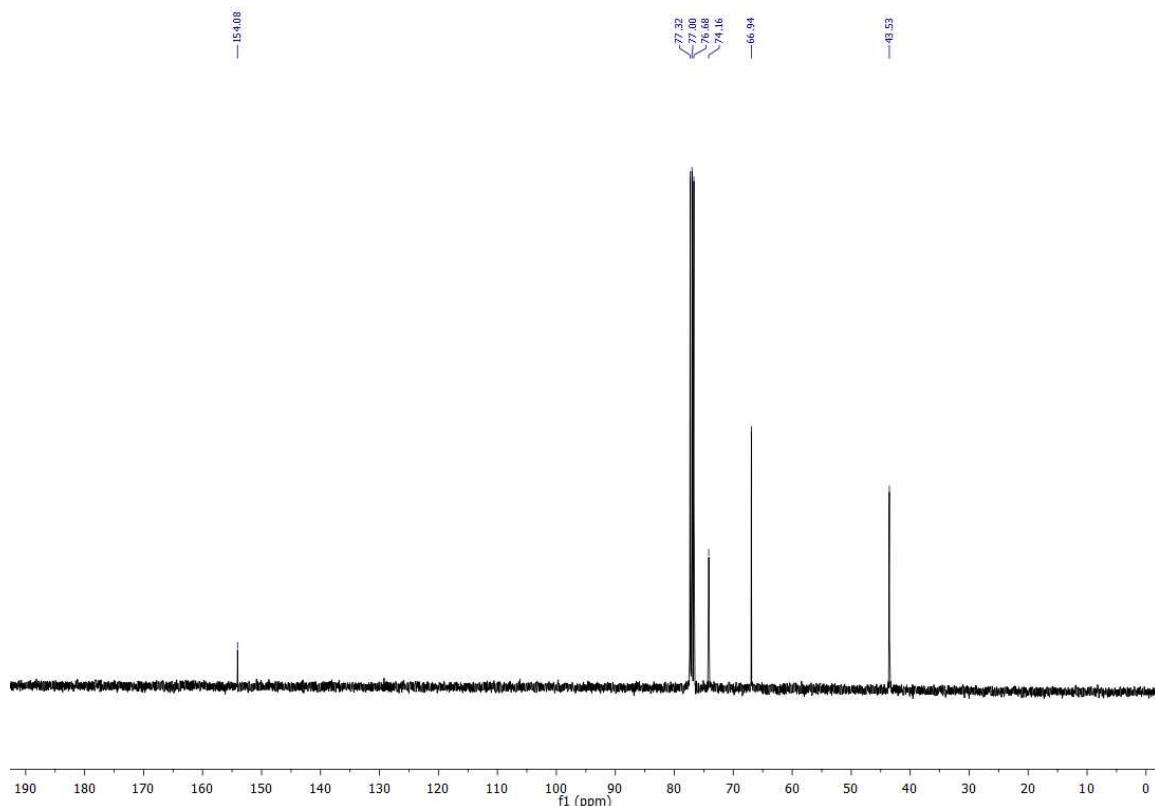


Figure S19b. ^{13}C - $\{{}^1\text{H}\}$ -NMR spectrum (400 MHz, 297 K, CDCl_3) for 3-chloropropylene carbonate **11e**.

ELECTRONIC SUPPLEMENTARY INFORMATION

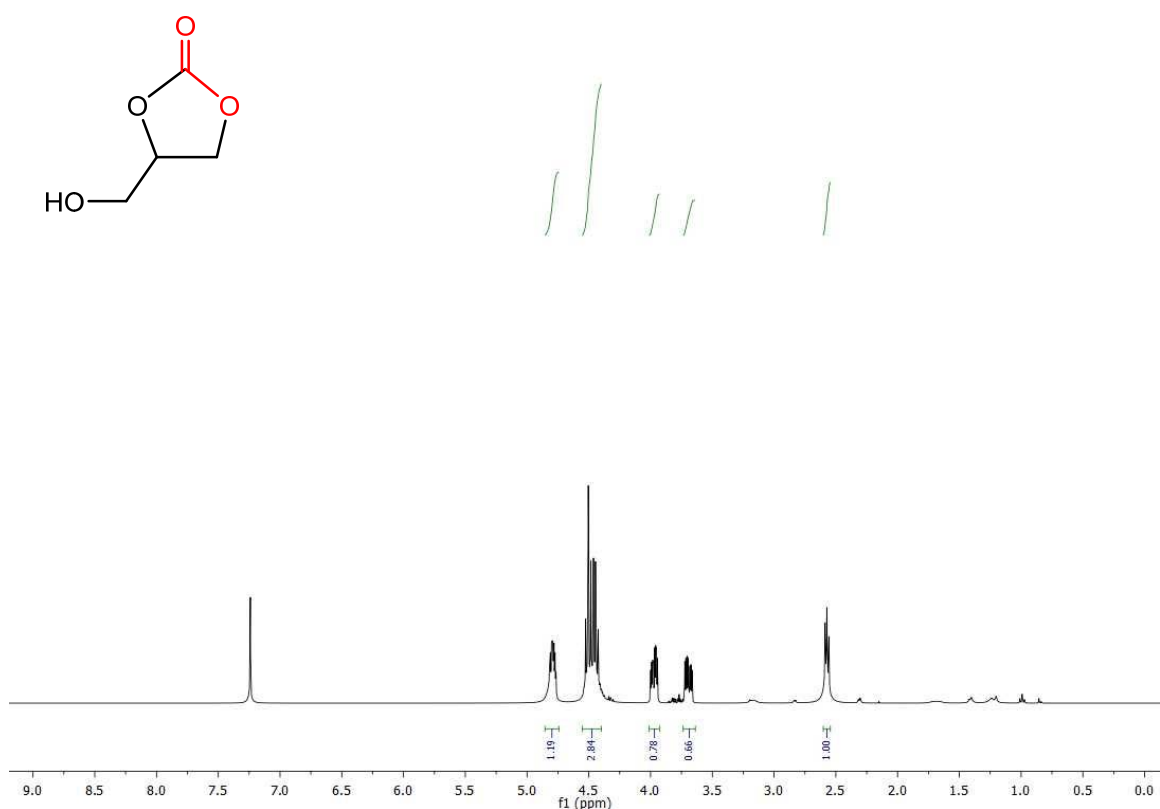


Figure S20a. ^1H NMR spectrum (500 MHz, 297 K, CDCl_3) for glycerol carbonate **11f**.

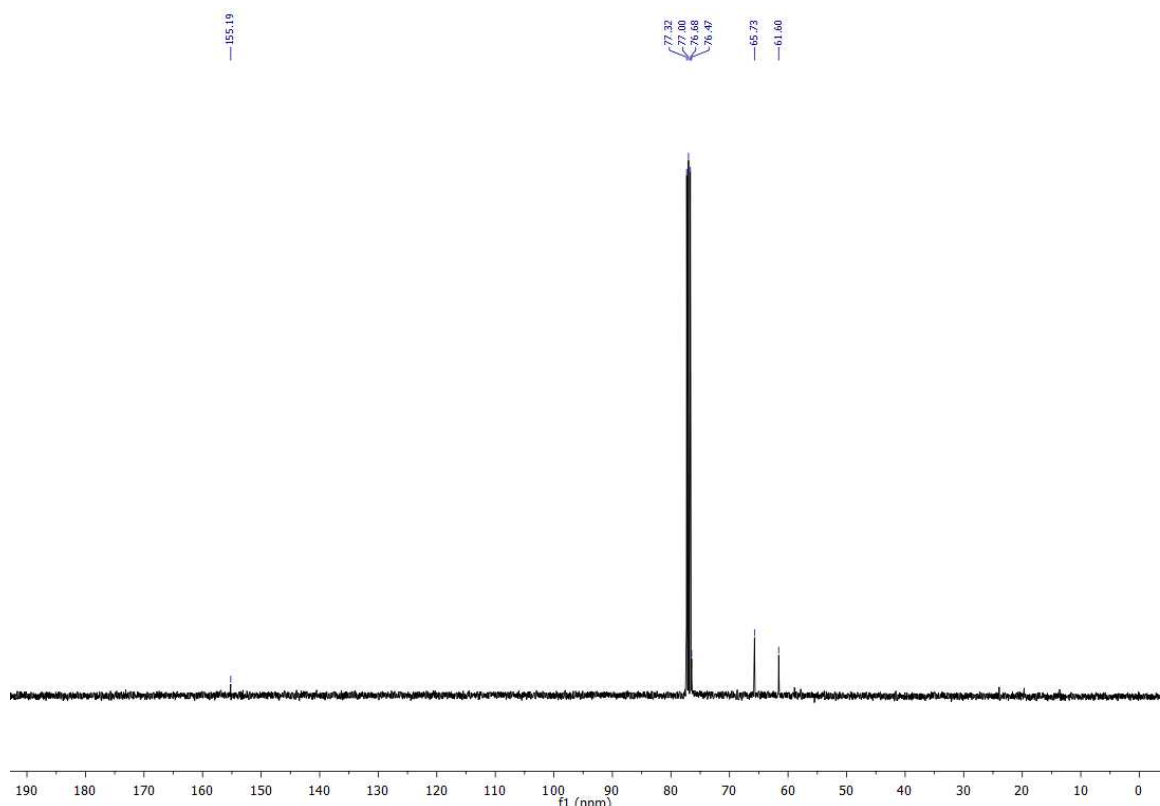


Figure S20b. ^{13}C -{ ^1H } -NMR spectrum (400 MHz, 297 K, CDCl_3) for glycerol carbonate **11f**.

ELECTRONIC SUPPLEMENTARY INFORMATION

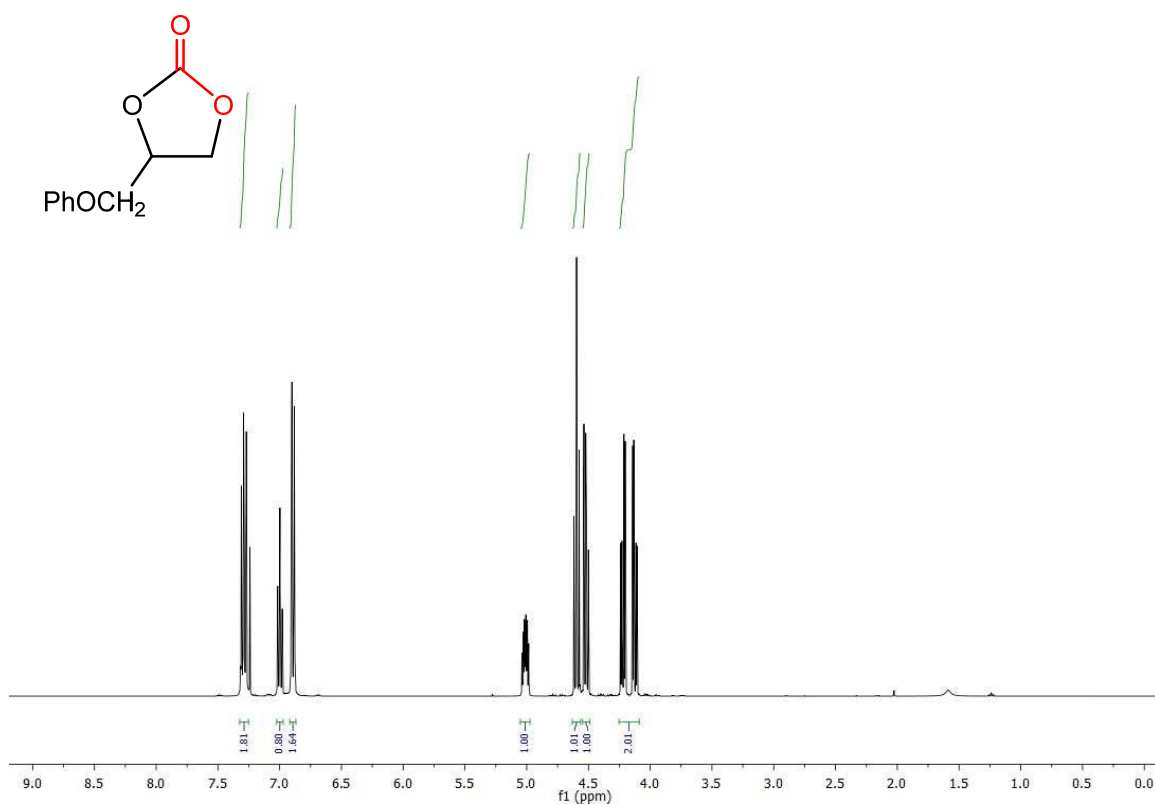


Figure S21a. ^1H NMR spectrum (400 MHz, 297 K, CDCl_3) for 3-phenoxypropylene carbonate **11g**.

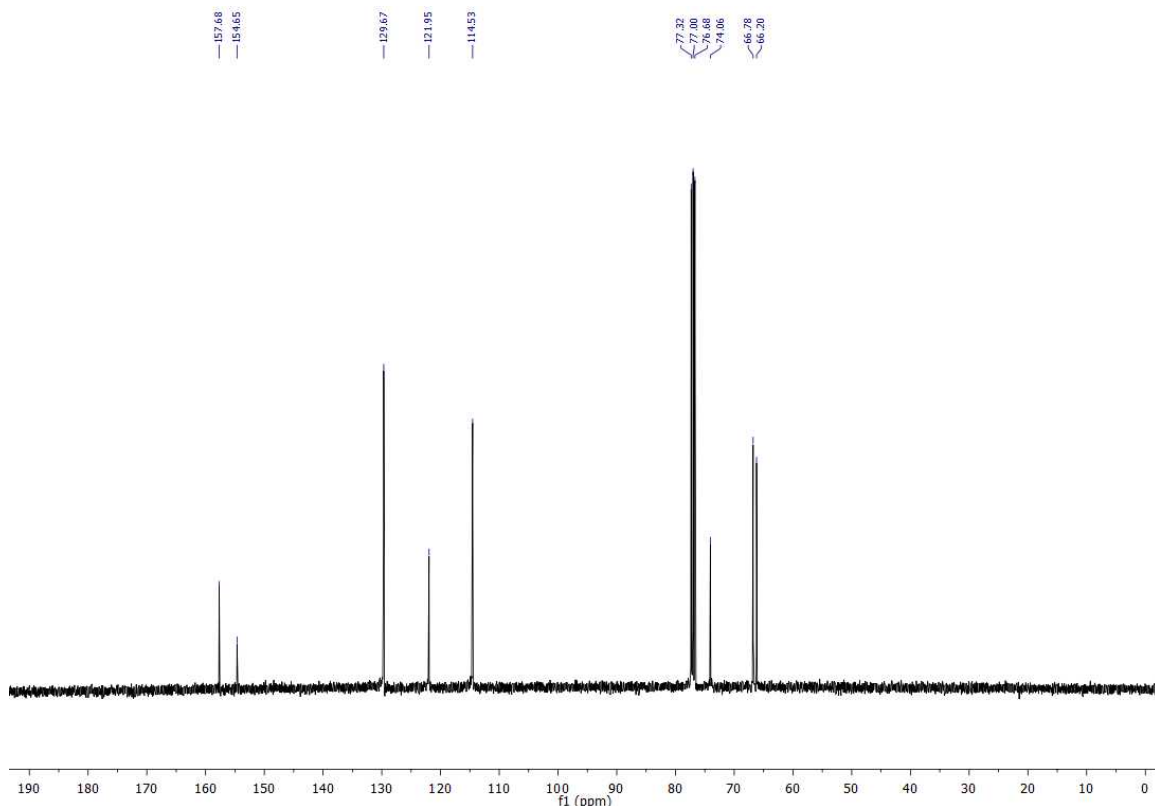


Figure S21b. ^{13}C - $\{^1\text{H}\}$ -NMR spectrum (400 MHz, 297 K, CDCl_3) for 3-phenoxypropylene carbonate **11g**.

ELECTRONIC SUPPLEMENTARY INFORMATION

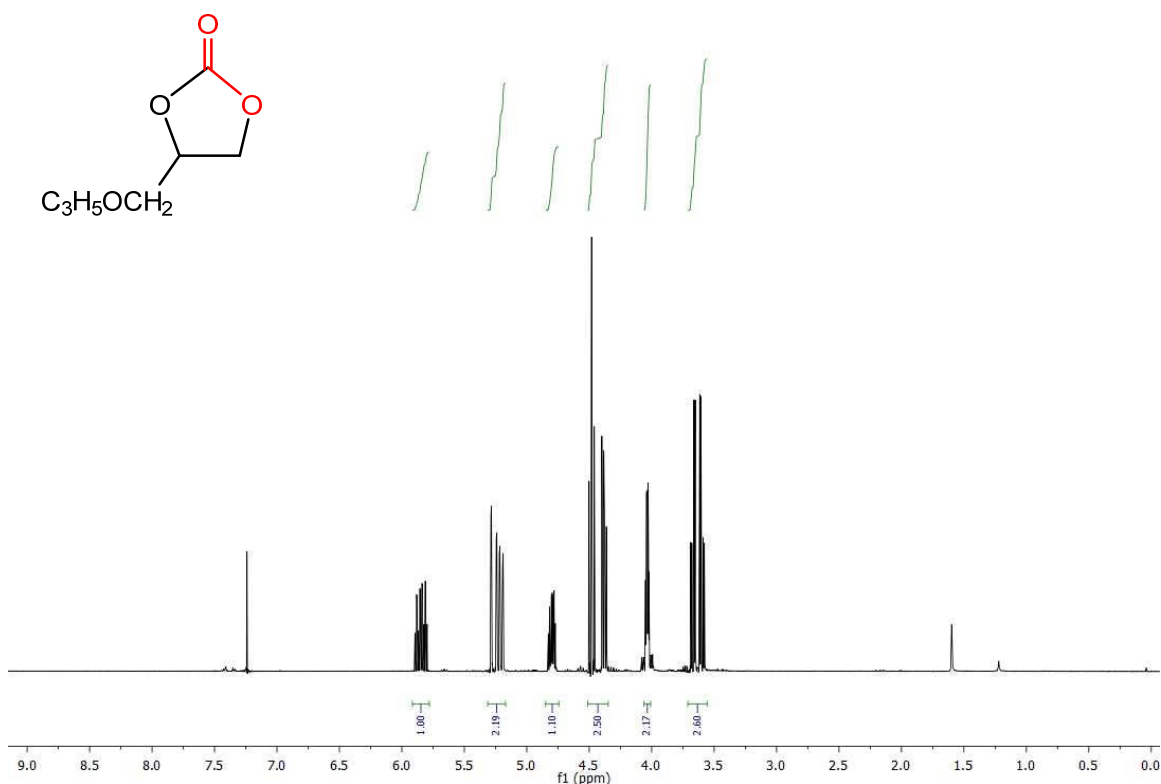


Figure S22a. ^1H NMR spectrum (400 MHz, 297 K, CDCl_3) for 3-vinyloxypropylene carbonate **11h**.

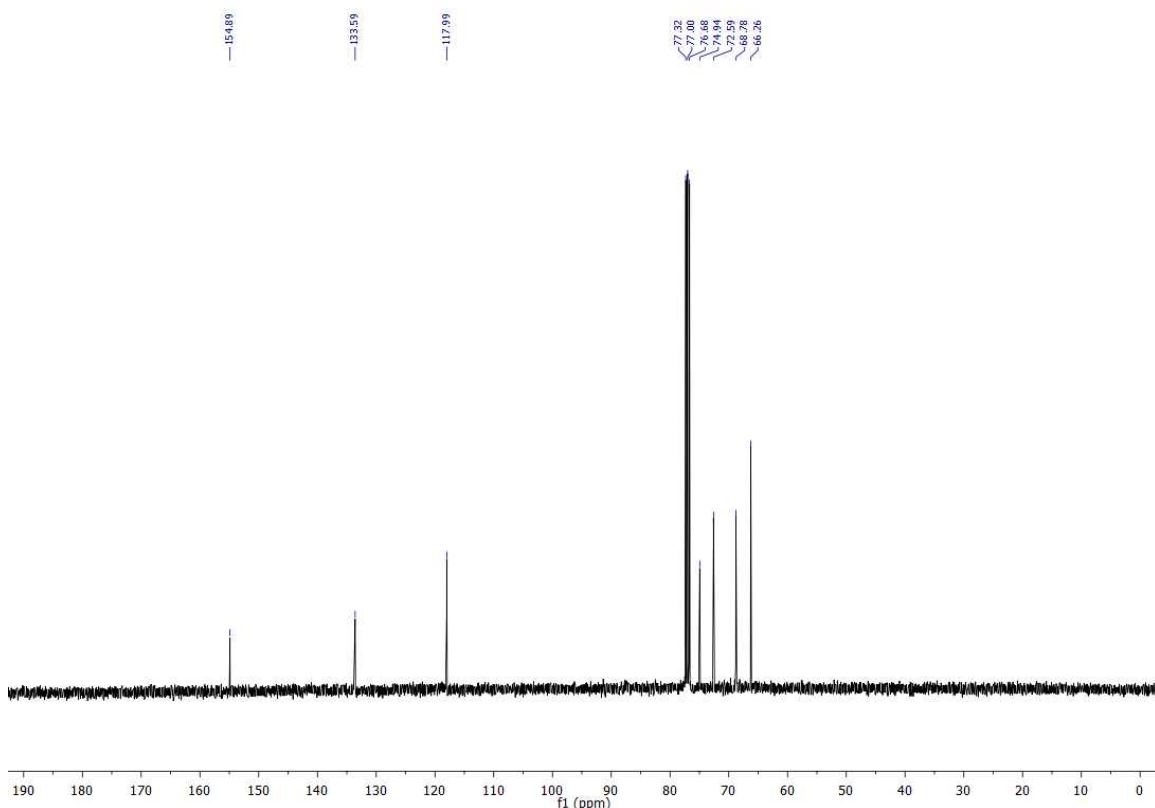


Figure S22b. ^{13}C -{ ^1H } NMR spectrum (400 MHz, 297 K, CDCl_3) for 3-vinyloxypropylene carbonate **11h**.

ELECTRONIC SUPPLEMENTARY INFORMATION

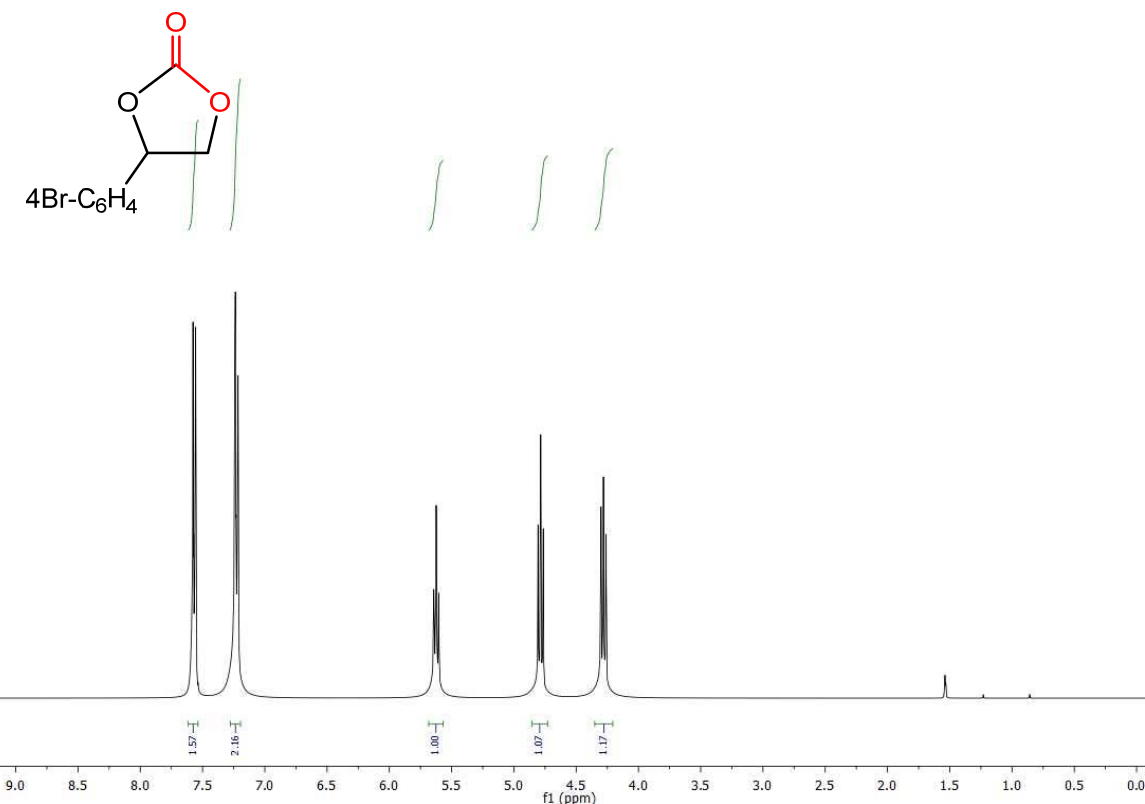


Figure S23a. ^1H NMR spectrum (400 MHz, 297 K, CDCl_3) for 4-bromostyrene carbonate **11i**.

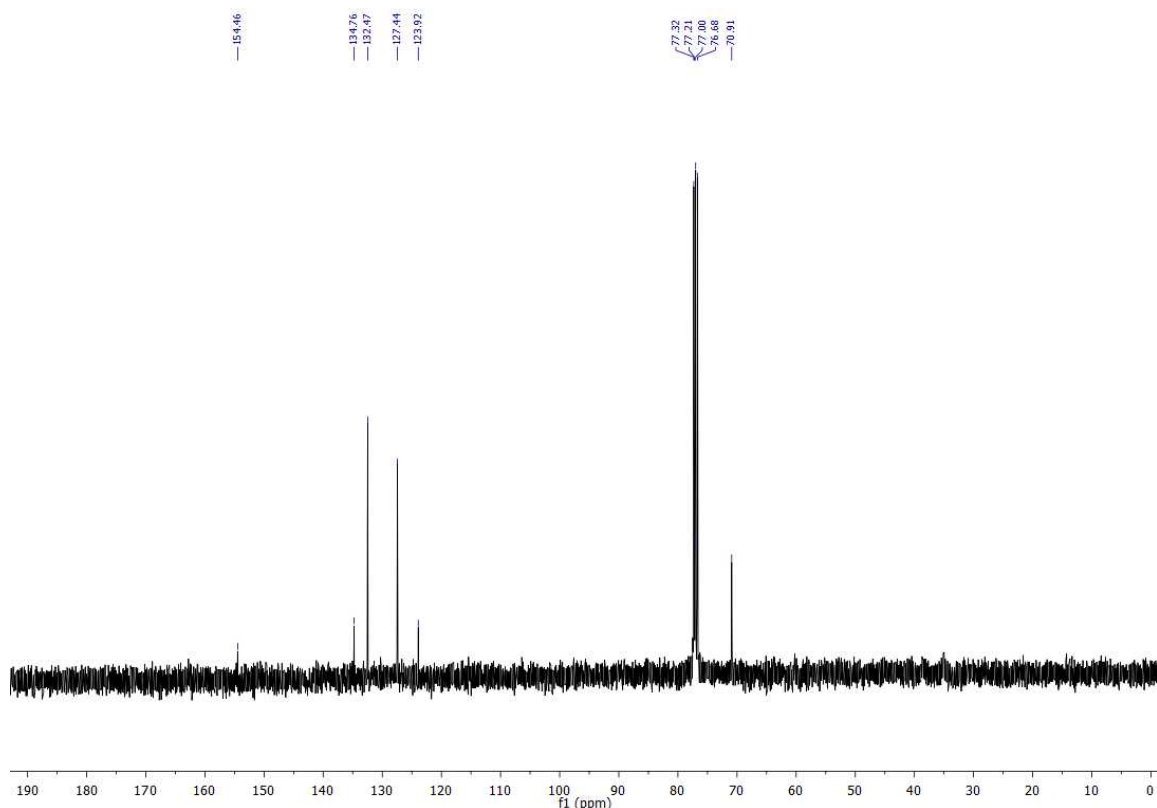


Figure S23b. ^{13}C - $\{{}^1\text{H}\}$ -NMR spectrum (400 MHz, 297 K, CDCl_3) for 4-bromostyrene carbonate **11i**.

ELECTRONIC SUPPLEMENTARY INFORMATION

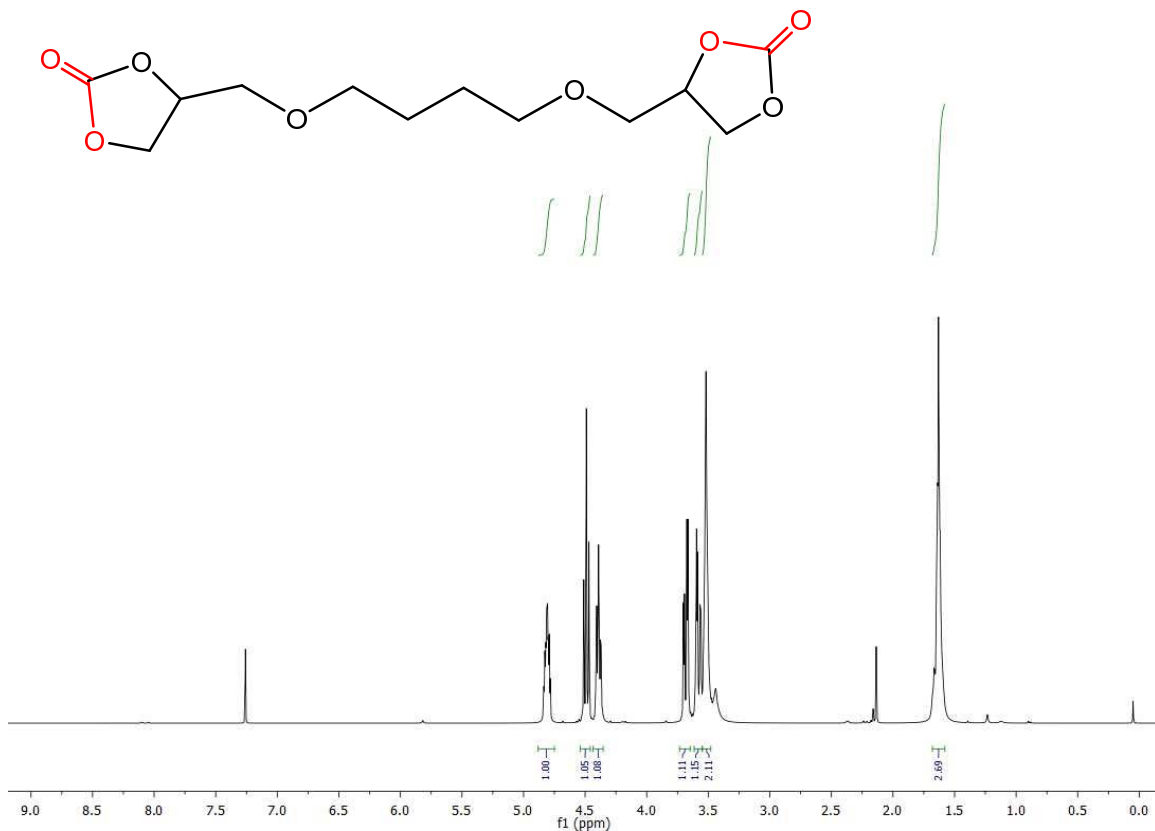
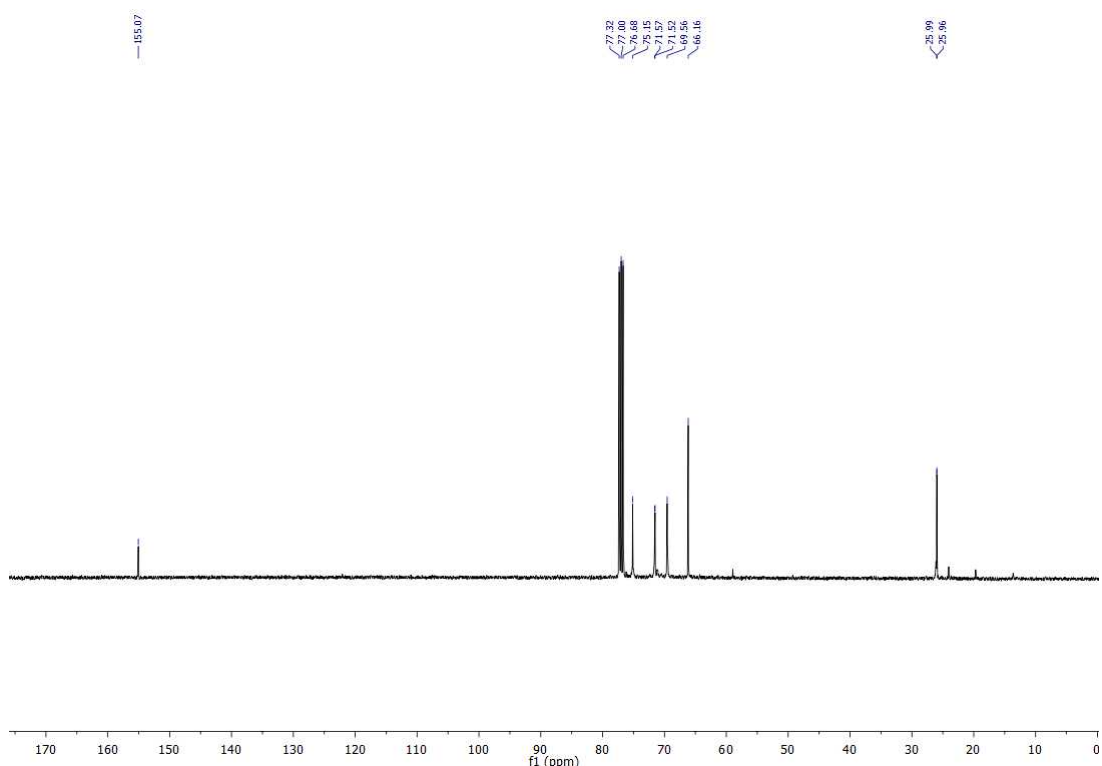


Figure S24a. ¹H-NMR spectrum (500 MHz, 297 K, CDCl₃) for 4,4'-(butane-1,4-diylbis(oxy))bis(methylene))bis(1,3-dioxolan-2-one) **11j**.



ELECTRONIC SUPPLEMENTARY INFORMATION

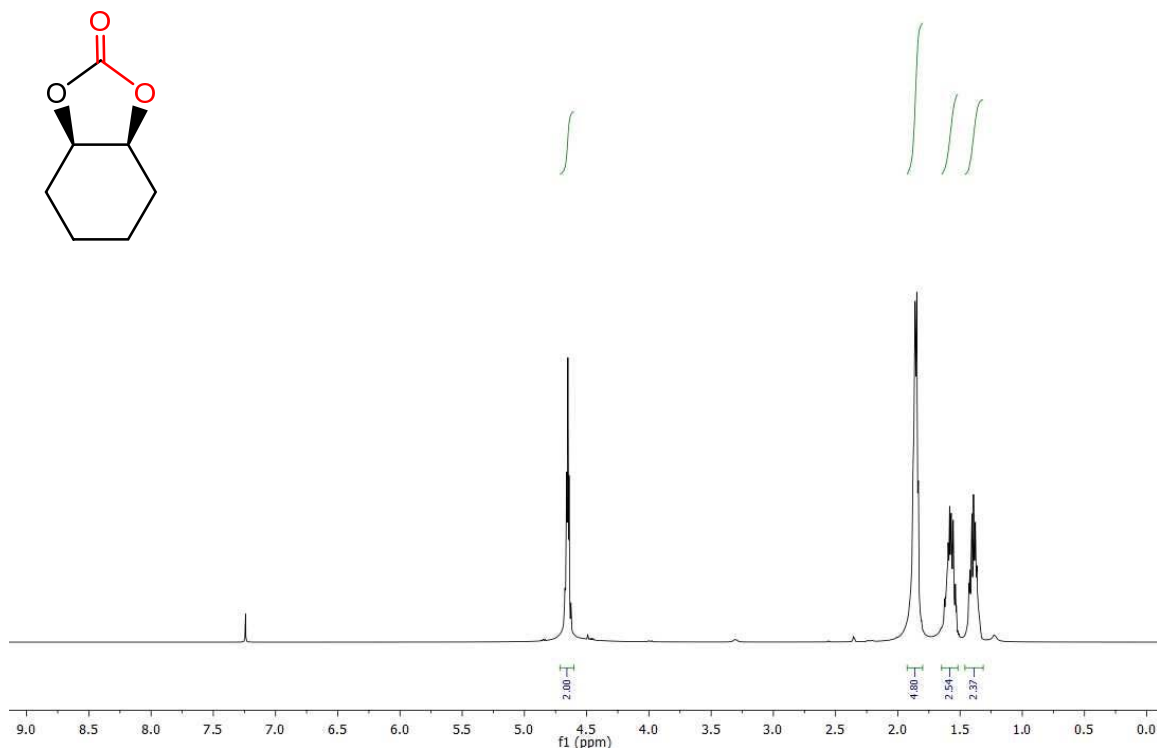


Figure S25a. ^1H NMR spectrum (400 MHz, 297 K, CDCl_3) for *cis*-1,2-cyclohexene carbonate **13a**.

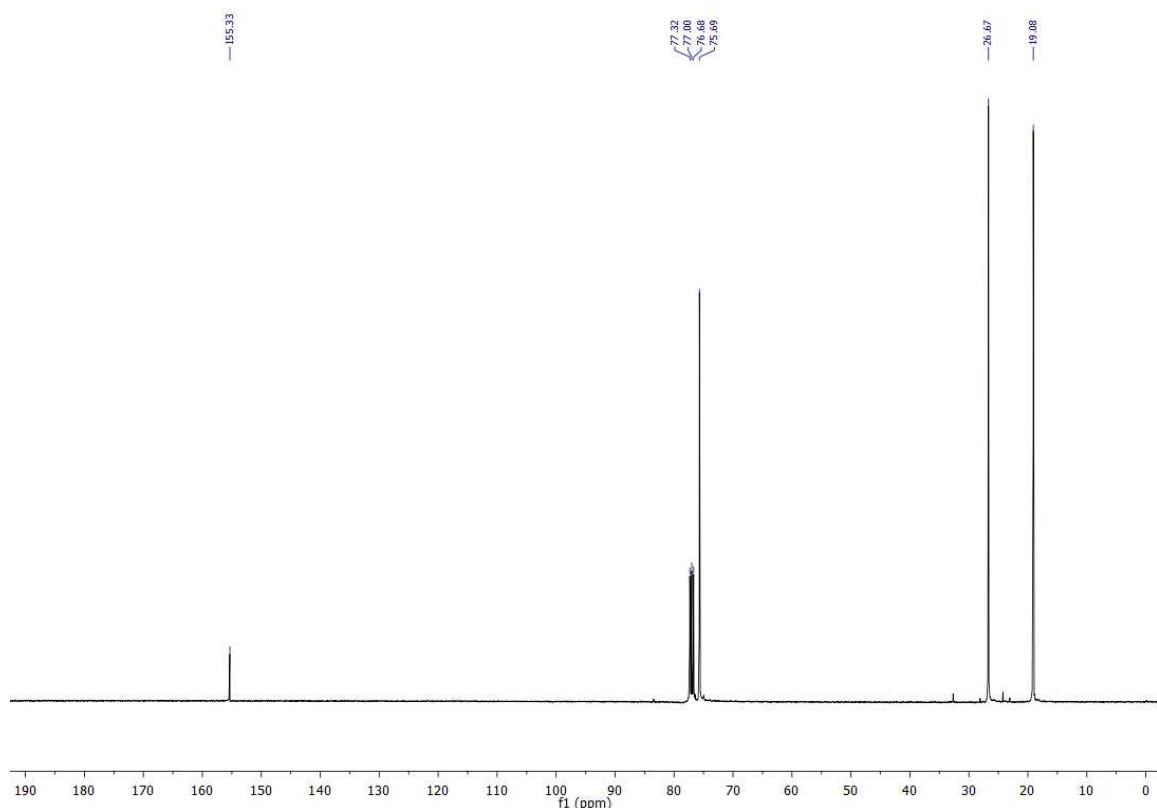


Figure S25b. ^{13}C -{ ^1H } NMR spectrum (400 MHz, 297 K, CDCl_3) for *cis*-1,2-cyclohexene carbonate **13a**.

ELECTRONIC SUPPLEMENTARY INFORMATION

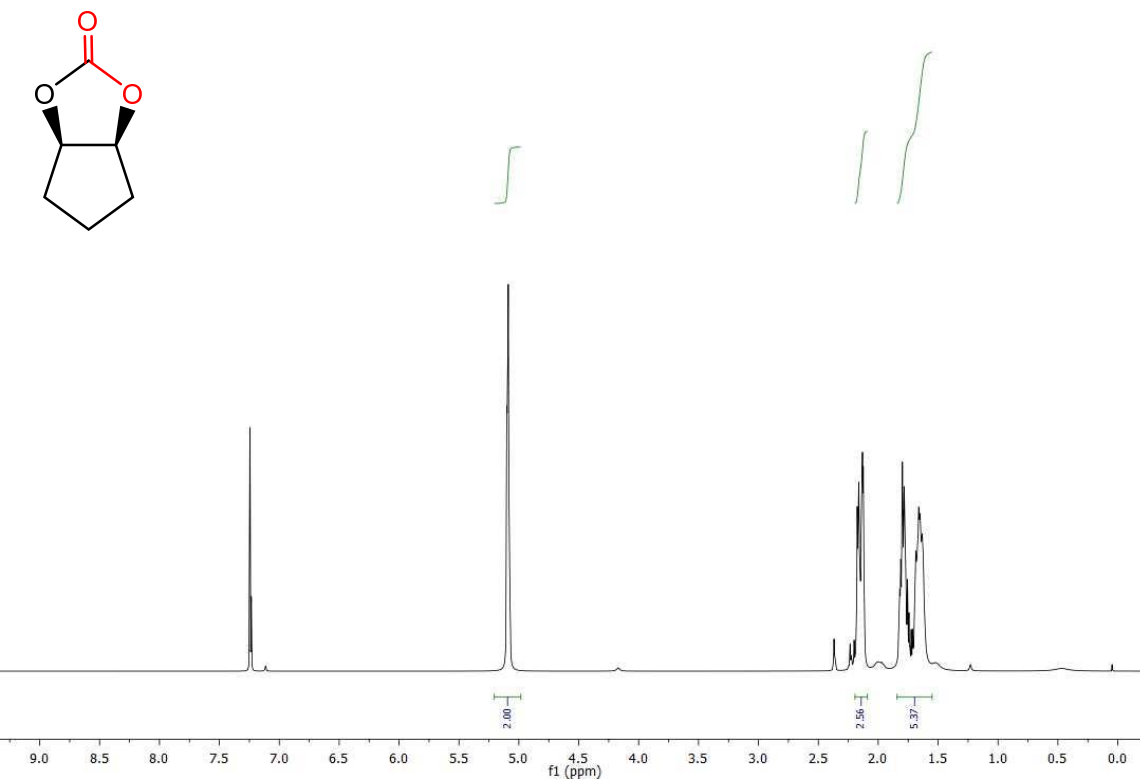


Figure S26a. ^1H NMR spectrum (400 MHz, 297 K, CDCl_3) for *cis*-1,2-cyclopentene carbonate **13b**.

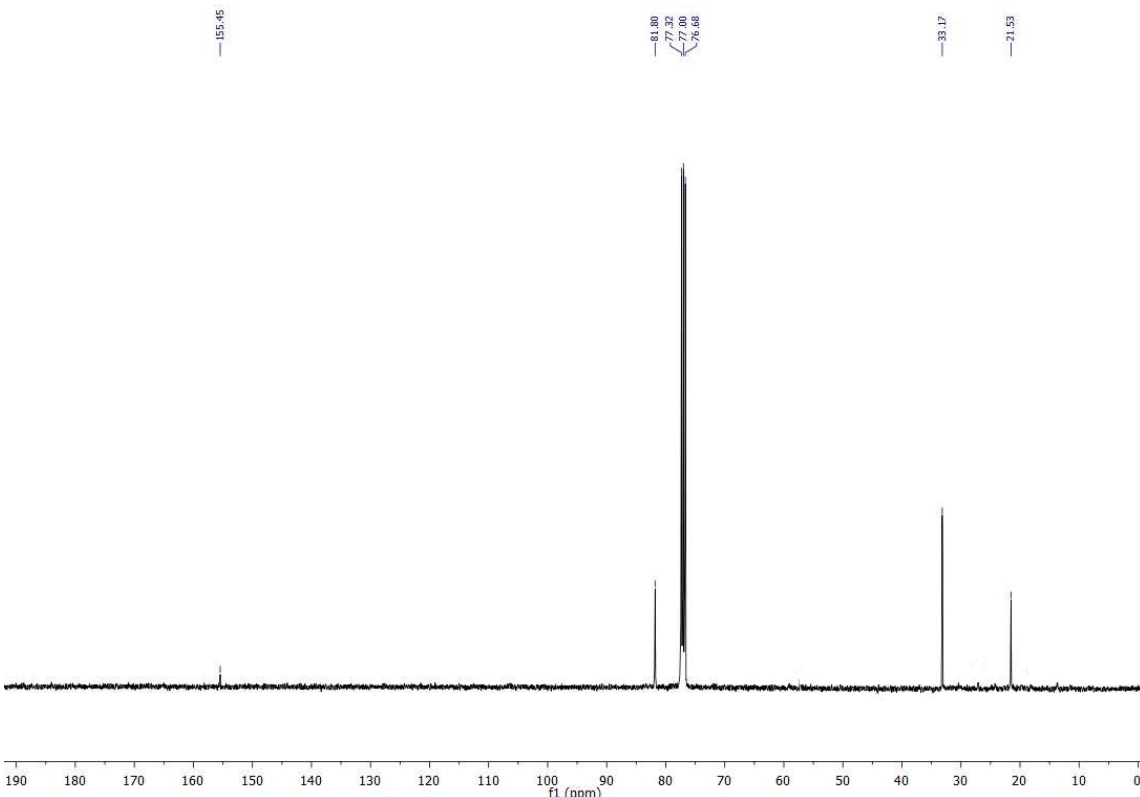


Figure S26b. ^{13}C - $\{{}^1\text{H}\}$ -NMR spectrum (400 MHz, 297 K, CDCl_3) for *cis*-1,2-cyclopentene carbonate **13b**.

ELECTRONIC SUPPLEMENTARY INFORMATION

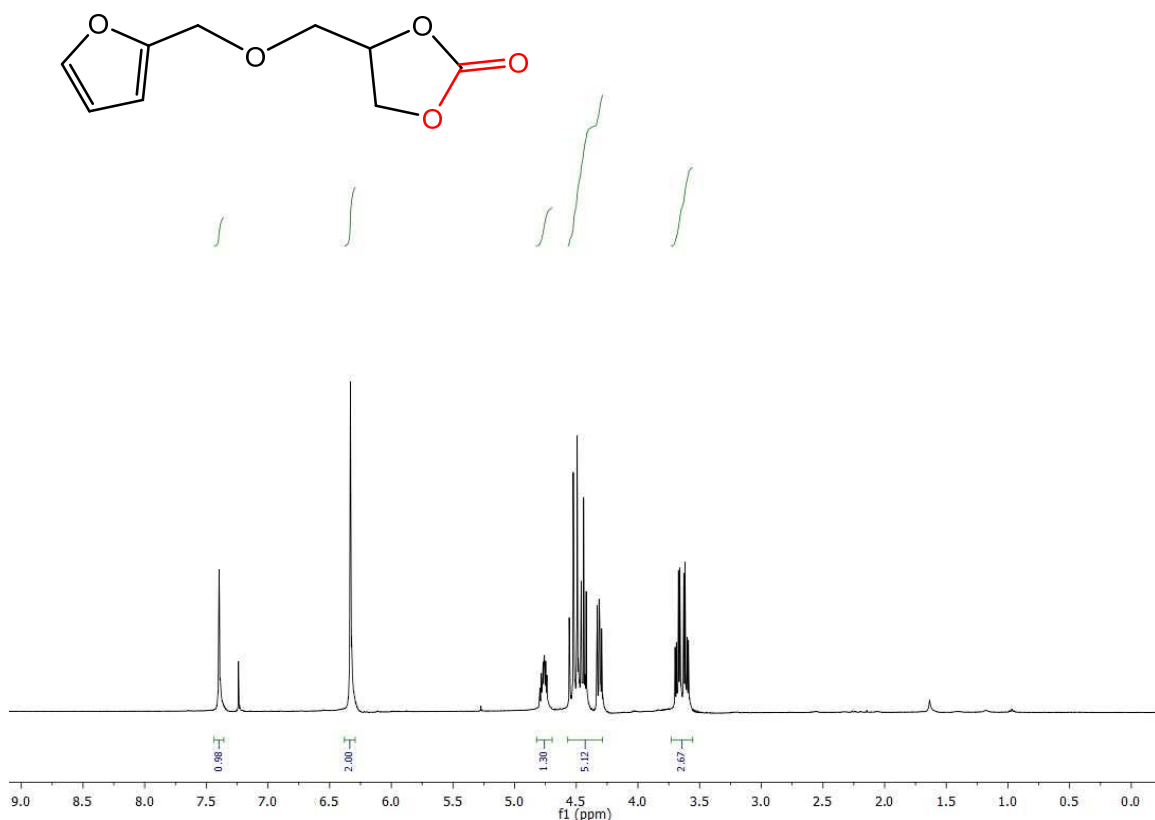


Figure S27a. ¹H-NMR spectrum (400 MHz, 297 K, CDCl₃) for 4-(furan-2-ylmethoxy)-1,3-dioxolan-2-one **13c**.

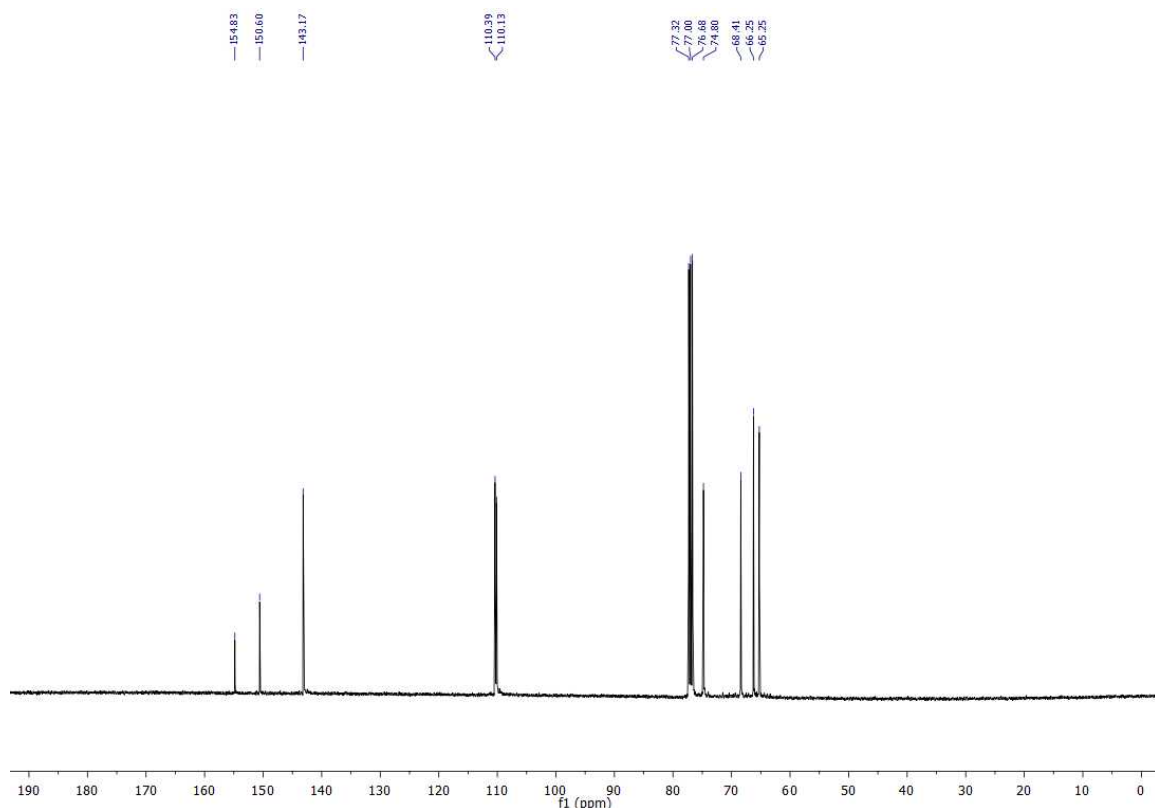


Figure S27b. ¹³C-{¹H}-NMR spectrum (400 MHz, 297 K, CDCl₃) for 4-(furan-2-ylmethoxy)-1,3-dioxolan-2-one **13c**.

ELECTRONIC SUPPLEMENTARY INFORMATION

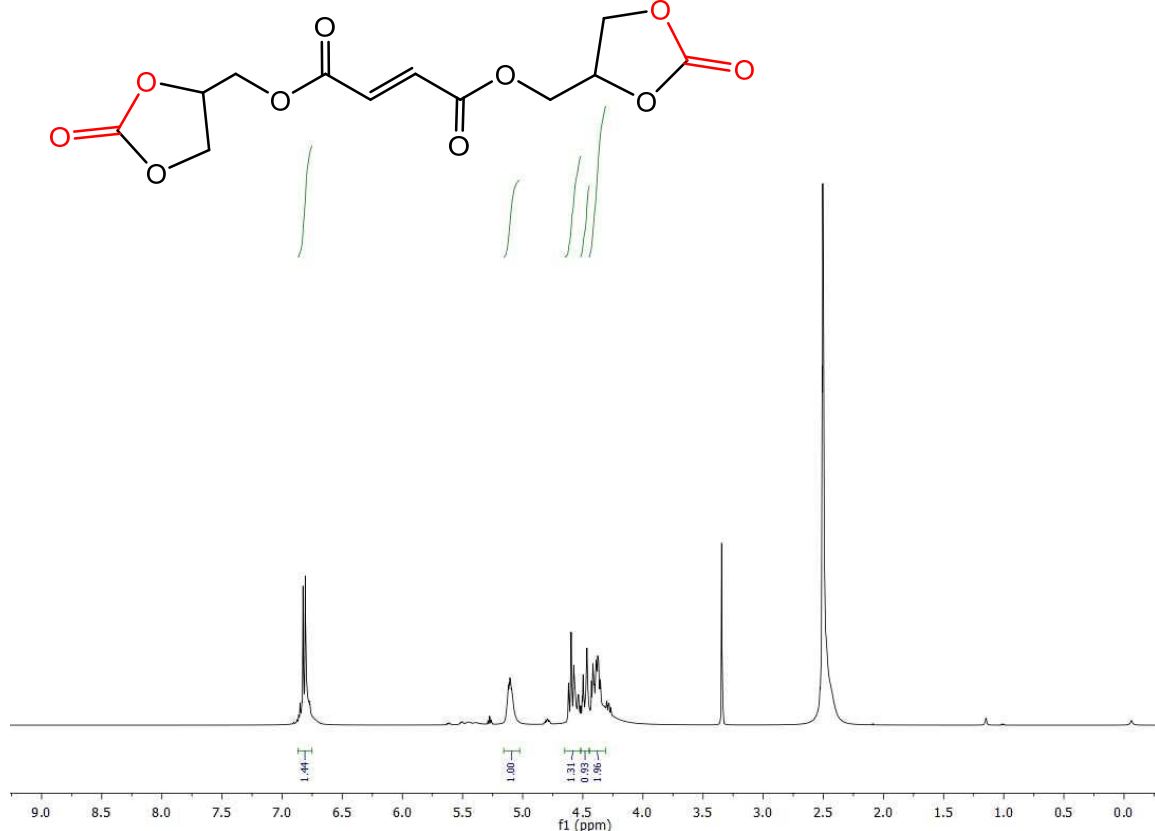


Figure S28a. ¹H-NMR spectrum (400 MHz, 297 K, DMSO-*d*₆) for bis((2-oxo-1,3-dioxolan-4-yl)methyl)fumarate **13d**.

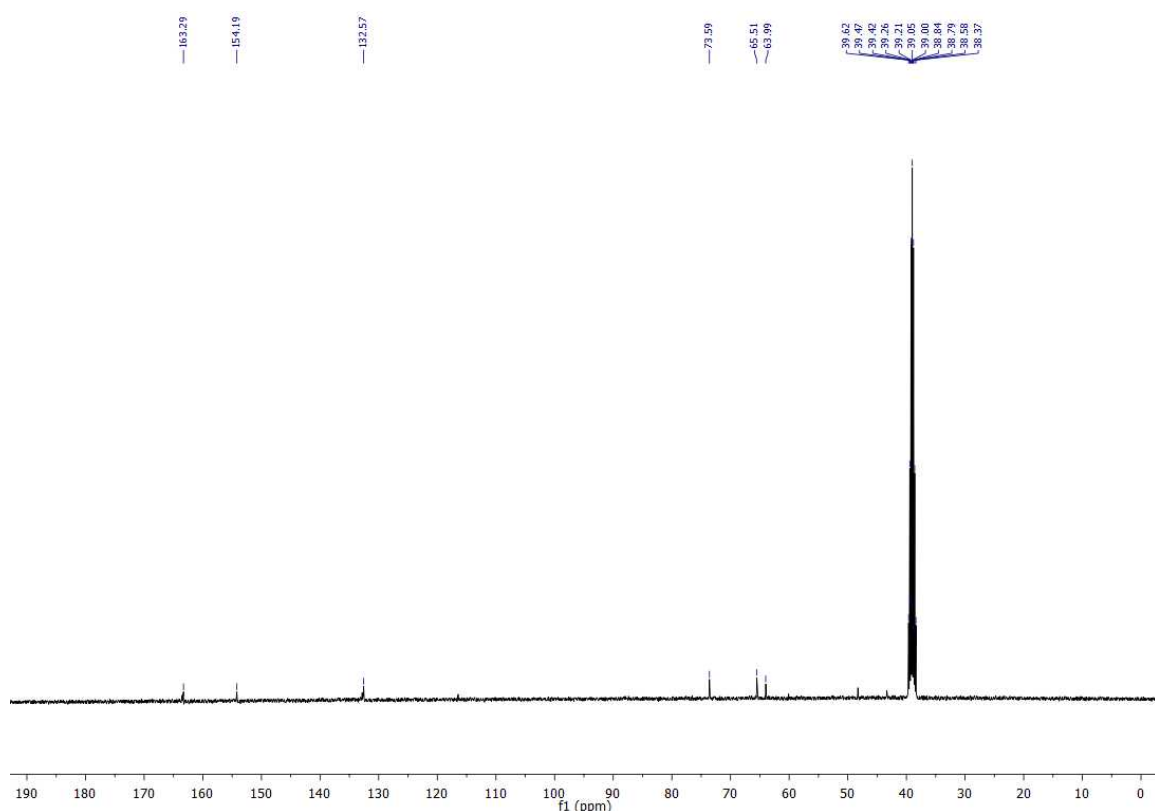


Figure S28b. ¹³C-{¹H}-NMR spectrum (400 MHz, 297 K, DMSO-*d*₆) for bis((2-oxo-1,3-dioxolan-4-yl)methyl)fumarate **13d**.

ELECTRONIC SUPPLEMENTARY INFORMATION

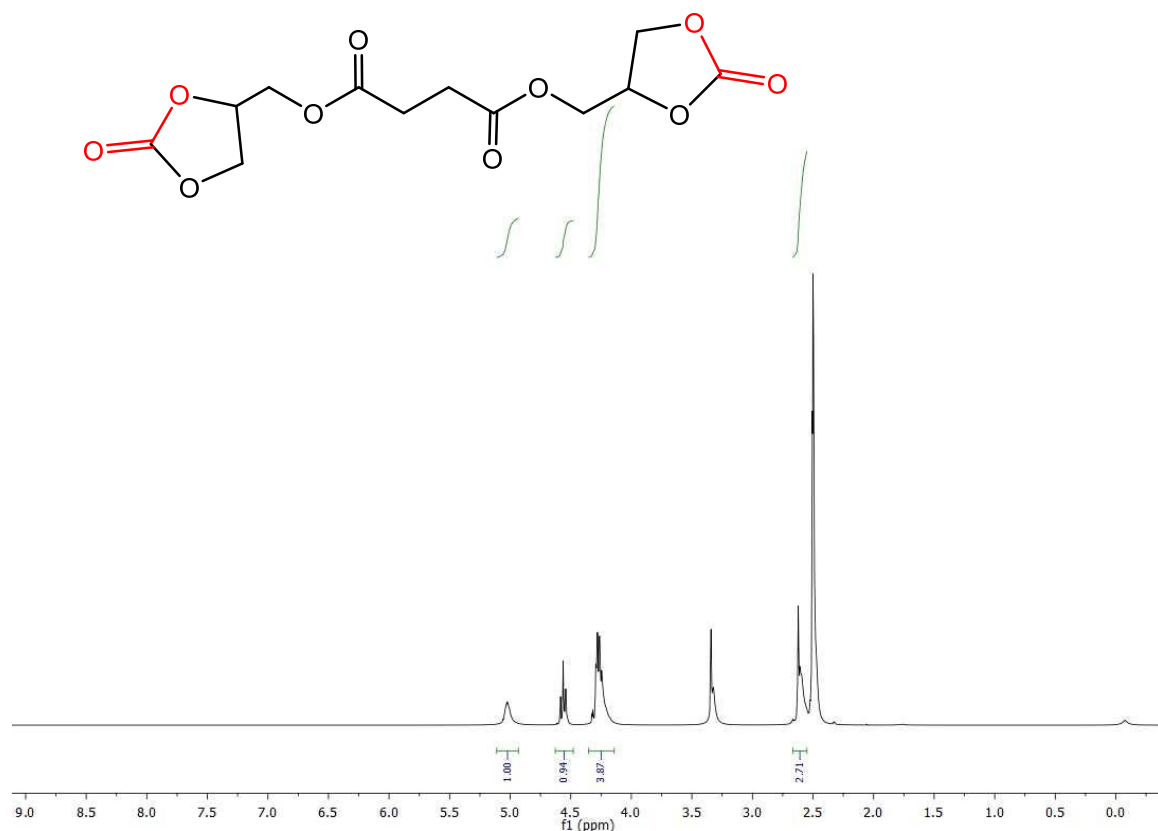


Figure S29a. ^1H -NMR spectrum (500 MHz, 297 K, $\text{DMSO}-d_6$) for bis((2-oxo-1,3-dioxolan-4-yl)methyl) succinate **13e**.

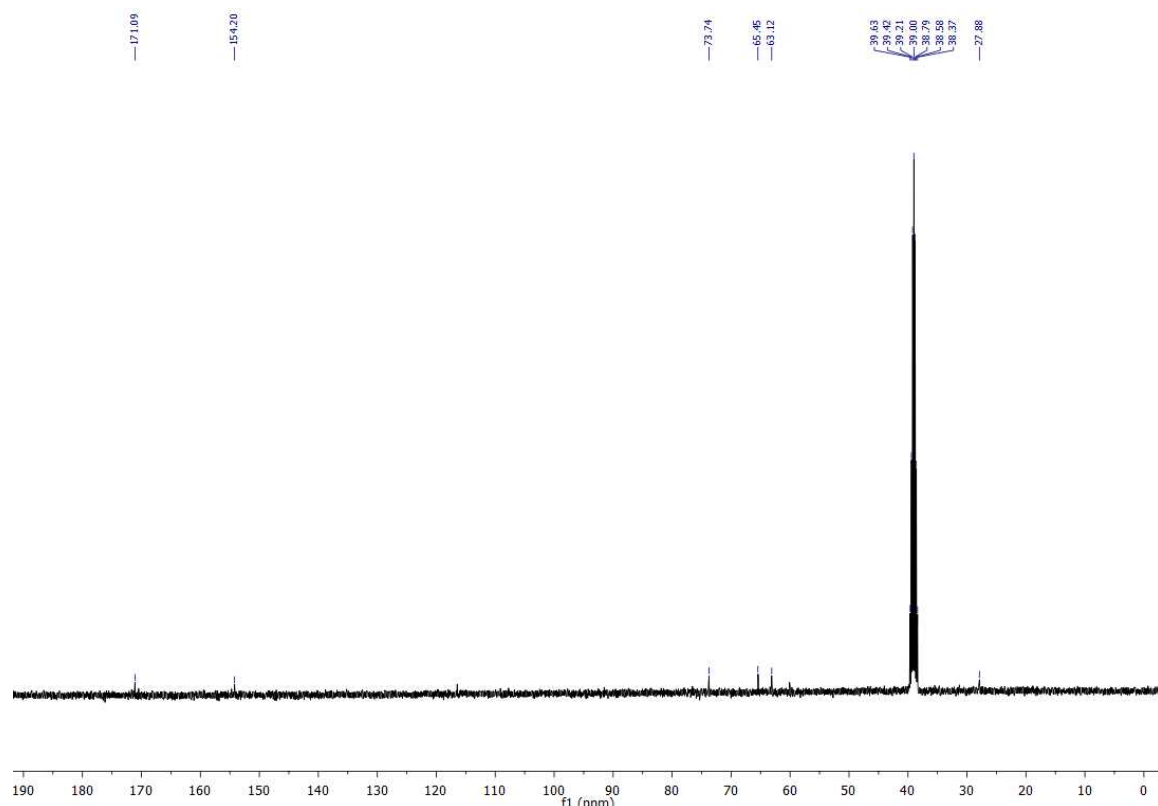


Figure S29b. ^{13}C - $\{{}^1\text{H}\}$ -NMR spectrum (400 MHz, 297 K, $\text{DMSO}-d_6$) for bis((2-oxo-1,3-dioxolan-4-yl)methyl) succinate **13e**.

ELECTRONIC SUPPLEMENTARY INFORMATION

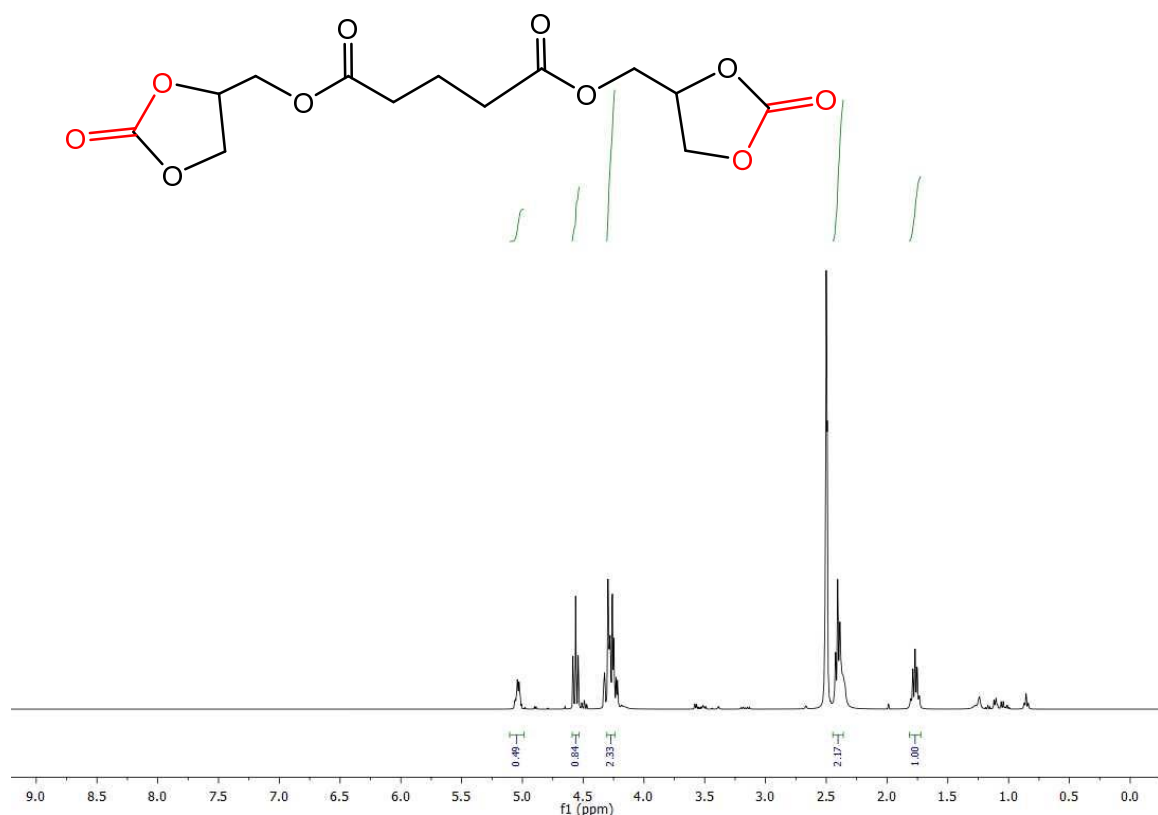


Figure S30a. ^1H -NMR spectrum (400 MHz, 297 K, $\text{DMSO}-d_6$) for bis((2-oxo-1,3-dioxolan-4-yl)methyl) glutarate **13f**.

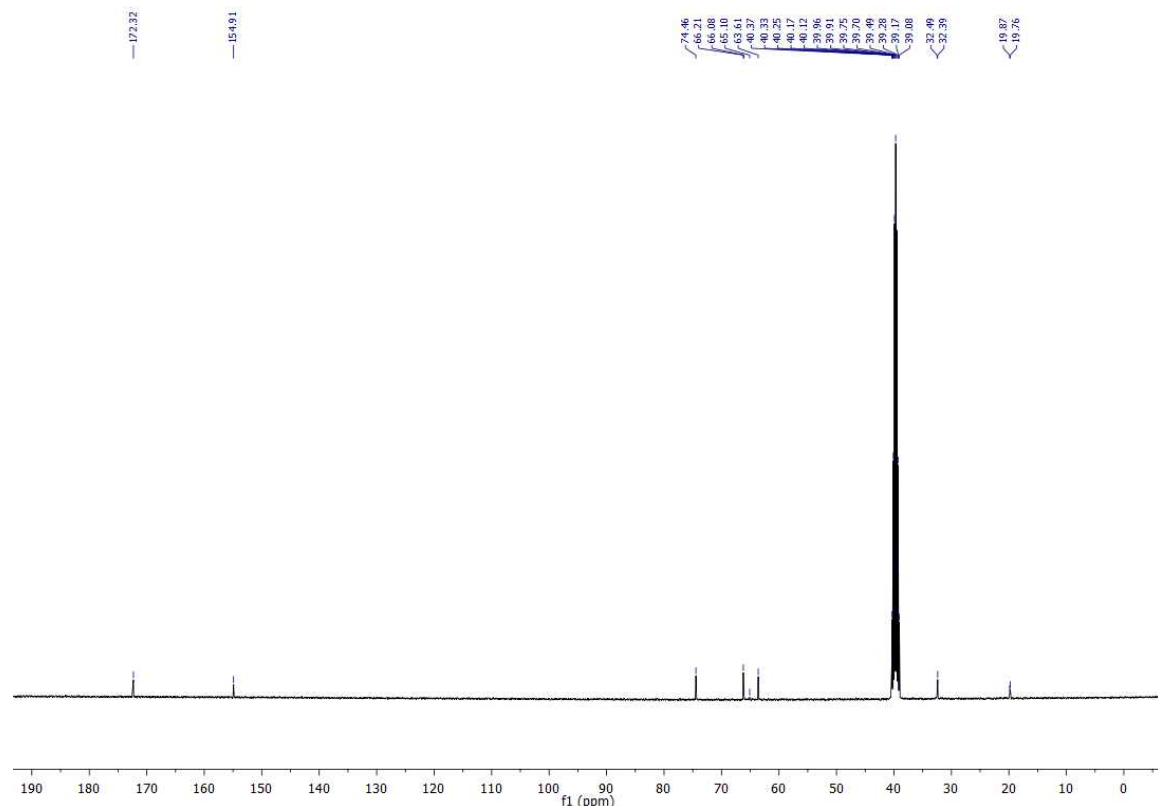


Figure S30b. ^{13}C - $\{{}^1\text{H}\}$ -NMR spectrum (400 MHz, 297 K, $\text{DMSO}-d_6$) for bis((2-oxo-1,3-dioxolan-4-yl)methyl) glutarate **13f**.

ELECTRONIC SUPPLEMENTARY INFORMATION

Figure S31. ^1H NMR spectra of commercial available *cis/trans* mixture of limonene oxide and *trans*-isomer isolated.

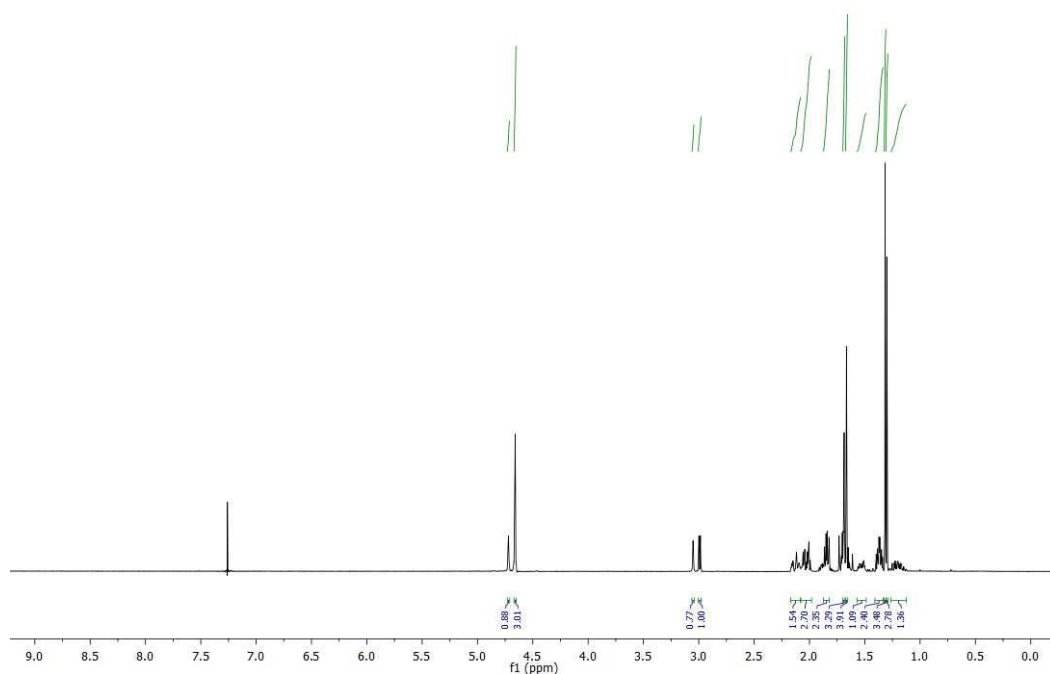


Figure S31a. ^1H -NMR spectrum (400 MHz, 297 K, CDCl_3) for commercially available *cis*- and *trans*-diastereomers of (*R*)-(+)-limonene oxide. 43:57 *cis/trans* proportion in the mixture.

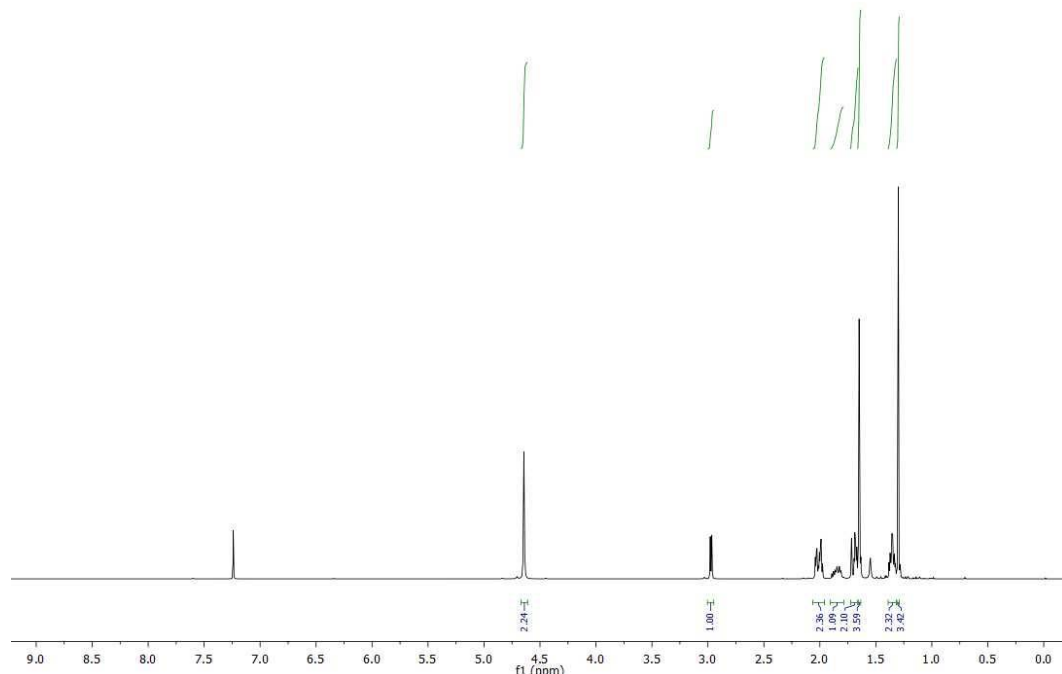


Figure S31b. ^1H -NMR spectrum (400 MHz, 297 K, CDCl_3) for *trans*-(*R*)-(+)-limonene oxide after purification.⁷

ELECTRONIC SUPPLEMENTARY INFORMATION

Figure S32. ^1H and ^{13}C - $\{^1\text{H}\}$ NMR spectra of compound **15**

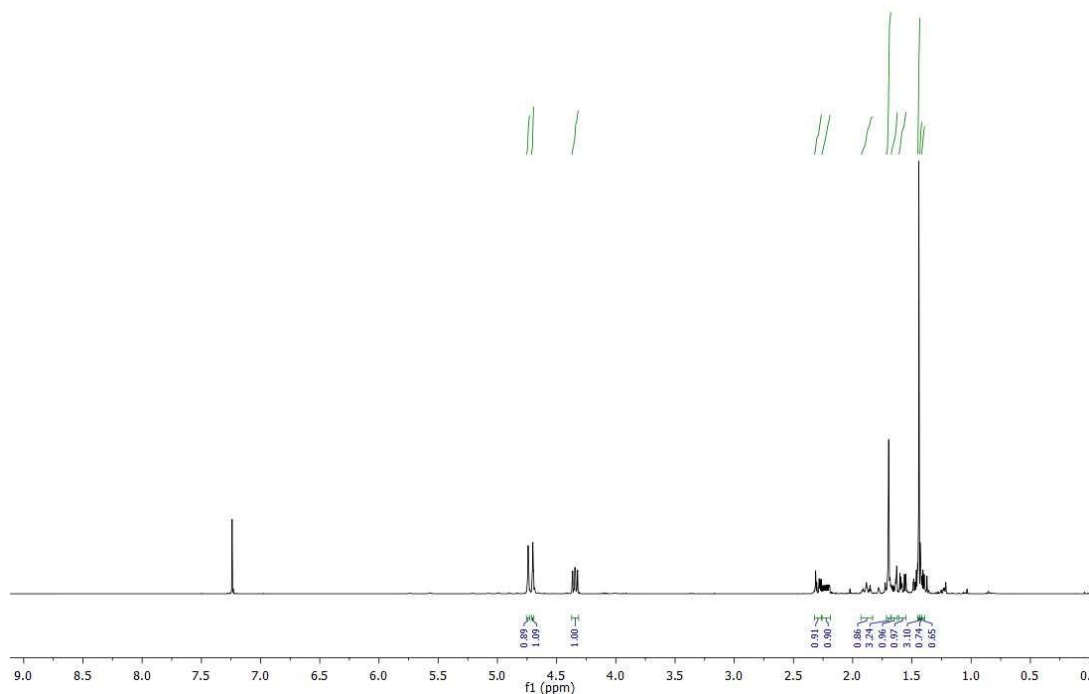


Figure S32a. ^1H -NMR spectrum (400 MHz, 297 K, CDCl_3) for 3a-methyl-6-(prop-1-en-2-yl)hexahydrobenzo[*d*][1,3]dioxol-2-one **15**.

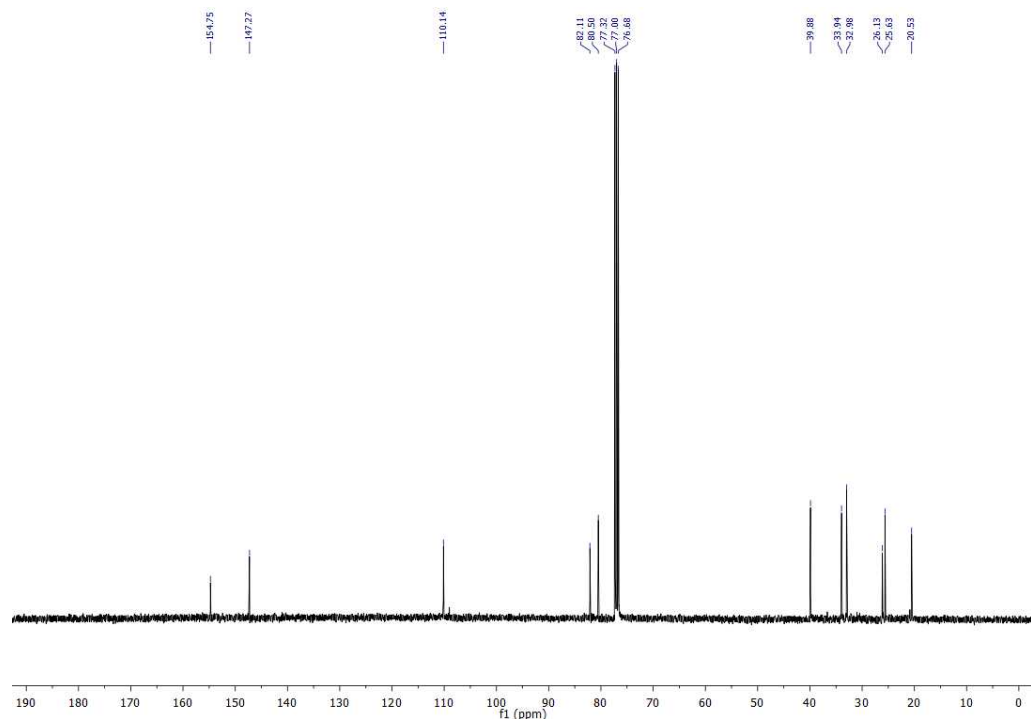


Figure S32b. ^{13}C - $\{^1\text{H}\}$ -NMR spectrum (400 MHz, 297 K, CDCl_3) for 3a-methyl-6-(prop-1-en-2-yl)hexahydrobenzo[*d*][1,3]dioxol-2-one **15**.

ELECTRONIC SUPPLEMENTARY INFORMATION

5. Kinetic studies to determine the order with respect the catalyst and cocatalyst

Typical kinetic procedure.

Styrene oxide **10a** (0.21, 1.81 mmol, 8.6 M), complex **4** (40 mg, 90.3 µmol), and TBAB (30 mg, 90.3 µmol), were placed in a sample vial fitted with a magnetic stirrer bar and placed in a large conical flask fitted with a rubber stopper pierced by a deflated balloon. The conical flask was placed in an oil bath thermostatted at 40 °C. Cardice pellets were added to the conical flask and the reaction mixture was stirred at this temperature during 5 hours. Samples of the mixture were withdrawn at different time intervals and the conversion of the epoxide to cyclic carbonate was determined by ¹H NMR analysis.

Similar experimental procedures were followed for additional runs but employing the corresponding amount of each substance according to the established loading for catalyst and/or co-catalyst (from 2 % to 5 %).

Kinetics analysis

Kinetics measurements as a function of catalyst and co-catalyst loading were performed at early stages of the cycloaddition reaction. Under these conditions, the epoxide acts as both substrate and solvent and its concentration does not change significantly, and therefore it can be considered as pseudo-constant. Therefore, the general rate equation may be written as shown in Equation (1). The reaction also proceeds in the presence of a large excess of CO₂ and therefore its concentration can be considered constant, they can be included in the observed reaction constant, giving Equation (2).

$$\text{Rate} = k [10a]^a [\text{CO}_2]^b [4]^c [\text{TBAB}]^d \quad (1)$$

$$\text{Rate} = k_{\text{obs}} [10a]^a [4]^c [\text{TBAB}]^d \text{ where } k_{\text{obs}} = k [\text{CO}_2]^b \quad (2)$$

Similarly, it could be assumed that the concentrations of catalyst **4** and the co-catalyst [TBAB] were constant during the reaction, giving Equation (3).

$$\text{Rate} = k_{1,\text{obs}} [10a]^a \text{ where } k_{1,\text{obs}} = k_{\text{obs}} [4]^c [\text{TBAB}]^d \quad (3)$$

Here, $k_{1,\text{obs}}$ is the pseudo-first-order observed rate constant for **10a** concentration and, a , b , c and d are the order of the reactions with respect to epoxide **10a**, [CO₂], catalyst **4** and co-catalyst [TBAB].

To study the order with respect to the concentration of complex **4** and TBAB two set of reactions were carried out at four concentrations. Initially, for determining the order with respect the catalyst, the amount of TBAB was fixed to 5 mol % with respect the epoxide, whilst concentration of complex **4** was varied between 2 % to 5 %. Equation (2) can rewritten as:

$$\text{Rate} = k'_{\text{obs}} [4]^c \text{ where } k'_{\text{obs}} = k_{\text{obs}} [\text{TBAB}]^d [10a]^a \quad (4)$$

Concentration of epoxide **10a** was plotted against time for the four runs (**Figure S33a**). By plotting log k'_{obs} against concentration of **4** is possible to determine the order with respect the catalyst from the slope of the curve (**Figure S33b**). The log $k'_{\text{obs}}/\log [4]$ plot showed slope of 0.99, indicating that the reaction is first order with respect to the concentration of **4**.

The order with respect co-catalyst was determined following a similar procedure but keeping concentration of complex **4** constant, 5% of initial epoxide concentration, and varying the concentration of TBAB from 2% to 5%. Concentration of epoxide **10a** was plotted against time for the four runs (**Figure S34a**).

In this case, Equation (2) can rewritten as:

$$\text{Rate} = k''_{\text{obs}} [\text{TBAB}]^d \text{ where } k''_{\text{obs}} = k_{\text{obs}} [4]^c [10a]^a \quad (5)$$

ELECTRONIC SUPPLEMENTARY INFORMATION

By plotting $\log k''_{\text{obs}}$ against concentration of TBAB is possible to determine the order with respect the co-catalyst from the slope of the curve (**Figure S34b**). The $\log k''_{\text{obs}}/\log[\text{TBAB}]$ plot showed slope of 0.99, indicating that the reaction is first order with respect to the concentration of TBAB.

Figures S33 and S34. Kinetic Plots to determine order with respect 4 and TBAB

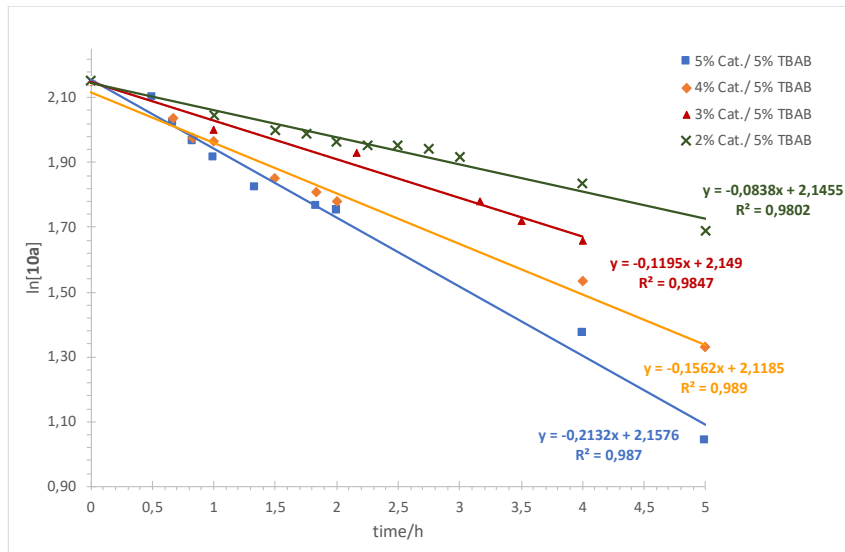


Figure S33a. First-order kinetic plot of $\ln[10\mathbf{a}]$ vs. time for the **4**/TBAB catalytic system. Reaction Conditions: $T = 40^\circ\text{C}$, $P_{\text{CO}_2} = 1 \text{ bar}$, catalyst 2-5.0 mol%, TBAB 5 mol%

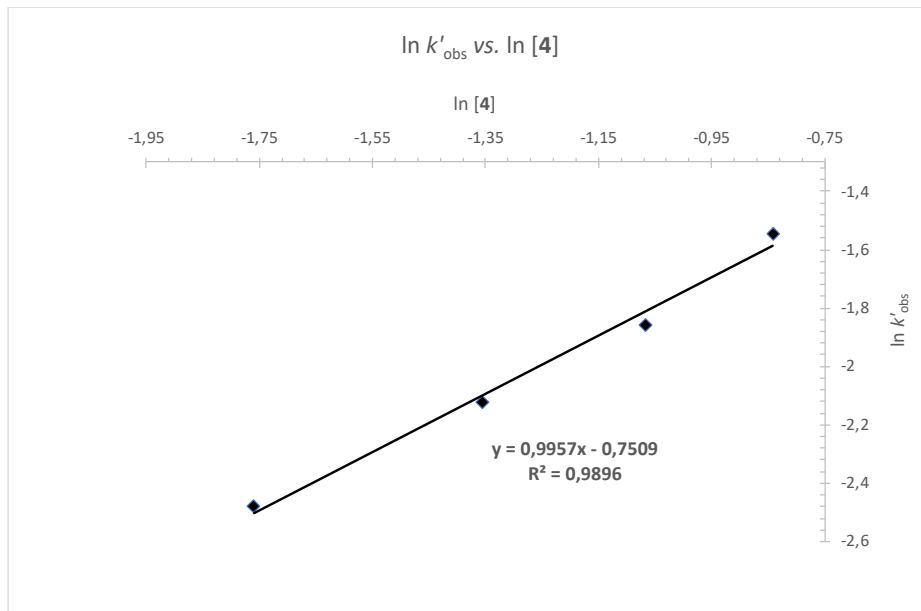


Figure S33b. Double logarithm plot of $\ln k'_{\text{obs}}$ vs $\ln [\mathbf{4}]$ for cycloaddition reaction of **10a** and CO_2 at four different concentrations of **4** (2-5 mol%). Reaction Conditions: $T = 40^\circ\text{C}$, $P_{\text{CO}_2} = 1 \text{ bar}$, catalyst 2-5.0 mol%, TBAB 5 mol%

ELECTRONIC SUPPLEMENTARY INFORMATION

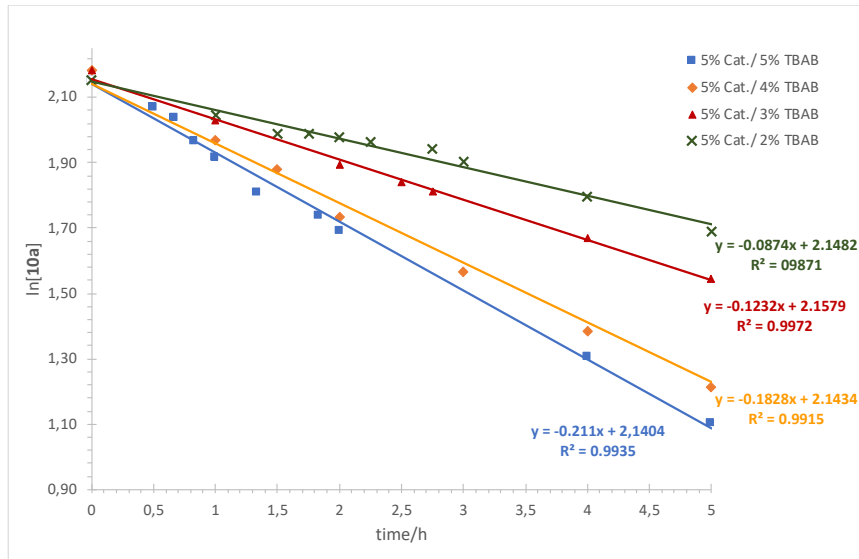


Figure S34a. First-order kinetic plot of $\ln[10a]$ vs. time for the **4**/TBAB catalytic system. Reaction Conditions: $T = 40^\circ\text{C}$, $P_{\text{CO}_2} = 1$ bar, catalyst 5.0 mol%, TBAB 2-5 mol%

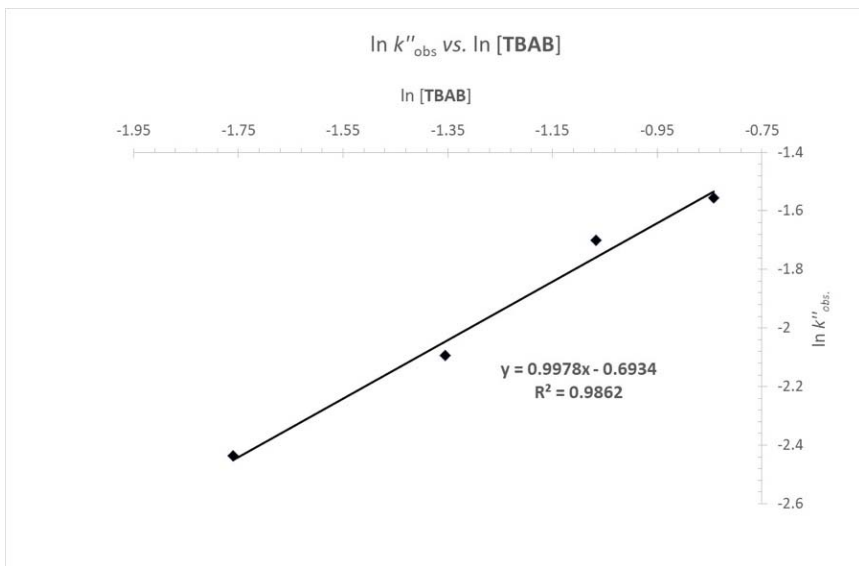


Figure S34b. Double logarithm plot of $\ln k''_{\text{obs.}}$ vs $\ln [\text{TBAB}]$ for cycloaddition reaction of **10a** and CO_2 of at four different concentrations of TBAB (2-5 mol%). Reaction Conditions: $T = 40^\circ\text{C}$, $P_{\text{CO}_2} = 1$ bar, catalyst 5.0 mol%, TBAB 2-5 mol%.

ELECTRONIC SUPPLEMENTARY INFORMATION

Tables S5a-b. Reaction rate constant and associated error for cycloaddition reaction of **10a** and CO₂.

Table S5a. First-order rate constant and associated error for cycloaddition reaction of **10a** and CO₂.^[a]

Conc. (M)	<i>k'</i> _{obs.} (h ⁻¹)	Error (h ⁻¹)	<i>k'</i> _{obs.} (h ⁻¹) × 10 ²	Error (h ⁻¹) ×	<i>k'</i> _{obs.} ± error (h ⁻¹) ×
0.172	8.38E-02	3.76E-03	8.4	0.4	8.4 ± 0.4
0.258	1.19E-01	7.46E-03	11.9	0.7	11.9 ± 0.4
0.344	1.56E-01	6.22E-03	15.6	0.6	15.6 ± 0.6
0.431	2.13E-01	8.65E-03	21.3	0.9	21.3 ± 0.9

^[a] Reaction Conditions: T= 40 °C, PCO₂ = 1 bar, catalyst **4** (2-5.0 mol%), TBAB 5 mol%

Reaction order with respect [**4**] = 0.99 ± 0.07

Table S5a. First-order rate constant and associated error for cycloaddition reaction of **10a** and CO₂.^[a]

Conc. (M)	<i>k'</i> _{obs.} (h ⁻¹)	Error (h ⁻¹)	<i>k'</i> _{obs.} (h ⁻¹) × 10 ²	Error (h ⁻¹) ×	<i>k'</i> _{obs.} ± error (h ⁻¹) ×
0.172	8.74E-02	3.33E-03	8.7	0.3	8.7 ± 0.3
0.258	1.23E-01	2.65E-03	12.3	0.3	12.3 ± 0.3
0.344	1.83E-01	6.92E-03	18.3	0.7	18.3 ± 0.7
0.431	2.11E-01	6.02E-03	21.1	0.6	21.1 ± 0.6

^[a] Reaction Conditions: T= 40 °C, PCO₂ = 1 bar, catalyst **4** 5.0 mol%, TBAB (2-5 mol%)

Reaction order with respect [TBAB]= 0.99 ± 0.08

ELECTRONIC SUPPLEMENTARY INFORMATION

6. References

- [1] A. Garcés, L. F. Sánchez-Barba, J. Fernández-Baeza, A. Otero, I. Fernández, A. Lara-Sánchez, A. M. Rodríguez, *Inorg. Chem.* **2018**, *57*, 12132-12142.
- [2] SAINT v8.37, Bruker-AXS (2016), APEX3 v2016.1.0. Madison, Wisconsin, USA.
- [3] SADABS, Krause, L., Herbst-Irmer, R., Sheldrick, G. M. & Stalke, D.. *J. Appl. Crystallogr.* **2015**, *48*, 3.
- [4] a) L. J. Farrugia, *J. Appl. Cryst.*, **2012**, *45*, 849. b). G. M. Sheldrick, SHELX-2014, Program for Crystal Structure Refinement, University of Göttingen, Göttingen, Germany, **2014**.
- [5] F. de la Cruz-Martínez, J. Martínez, M. A. Gaona, J. Fernández-Baeza, L. F. Sánchez-Barba, A. M. Rodríguez, J. A. Castro-Osma, A. Otero, A. Lara-Sánchez, *ACS Sustainable Chem. Eng.* **2018**, *6*, 5322-5332.
- [6] J. Martínez, J. A. Castro-Osma, C. Alonso-Moreno, A. Rodríguez-Díéguez, M. North, A. Otero, A. Lara-Sánchez, *ChemSusChem* **2017**, *10*, 1175-1185.
- [7] D. Steiner, L. Ivison, C. T. Goralski, R. B. Appell, J. R. Gojkovic, B. Singaram, *Tetrahedron: Asymmetry* **2002**, *13*, 2359-2363.
- [8] L. Peña-Carrodeguas, J. González-Fabra, F. Castro-Gómez, C. Bo, A. W. Kleij, *Chem. Eur. J.* **2015**, *21*, 6115-6122.